Large-scale Increases in Vegetation Productivity Inferred from Satellite Data

by
Jingfeng Xiao

A dissertation submitted to the faculty of the University of North Carolina at Chapel Hill in partial fulfillment of the requirement for the degree of Doctor of Philosophy in the Department of Geography.

Chapel Hill
2006

Approved by:

Aaron Moody, Advisor

Lawrence E. Band, Reader

William A. Hoffmann, Reader

Robert K. Peet, Reader

Conghe Song, Reader

ABSTRACT

Jingfeng Xiao

Large-Scale Increases in Vegetation Productivity Inferred from Satellite Data
(Under the direction of Dr. A. Moody)

Terrestrial vegetation plays an important role in the exchanges of carbon, water, and energy at the land surface. Changes in vegetation productivity at regional or larger scales have important implications for regulating the atmospheric CO_2 concentration and climate and affecting food production. The characterization of large-scale increases in vegetation productivity will lead to a better understanding of the distribution and dynamics of carbon sources/sinks and climate change. In this dissertation, I examined the increases in vegetation productivity at multiple scales. First, I examined the increases in vegetation productivity and their associations with climate variability at the global scale over the period 1982 to 1998 using satellite data and ground-based climatology data. Temperature, and, in particular spring warming, was the primary climatic factor associated with greening in the northern high latitudes, Western Europe, U.S. Pacific Northwest, tropical and subtropical Africa, and eastern China. Precipitation was a strong correlate of greening in fragmented regions only. Globally, greening trends are a function of both climatic and non-climatic factors, such as forest regrowth, CO_2 enrichment, woody plant proliferation, and trends in agricultural practices. Second, I analyzed the responses of vegetation productivity to climate both within and across biomes for the

conterminous US using satellite data and climate data. Forested and non-forested biomes differed sharply in their response to spatial gradients in temperature and precipitation. Precipitation affected the productivity of all biomes, and the influence of precipitation on productivity differed across biomes. The effect of seasonal Tmax and Tmin was only apparent for forested biomes, which are less likely to be water limited. The seasonality of temperature relations, and the relatively greater importance of Tmin for some biomes, suggest that the dominant effect of temperature is through its influence on growing-season length. Third, I looked at the rates of western juniper expansion and the resulting C uptake in central Oregon over the period 1975-2000 using satellite data, forest inventory data, and field measurements. Western juniper expanded at the rate of 0.15% per year over the 25-year period. The results suggest that the expansion of western juniper caused C accumulation of 0.27 Mg C ha^{-1} yr^{-1} in aboveground woody biomass. Total C stock in aboveground woody biomass increased from 0.13 Tg in 1975 to 0.21 Tg in 2000. Western juniper expansion may have a significant impact on the regional C budget.

ACKNOWLEDGEMENTS

I would like to acknowledge many people for helping me during my doctoral work. I would especially like to thank my advisor, Dr. Aaron Moody, for his generous time and commitment. I greatly improved independent thinking, research skills, and scientific writing with his help throughout my doctoral work.

I wish to thank my committee members, Drs. Larry Band, Conghe Song, Bill Hoffmann, and Bob Pete for their continual help and support.

I would like to thank Dr. Steve Walsh for his support and encouragement. I have learned a lot from him throughout these years.

I extend my thanks to my colleagues and friends, especially David Tenebaum, Peter Shin, and those who kindly provided me scientific data sets used in my dissertation work.

Finally, I would like to thank my family. I am grateful to my parents, Youguo Xiao and Peimei Chen, for their love, support and encouragement over the years. I aslo thank my brother, Jingsong Xiao and sister, Fuying Xiao for their encouragement. I am especially grateful to my wife, Jumei, for her love and support and my two-year-old son, Vincent for bringing me so much happiness and laughters everyday.

This research was partially funded a NASA Earth System Science Fellowship award (09/2003-08/2006).

CONTENTS

LIST OF TABLES

LIST OF FIGURES

Chapter 1

Introduction

1.1 Introduction

Atmospheric CO_2 concentration has been increasing since the industrial revolution. Measurements taken Mauna Loa, Hawaii show that mean annual CO_2 concentration increased approximately 19% from about 316 ppmv in 1958 to about 377 ppmv in 2004 (Keeling & Whorf 2005). The dramatic rise of this greenhouse gas in the atmosphere is increasingly thought to be a major factor causing global warming.

The two major sources of CO_2 in the atmosphere are the combustion of fossil fuels and deforestation (IPCC 2001). The worldwide consumption of fossil fuels (coal, oil, and natural gas) released 6.3 ± 0.4 Pg C yr^{-1} into the atmosphere in the 1990s (IPCC 2001). About 10 to 30% of the current total anthropogenic emissions of CO_2 are estimated to be caused by land-use conversion, particularly deforestation (IPCC 2001). For example, Houghton (2000) estimated that the net flux due to land-use change was 1.7 ± 0.8 Pg C yr, almost entirely due to deforestation in tropical regions.

Not all the carbon (C) released by anthropogenic activities is absorbed by the atmosphere. The atmosphere only absorbs 3.2 ± 0.1 Pg C yr^{-1} during the 1990s, while the oceans absorb another 1.5-2.2 Pg C yr^{1} during the 1980s and 1990s (IPCC 2001). The residual C sink is estimated at 1.96 ± 1.6 Pg C yr for the 1990s (IPCC 2001), and this sink has been attributed to terrestrial ecosystems (Schimel et al. 2001).

Terrestrial vegetation plays a major role in the exchanges of C at the land surface (Tans et al. 1990, Hoffmann & Jackson 2000, Wu & Lynch 2000). There is general agreement that terrestrial ecosystems in the northern hemisphere provide a C sink of 1 to 2 Pg C yr^{-1} (Battle et al. 2000, IPCC 2001, Schimel et al. 2001). Changes in vegetation productivity, especially at regional or larger scales, affect atmospheric CO_2 concentrations, and produce variability in global C budgets and uncertainty in their approximation (Schimel et al. 1996). Regionally, net C uptake has been attributed to increases in vegetation activity due to fire suppression (Houghton et al. 2000), forest regrowth after agricultural abandonment (Caspersen et al. 2000), CO_2 enrichment (Hamilton et al. 2002), climate change (Nemani et al. 2002), N deposition (Nadelhoffer et al. 1999), forest plantations (Goodale et al. 2002), and woody plant proliferation (Houghton et al. 1999, 2000, Pacala et al. 2001). Understanding the modes and drivers of changes in terrestrial plant productivity can, therefore, help us to understand and account for this source of variability.

The modes and drivers of increases in terrestrial plant productivity have been documented at regional to global scales (e.g., Myneni et al. 1997, Cao & Woodward 1998, Zhou et al. 2001). There is growing evidence that vegetation productivity has been increasing in the northern middle and high latitudes during the past two decades, suggesting that the earth has become greener due to natural factors and anthropogenic activities (Fan et al. 1998, Bousquet et al. 1999, Zhou et al. 2001, Goodale et al. 2002). This evidence has been obtained from analysis of atmospheric CO_2 data (Tans et al. 1990, Keeling et al. 1996), forest inventory data (Birdsey et al. 1993, Turner et al. 1995, Goodale et al. 2002), studies of land-use change (Houghton et al. 1999, Caspersen et al.

2000), ground-based phenological observations (Cayan et al. 2001, Fitter & Fitter 2002), analysis of satellite data (Myneni et al. 1997, 2001, Zhou et al. 2001), and simulations using biogeochemical models (Cao & Woodward 1998, Hicke et al. 2002, Lucht et al. 2002).

The investigation of large-scale increases in vegetation productivity has been largely limited to northern high latitudes (e.g., Myneni et al. 1997, Tucker et al. 2001, Zhou et al. 2001). Temperature is thought to be the leading climatic factor controlling the high-latitude greening trend. Elevated temperature enhances plant growth by lengthening the growing season (Myneni et al. 1997). The geographic distribution and patterns of the increases in vegetation productivity at the global scale are not well understood. The following three questions remain regarding the distribution and drivers of changes in vegetation productivity: (1) What is the geographic distribution of dominant trends in vegetation activity globally? (2) What are the primary climatic correlates of these trends and patterns? (3) What are the rates of woody plant proliferation and the resulting C uptake?

Among the modes of increases in vegetation productivity, woody plant proliferation is unique in that it involves increases in stem density and/or represents a transition from one biome type to another, and has important implications for US C budgets. This phenomenon has been attributed to fire suppression (Houghton et al. 2000, Tilman et al. 2000), over-grazing (Archer 1989), climate change (Brown et al. 1997), atmospheric CO_2 enrichment (Polley et al. 2002), nitrogen deposition (Köchy & Wilson 2001), and a combination of two or more of these factors (Van Auken 2000). Woody plant proliferation includes woody encroachment (Van Auken 2000) and woody thickening

(Hicke et al. 2004). Woody encroachment is the process by which woody plants expand into grasslands or shrublands (e.g., Archer et al. 2001), whereas woody thickening occurs when woody plants increases in stem density (e.g., Covington & Moore 1994). Woody plant proliferation has been documented primarily at local scales (Schlesinger et al. 1990, Miller & Rose 1995, Brown et al. 1997, Briggs et al. 2002a, b, Asner et al. 2003).

Woody encroachment and/or woody thickening have significant implications for C budgets. About 21-40% of the US C sink has been attributed to woody plant proliferation in the non-forested areas in the western US (Houghton et al. 1999, 2000, Pacala et al. 2001). However, these studies emphasized the large uncertainty in their estimates. Neither the rates of change nor the geographical extent of woody plant proliferation has been systematically quantified, not to mention the resulting C uptake and the implications on regional C budgets (Anser et al. 2003). Regional-scale analysis of the rates, geographical extent, and C stocks of woody plant proliferation are needed in order to reduce the uncertainty in the estimate of the C sink resulting from woody plant proliferation and thus to refine the US C sink (Goodale & Davidson 2002, Asner et al. 2003).

In the current study, I characterized increases in vegetation productivity and their associations with climate variability at the global scale over the period 1982-1998 using satellite data and ground-based climatology data (Chapter 2); examined the responses of vegetation productivity to climate within and across biomes for the conterminous US using satellite data along with climate data (Chapter 3); and looked at the rates of western juniper expansion and the resulting C uptake in aboveground woody biomass in central Oregon using satellite data, forest inventory data, and field measurements (Chapter 4). In

Chapter 5, I synthesized the previous chapters' results and discussed my future work in this direction.

1.2 References

Archer, S., 1989. Have southern Texas savannas been converted to woodlands in recent history. *American Naturalist*, **134**, 545-561.

Archer, S., Boutton, T.W., & Hibbard, K.A., 2001. Trees in grasslands: biogeochemical consequences of woody plant proliferation. In *Global Biogeochemical Cycles in the Climate System*. Edited by E.-D. Schulze, S. Harrison, M. Heimann, E. Holland, J. Lloyd, I. Prentice, and D. Schimel. Academic Press Inc., San Diego. pp. 115-133.

Asner, G.P., Archer, S., Hughes, R.F., Ansley, R.J., & Wessman, C.A., 2003. Net changes in regional woody vegetation cover and carbon storage in Texas Drylands, 1937-1999. *Global Change Biology*, **9**, 316-335.

Battle, M., Bender, M.L., Tans, P.P., White, J.W.C., Ellis, J.T., Conway, T., & Francey, R.J., 2000. Global sinks and their variability inferred from atmospheric O_2 and $\delta^{13}C$. *Science*, **287**, 2467-2470.

Birdsey, R.A., Plantinga, A.J., & Heath, L.S., 1993. Past and prospective carbon storage in United States forests. *Forest Ecology & Mangement*, **58**, 33-40.

Bousquet, P., Ciais, P., Peylin, P., Ramonet, M., & Monfray, P., 1999. Inverse modeling of annual atmospheric CO_2 sources and sinks. 1. Method and control inversion. *Journal of Geophysical Research*, **104**, 26161-26178.

Briggs, J.M., Knapp, A.K., & Brock, B.L., 2002a. Expansion of woody plants in tallgrass prairie: a fifteen-year study of fire and fire-grazing interactions. *American Midland Naturalist*, **147**, 287-294.

Briggs, J.M., Hoch, G.A., & Johnson, L.C., 2002b. Assessing the rate, mechanisms, and consequences of the conversion of tallgrass prairie to Juniperus virginiana forest. *Ecosystems*, **5**, 578-586.

Brown, J.H., Valone, T.J., & Curtin, C.G. 1997. Reorganization of an arid ecosystem in response to recent climate change. *Proc. Natl. Acad. Sci. USA*, **94**, 9729-9733.

Cao, M., & Woodward, F.I., 1998. Dynamic responses of terrestrial ecosystem carbon cycling to global climate change. *Nature*, **393**, 249-252.

Caspersen, J.P., Pacala, S.W., Jenkins, J.C., Hurtt, G.C., Moorcroft, P.R., & Birdsey, R.A. 2000. Contributions of land-use history to carbon accumulation in U.S. forests. *Science*, **290**, 1148-1151.

Cayan, R.C., Kammerdiener, S.A., Dettinger, M.D., Caprio, J.M., & Peterson, D.H., 2001. Changes in the onset of spring in the western United States. *Bulletin of the American Meteorological Society*, **82**, 399-415.

Covington, W.W., & Moore, N.M., 1994. Southwestern ponderosa forest structure: changes since Euro-American settlement. *Journal of Forestry*, **92**, 39-47.

Fan, S., Gloor, M., Mahlman, J., Pacala, S., Sarmiento, J., Takahashi, T., Tans, P. 1998. A large terrestrial carbon sink in North American implied by atmospheric and oceanic carbon dioxide data and models. *Science*, **282**, 442-446.

Fitter, A.H., & Fitter, R.S.R., 2002. Rapid changes in flowering time in British plants. *Science*, **296**, 1689-1691.

Goodale, C.L., Apps, M.J., Birdsey, R.A., Field, C.B., Heath, L.S. et al. 2002. Forest carbon sinks in the northern hemisphere. *Ecological Applications*, **12**, 891-899.

Goodale, C.L., & Davidson, E.A., 2002. Uncertain sinks in the shrubs. *Nature*, **418**, 593-594.

Hamilton, JG, DeLucia, EH, George, K et al. 2002. Forest carbon balance under elevated CO_2. *Oecologia*, **131**, 250-260.

Hicke, J.A., Asner, G.P., Randerson, J.T., Tucker, C., Los, S. et al., 2002. Satellite-derived increases in net primary productivity across North America, 1982-1998. *Geophysical Research Letters*, **29**, 1427, 10.1029/2001GL013578.

Hicke, J.A., Sherriff, R.L., Veblen, T.T., & Asner, G., 2004. Carbon accumulation in Colorado ponderosa pine stands. *Canadian Journal of Forest Research*, **34**, 1283-1295.

Hoffmann, W.A., & Jackson, R.B., 2000. Vegetation-climate feedbacks in the conversion of tropical savanna to grassland. *Journal of Climate*, **13**, 1593-1602.

Houghton, R.A., Hackler, J.L., & Lawrence, K.T. 1999. The U.S. carbon budget: contributions from land-use change. *Science*, **285**, 574-578.

Houghton, R.A., 2000: A new estimate of global sources and sinks of carbon from land-use change. *EOS*, **81**, supplement, s281.

Houghton, R.A., Hackler, J.L., & Lawrence, K.T. 2000. Changes in terrestrial carbon storage in the United States. 2: The role of fire and fire management. *Global Ecology & Biogeography*, **9**, 145-170.

Intergovernmental Panel on Climate Change (IPCC), 2001. *Climate Change 2001: The Scientific Basis*. Contribution of Working Group I to the Third Assessment Report of the Intergovernmental Panel on Climate Change (IPCC). J. T. Houghton, Y. Ding, D.J. Griggs, M. Noguer, P. J. van der Linden and D. Xiaosu (Eds.). Cambridge University Press, UK. pp 944.

Keeling, C.D., Chin, J.F.S., & Whorf, T.P., 1996. Increased activity of northern vegetation inferred from atmospheric CO_2 measurements. *Nature*, **382**, 146-149.

Keeling, C.D. and T.P. Whorf. 2005. Atmospheric CO_2 records from sites in the SIO air sampling network. In Trends: A Compendium of Data on Global Change. Carbon Dioxide Information Analysis Center, Oak Ridge National Laboratory, U.S. Department of Energy, Oak Ridge, Tenn., U.S.A.

Köchy, M., & Wilson, S.D., 2001. Nitrogen deposition and forest expansion in the northern Great Plains. *Journal of Ecology*, **89**, 807-817.

Lucht, W., Prentice, I.C., Myneni, R.B., Sitch, S., Friedlingstein, P. et al., 2002, Climatic control of the high-latitude vegetation greening trend and Pinatubo effect. *Science,* **296**, 1687-1689.

Miller, R.F., Rose, J.A., 1995. Historic expansion of Juniperus occidentalis (western juniper) in southeastern Oregon. *Great Basin Naturalist*, **55**, 37-45.

Myneni, R.B., Keeling, C.D., Tucker, C.J., Asrar, G., & Nemani, R.R., 1997. Increased plant growth in the northern high latitudes from 1981 to 1991. *Nature*, **386**, 698-702.

Myneni, R.B., Dong, J., Tucker, C.J., Kaufmann, R.K., Kauppi, P.E. et al. 2001. A large carbon sink in the woody biomass of northern forests. *Proc. Natl. Acad. Sci. USA*, **98**, 14784-14789.

Nadelhoffer, KJ, Emmett, BA, Gundersen, P et al. 1999. Nitrogen deposition makes a minor contribution to carbon sequestration in temperate forests. *Nature*, **398**, 145-148.

Nemani, R., White, M., Thornton, P., Nishida, K., Reddy, S., Jenkins, J., & Running, S. 2002. Recent trends in hydrologic balance have enhanced the terrestrial carbon sink in the United States. *Geophysical Research Letters*, **29**, 1468, doi:10.1029/2002GL014867.

Pacala, S.W., Hurtt, G.C., Baker, D., Peylin, P., Houghton, R.A., et al. 2001. Consistent land- and atmosphere-based U.S. carbon sink estimates. *Science*, **292**, 2316-2320.

Polley, H.W., Johnson, H.B., & Tischler, C.R., 2002. Woody invasion of grasslands: evidence that CO_2 enrichment indirectly promotes establishment of Prosopis glandulosa. *Plant Ecology,* **164**, 85-94.

Schimel, D.S., Alves, D., Enting, I., Himann, M., Joos, F., Raynaud, D., and Wigley, T., 1996, CO2 and the carbon cycle, in *Climate Change 1995: The Science of Climate Change*, edited by J. T. Houghton et al., pp. 76-86, Cambridge University Press, New York, 1996.

Schimel, D.S., House, J.I., Hibbard, K.A., Bousquet, P., Ciais, P. et al., 2001. Recent patterns and mechanisms of carbon exchange by terrestrial ecosystems. *Nature*, **414**, 169-172.

Schlesinger, W.H., Reynolds, J.F., Cunningham, G.L., Huenneke, L.F., Jarrell, W.M., et al., 1990. Biological feedbacks in global desertification. *Science*, **247**, 1043-1048.

Tans, P. P., Fung, I. Y., and Takahashi, T. 1990. Observation constraints on the global atmospheric CO_2 budget. *Science*, **247**, 1431-1438.

Tilman, D., Reich, P., Phillips, H., Menton, M., Patel, A. et al., 2000. Fire suppression and ecosystem carbon storage. *Ecology,* **81***,* 2680-2685.

Tucker, C.J., Slayback, D.A., Pinzon, J.E., Los, S.O., Myneni, R.B., and Taylor, M.G., 2001, Higher northern latitude normalized difference vegetation index and growing season trends from 1982 to 1999. *International Journal of Biometeorology,* **45**, 184-190.

Turner, D.P., Koerper, G.J., Harmon, M.E., & Lee, J., 1995. A carbon budget for forests of the conterminous United States. *Ecological Applications*, **5**, 421-436.

Van Auken, W.O., 2000. Shrub invasions of North American semiarid grasslands. *Annual Review of Ecology and Systematics*, **31**, 197-216.

Wu, W., & Lynch, A.H., 2000. Response of the seasonal carbon cycle in high latitudes to climate anomalies. *Journal of Geophysical Research*, **105**, 22897-22908.

Zhou, L., Tucker, C.J., Kaufmann, R.K., Slayback, D., Shabanov, N.V., and Myneni, R.B., 2001, Variations in northern vegetation activity inferred from satellite data of vegetation index during 1981 to 1999. *Journal of Geophysical Research,* **106**, 20069-20083.

Chapter 2

Geographic distribution of global greening trends and their climatic correlates: 1982-1998

2.1 Introduction

The global surface air temperature increased by about 0.5℃ between the mid-1970s and the late 1990s (Hansen et al. 1999). These changes are geographically stratified. The northern middle and high latitudes have warmed most rapidly, by about 0.8℃ since the early 1970s, while the tropics have warmed only moderately (Hansen et al. 1999). In addition, global land precipitation increased by about 2% during the 20th century (Jones and Hulme 1996, Hulme et al. 1998). Precipitation changes have also exhibited substantial spatial and temporal variability (Karl and Knight 1998, Doherty et al. 1999, Mekis and Hogg 1999, Zhai et al. 1999).

Increases in temperature and moisture may increase vegetation activity by lengthening the period of carbon uptake (Nemani et al. 2002), enhancing photosynthesis (Keeling et al. 1996, Randerson et al. 1999), and changing nutrient availability by accelerating decomposition or mineralization (Melillo et al. 1993). Such processes have important implications for carbon sink/source dynamics, changes in the distribution of terrestrial biomes, and food production (Tans et al. 1990, Schimel et al. 1996).

Several studies have documented greening trends in the northern high latitudes (Zhou et al. 2001, Tucker et al. 2001, Bogaert et al. 2002, Slayback et al. 2003) as well as in other large geographic regions (e.g., Kawabata et al. 2001, Nemani et al. 2003, Xiao and Moody 2004a). However, numerous questions remain regarding the distribution and drivers of trends in vegetation greenness. The focus of this paper is on two questions: (1) What is the geographic distribution of dominant trends in vegetation activity globally? (2) What are the primary climatic correlates of these trends and patterns? To address these questions, I used a recently developed satellite-measured vegetation index data set, in conjunction with a gridded global climate data set, to examine trends in vegetation activity and their associations to climatic drivers in the period 1982-1998. In particular, I emphasize the geographical variability in these bioclimatological associations.

2.2 Background

The satellite-measured normalized difference vegetation index (NDVI) has been widely used to characterize vegetation activity (Asrar et al. 1984, Myneni et al. 1995, 1997, Zhou et al. 2001, Tucker et al. 2001, Xiao and Moody 2004b). NDVI captures the contrast between the visible-red and near-infrared reflectance of vegetation canopies, and is indicative of the abundance and activity of leaf chlorophyll pigments (Asrar et al. 1984, Myneni et al. 1995). NDVI is closely correlated to the fraction of photosynthetically active radiation (fPAR) absorbed by vegetation canopies, and thus can be used as a proxy for photosynthetic activity of terrestrial vegetation at a global scale (Asrar et al. 1984, Myneni et al. 1995).

Satellite-based NDVI observations over the past two decades (Zhou et al. 2001, Tucker et al. 2001, Bogaert et al. 2002, Slayback et al. 2003), as well as model

predictions based on observed climate data (Lucht et al. 2002), have identified a vegetation greening trend in the northern high latitudes (40ºN–70ºN), especially in Eurasia. The greening trend corresponds to the pronounced warming, particularly during winter and spring over Alaska, northern Canada, and northern Eurasia (Hansen et al. 1999). The greening trend is also consistent with ground-based phenological observations (Colombo 1998, Cayan et al. 2001, Fitter and Fitter 2002), as well as reports of increased terrestrial carbon stock in woody biomass in these regions (Fan et al. 1998, Myneni et al. 2001, Schimel et al. 2001). Temperature is thought to be the leading climatic factor controlling the high-latitude greening trend, which has been attributed to an early spring and a delayed autumn (Zhou et al. 2001, Tucker et al. 2001, Bogaert et al. 2002, Lucht et al. 2002). Precipitation has been assumed to play a minor role in increasing vegetation activity and has not been fully considered in most studies.

At the global scale, Kawabata et al. (2001) and Ichii et al. (2002) used the NOAA/NASA Pathfinder AVHRR Land (PAL) NDVI dataset (James and Kalluri 1994) combined with gridded climate data, to examine correlations between trends in vegetation activity and climate for the period 1982-1990. Even over this short period, their results illustrated the strong correlation between northern mid-to-high latitude greening and temperature increases. They also identified decreases in greeness in the southern hemisphere tropics to mid latitudes. These were correlated with variability in precipitation. Nemani et al. (2003) modeled the changes in net primary production (NPP) globally from 1982 to 1999 using both climatic and satellite observations, and indicated that net primary production increased 6%, and the largest increase was in tropical ecosystems. Xiao and Moody (2004a) examined trends in vegetation activity and their

climatic correlates in China between 1982 and 1998 using both climatic and satellite data. Temperature was the leading climatic factor controlling greening patterns in China, but trends in agricultural practices, such as increased use of high-yield crops and application of chemical fertilizers, along with land-use changes such as afforestation and reforestation probably have made a greater contribution to the greening trend than temperature (Xiao and Moody, 2004a).

Trends in vegetation productivity may indicate changes in terrestrial carbon stock in vegetation biomass, and thus have implications for the global carbon cycle (Goulden et al. 1996, Keeling et al. 1996, Myneni et al. 1997). However, the relative contributions of temperature and precipitation to observed greening trends, and in particular their geographical distribution, patterns and drivers are not resolved. Zhou et al. (2001), Tucker et al. (2001), Lucht et al. (2002), and Ichii et al. (2002) argued that temperature is the leading climatic factor in controlling the greening trend in the northern high latitudes. In the conterminous U.S., by contrast, Nemani et al. (2002) showed that increases in precipitation and humidity are the most important factors enhancing vegetation activity.

In this paper I present an analysis of greening trends, bioclimatological patterns and associations at the global scale. Compared to recent studies by Kawabata et al. (2001) and Ichii et al. (2002) I extend the period of analysis from 1982-1990 (9 years) to 1982-1998 (17 years). This extension is possible due to the recent availability of global, half-degree AVHRR NDVI data (Nemani et al. 2003) that has been reprocessed and substantially improved over the earlier, shorter-term version of the PAL dataset (James and Kalluri 1994). This data set not only allows the evaluation of the longevity and change in the

trends reported by Kawabata et al. (2001) and Ichii et al. (2002), but also permits more statistically conservative and reliable assessment of these trends and relationships.

2.3 Data & Methods

2.3.1 Data

2.3.1.1 Satellite data

I analyzed data for the period 1982-1998 for which I had access to both satellite and climate data. I used a recently developed Version 3 Pathfinder NDVI data set (Nemani et al. 2003) derived from Advanced Very High Resolution Radiometer (AVHRR) on board the National Oceanic and Atmospheric Administration's (NOAA) series of polar-orbiting meteorological satellites (NOAA 7, 9, 11, and 14). This NDVI data set is the improved version of the NOAA/NASA PAL NDVI data set (James & Kalluri, 1994). The NDVI captures the contrast between the visible-red and near-infrared reflectance of vegetation canopies. It is defined as

$$NDVI = (NIR - RED) / (NIR + RED) \quad (1)$$

where NIR and RED are the visible-red (0.58-0.68μm) and near-infrared (0.725-1.1μm) reflectance, respectively. The NDVI is scaled between -1 and +1, and typically varies from -0.2 to 0.1 for snow, inland water bodies, deserts, and bare soils, and increases from about 0.1 to 0.75 for progressively increasing amounts of vegetation (Tucker et al., 1986). The Version 3 Pathfinder NDVI data set was produced by the Dr. Ranga Myneni group at Department of Geography, Boston University, and referred to by Nemani et al. (2003). In the Version 3 Pathfinder NDVI data set, remaining noise associated with residual atmospheric effects, orbital drift effects, intersensor variations, and stratospheric aerosol effects (Myneni et al. 1998, Kaufmann et al. 2000) was further reduced by a series of

corrections, including temporal compositing, spatial compositing, orbital correction, and climate correction (Nemani et al. 2003). The Version 3 Pathfinder NDVI data set provides a valuable basis to infer the interannual variability in vegetation activity at a global scale. This data set is available at two different resolutions, including 16 km and 0.5 degree. The 0.5-degree NDVI data was used for this global-scale study.

2.3.1.2 Climate data

I used a global monthly climatology data set gridded at 0.5-degree resolution (New et al. 2000). This global climatology dataset includes seven climate variables: precipitation, mean temperature, diurnal temperature range, wet-day frequency, vapor pressure, cloud cover, and ground frost frequency. I used two variables, precipitation and mean temperature. Both variables were interpolated from station observations (New et al. 2000). This data set has higher spatial resolution, longer temporal coverage, and more strict temporal fidelity than other global climatology data sets (New et al. 2000).

2.3.2 Methods

I produced spatially averaged time series of annual average NDVI, annual mean temperature, and annual precipitation for all vegetated pixels within the northern high latitudes (40°N-70°N), the northern middle latitudes (23.5°N-40°N), and the tropics (23.5°S-23.5°N). These time series were not analyzed for climate zones in the southern hemisphere because these zones exhibit no prevalent greening pattern as shown later. Previous studies have shown increasing vegetation activity and carbon stock in the conterminous U.S. (e.g., Pacala et al. 2001, Nemani et al. 2002) and China (e.g., Goodale et al. 2002, Xiao and Moody 2004a). Thus, these time series were also produced both U.S. and China. Each time series was standardized by subtracting the mean of the series from

the original time series and then dividing by the standard deviation of the series in order to constrain the variance of these time series to the same range and therefore make their intercomparisons more straightforward. The linear trends of spatially averaged NDVI were determined by linearly regressing these variables as a function of time over the period from 1982 to 1998 for each geographical region. I then analyzed the correlations between NDVI and climate data to assess the associations between vegetation changes and climate changes on a regional basis.

The trends of spatially averaged NDVI may hide the geographical variability of NDVI trends over space. I thus analyzed the spatial patterns of NDVI from 1982 to 1998. I identified the vegetated pixels with linear trends in NDVI that are statistically significant ($p < 0.05$) over the 17-year period. For these pixels, I then analyzed the correlation between annual average NDVI and annual mean temperature and the correlation between annual mean NDVI and annual precipitation. These analyses were repeated using seasonal mean NDVI, seasonal mean temperature, and seasonal precipitation totals. The relative strength of associations between NDVI and climate variables were mapped and evaluated for different geographical regions.

2.4 Results

2.4.1 Trends of spatially averaged NDVI

2.4.1.1 Northern high latitudes

The spatially averaged time series of annual NDVI and annual mean temperature for vegetated areas within the northern high latitudes exhibited upward trends that are statistically significant at 0.01 and 0.05, respectively (Fig. 2.1 (a), table 2.1). From 1982 to 1998, annual NDVI averages increased by 13.02%, and annual mean temperature

increased by 0.74℃ (table 2.1). Annual NDVI averages and annual mean temperature were significantly correlated over the 17-year period within this region ($p < 0.05$) (table 2.2). There is no significant correlation between NDVI and precipitation.

2.4.1.2 Northern middle latitudes

Within the northern middle latitudes, NDVI exhibited an upward trend between 1982 and 1998 (Fig. 2.1 (b), table 2.1). This corresponds to an overall greening of 6.63% for the northern middle latitudes as a whole over the 17-year period.

Annual mean temperature increased by 0.56℃ from 1982 to 1998 (table 2.1). Annual NDVI averages are significantly correlated to annual mean temperature (table 2.2). NDVI is not significantly related to precipitation.

Over the conterminous U.S., NDVI increased by 9.14% (Fig. 2.1 (d), table 2.1). The spatially averaged time series of annual NDVI was significantly correlated to annual mean temperature over this area (table 2.2). There was no significant relationship between annual NDVI averages and annual precipitation.

NDVI increased by 7.99% in China over the study period (Fig. 2.1 (e), table 2.1). Annual mean temperature increased by about 0.87℃ (table 2.1). The spatially averaged time series of annual NDVI was significantly related to that of annual mean temperature in China (table 2.2). There was no significant relationship between annual NDVI averages and annual precipitation in China.

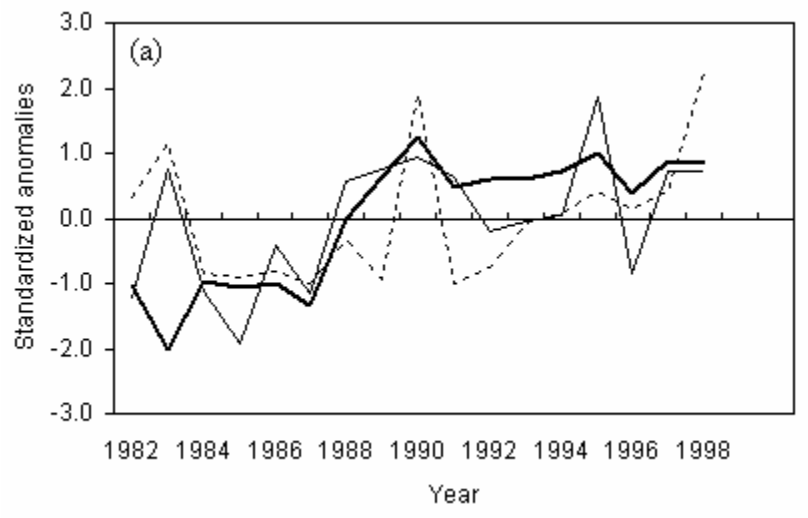
(a)
Standardized anomalies
3.0
2.0
1.0
0.0
-1.0
-2.0
-3.0
1982 1984 1986 1988 1990 1992 1994 1996 1998
Year

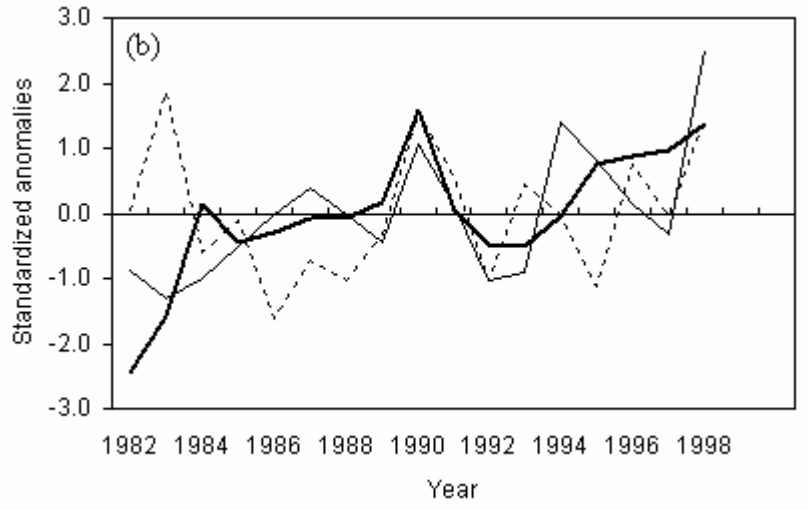
(b)
Standardized anomalies
3.0
2.0
1.0
0.0
-1.0
-2.0
-3.0
1982 1984 1986 1988 1990 1992 1994 1996 1998
Year

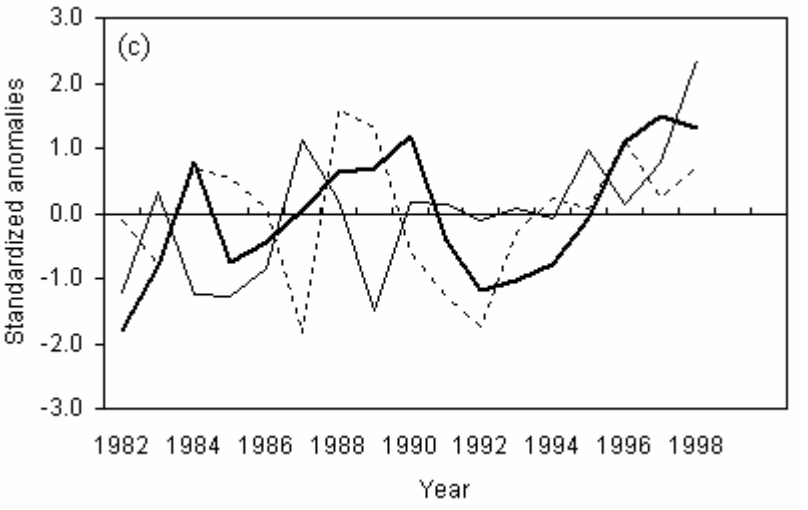
(c)
Standardized anomalies
3.0
2.0
1.0
0.0
-1.0
-2.0
-3.0
1982 1984 1986 1988 1990 1992 1994 1996 1998
Year

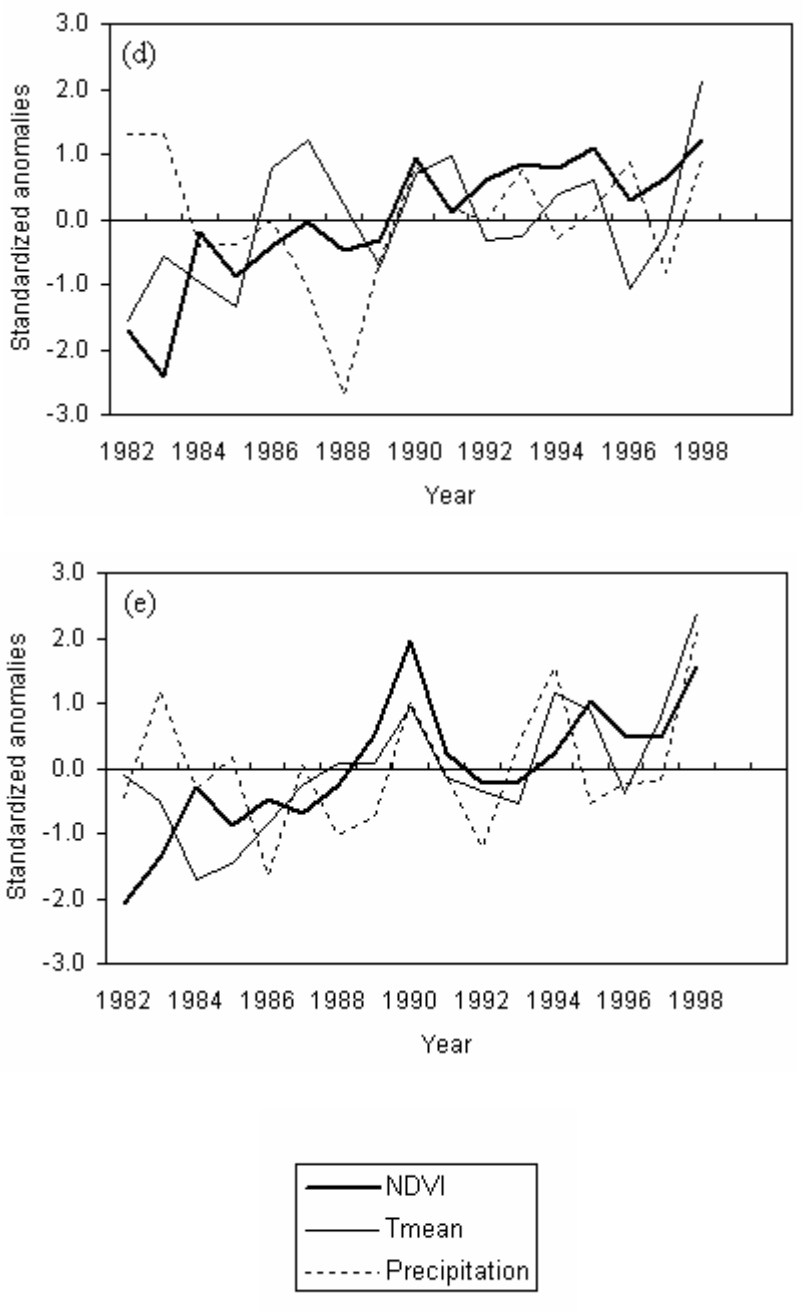

Fig. 2.1 Spatially averaged time series of annual NDVI, annual mean temperature, and annual precipitation in vegetated areas within the northern high latitudes (a), the northern middle latitudes (b), the tropics (c), the conterminous U.S. (d), and China (e) from 1982 to 1998.

Table 2.1 Trends of spatially averaged NDVI, temperature, and precipitation for different geographical regions from 1982 to 1998. All the trends are positive.

(a) NDVI

Region	Annual NDVI changes in the 17-year period		
	Absolute Value	R^2	*p* value
Northern high latitudes	0.043	0.69	0.00003
Northern middle latitudes	0.028	0.51	0.001
Tropics	0.020	0.21	0.07
Conterminous U.S.	0.036	0.71	0.00002
China	0.030	0.56	0.0006

(b) Temperature

Region	Annual temperature changes in the 17-year period		
	Absolute Value (ºC)	R^2	*p* value
Northern high latitudes	0.74	0.24	0.04
Northern middle latitudes	0.56	0.35	0.01
Tropics	0.48	0.41	0.006
Conterminous U.S.	0.63	0.19	0.08
China	0.87	0.46	0.003

(c) Precipitation

Region	Annual precipitation changes in the 17-year period		
	Absolute Value (mm)	R^2	*p* value
Northern high latitudes	14.58	0.12	0.17
Northern middle latitudes	16.44	0.02	0.59
Tropics	20.07	0.01	0.65
Conterminous U.S.	4.95	0.00	0.89
China	40.51	0.07	0.30

Table 2.2 Correlations between spatially averaged NDVI and spatially averaged annual mean temperature and correlations between spatially averaged NDVI and spatially averaged annual precipitation for different geographical regions from 1982 to 1998. All correlations except the correlation between NDVI and precipitation for the conterminous U.S. are positive.

Region	NDVI versus temperature		NDVI versus precipitation	
	R^2	*p* value	R^2	*p* value
Northern high latitudes	0.35	0.012	0.09	0.24
Northern middle latitudes	0.44	0.004	0.01	0.66
Tropics	0.14	0.14	0.20	0.07
Conterminous U.S.	0.29	0.027	0.01	0.77
China	0.42	0.005	0.09	0.23

2.4.1.3 Tropical regions

In the tropics, NDVI showed no significant trend from 1982 to 1998, although both annual mean temperature and annual precipitation increased during this period (table 2.1). Thus, there is no overall greening trend for the tropics as a whole over the 17-year period.

2.4.2 Spatial patterns of NDVI trends

Spatially averaging over large regions conceals the geographical variability of NDVI trends. Thus, I evaluated the spatial patterns of NDVI trends and climatic effects for all the vegetated pixels at a global scale. Fig. 2.2 shows areas where linear trends in NDVI are statistically significant ($p < 0.05$).

2.4.2.1 Northern high latitudes

In the northern high latitudes, 52.99% of the vegetated pixels exhibited significant increases in annual NDVI from 1982 to 1998 (Fig. 2.2 (a), table 2.3). The greening trend was observed over a broad contiguous swath of land from Alaska and Canada, and extending across the Eurasian land mass from Central Europe through Russia and northeastern China (Fig. 2.2 (a)).

The high-latitude greening pattern varied by season (Fig. 2.2 (b)-(e), table 2.3). In March-May, 24.61% of the vegetated pixels showed significant increases in NDVI, mainly in Alaska, western Europe, and much of Russia. In June-August, 33.67% of the vegetated pixels exhibited significant NDVI increases, primarily in northern U.S. and central Canada, Central Europe, and Russia. There were 21.96% and 29.73% of the vegetated pixels showing significant NDVI increases over September-November and

December-February, respectively. The greening trend over September-November and December-February was mainly observed in Canada, Europe, and Russia.

2.4.2.2 Northern middle latitudes

In the northern middle latitudes, 48.06% of the vegetated pixels showed significant increases in annual NDVI (Fig. 2.2 (a), table 2.3). The greening trend was observed mainly in the southeastern U.S., northern India, and southeastern China.

The greening pattern in the northern middle latitudes also varied by season (Fig. 2.2 (b)-(e), table 2.3). In the conterminous U.S., the greening trends over March-May, June-August, September-November, and December-February were observed in eastern, central, and northwestern U.S., respectively. In China, the percentages of the vegetated pixels that showed significant NDVI increases are 48.63% in March-May, 18.00% in June-August, 20.14% in September-November, and 16.55% in December-February.

2.4.2.3 Tropical regions

In the tropics, 32.84% of the vegetated pixels showed significant increases in annual NDVI (Fig. 2.2 (a), table 2.3). Spatially contiguous greening patterns were observed in tropical Africa, India, the north portion of South America, and Central America. Spatially fragmented greening patterns were observed in Southeast Asia.

In the southern middle and high latitudes, a greening trend was observed in the southernmost portion of South America, and southwestern Australia. Noticeably, a decreasing NDVI trend was observed in parts of southern Africa, South America (e.g., Argentina), and central Australia (Fig. 2.2 (a)-(e)).

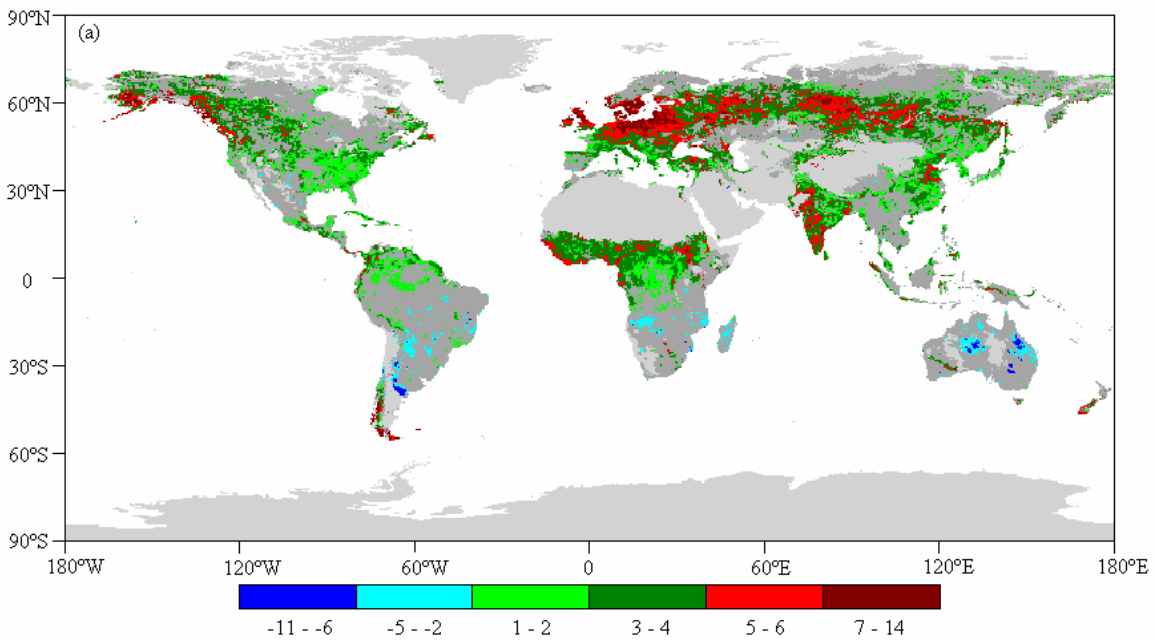
(a)
90°N
60°N
30°N
0
30°S
60°S
90°S
180°W
120°W
60°W
0
60°E
120°E
180°E
-11 - -6
-5 - -2
1 - 2
3 - 4
5 - 6
7 - 14

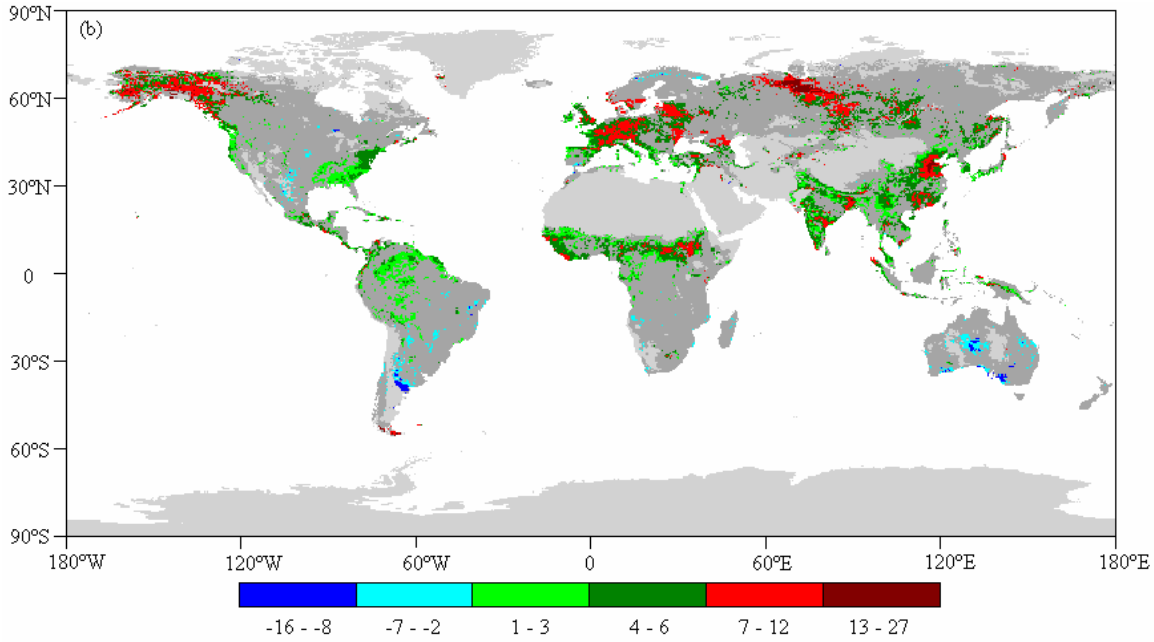
(b)
90°N
60°N
30°N
0
30°S
60°S
90°S
180°W
120°W
60°W
0
60°E
120°E
180°E
-16 - -8
-7 - -2
1 - 3
4 - 6
7 - 12
13 - 27

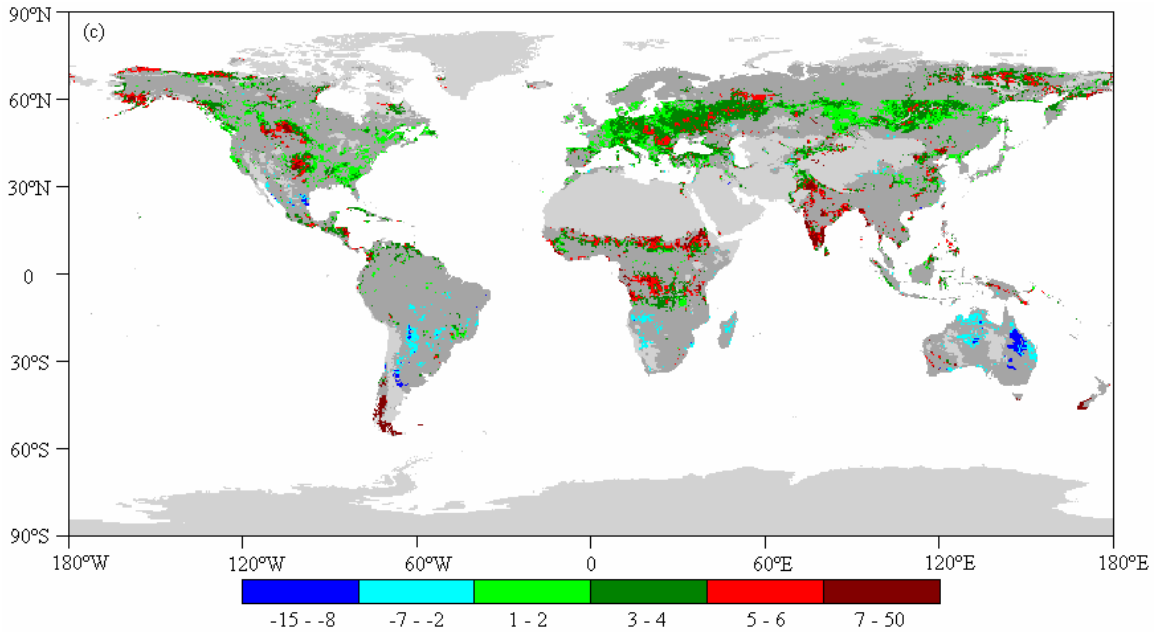
(c)
90°N
60°N
30°N
0
30°S
60°S
90°S
180°W
120°W
60°W
0
60°E
120°E
180°E
-15 - -8
-7 - -2
1 - 2
3 - 4
5 - 6
7 - 50

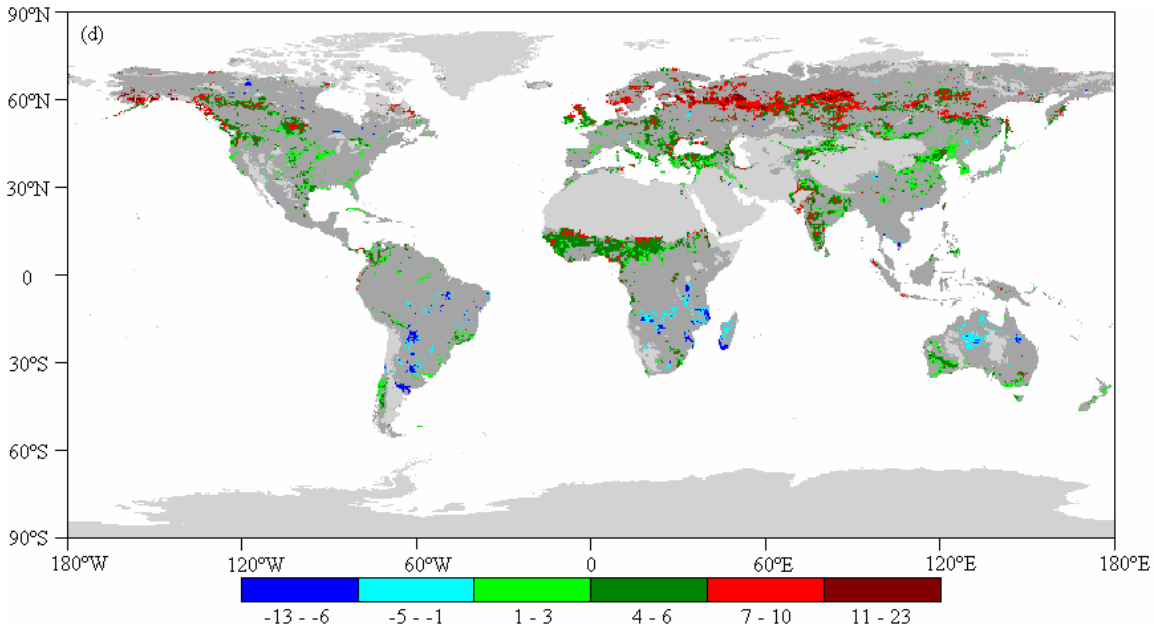
(d)
90°N
60°N
30°N
0
30°S
60°S
90°S
180°W
120°W
60°W
0
60°E
120°E
180°E
-13 - -6
-5 - -1
1 - 3
4 - 6
7 - 10
11 - 23

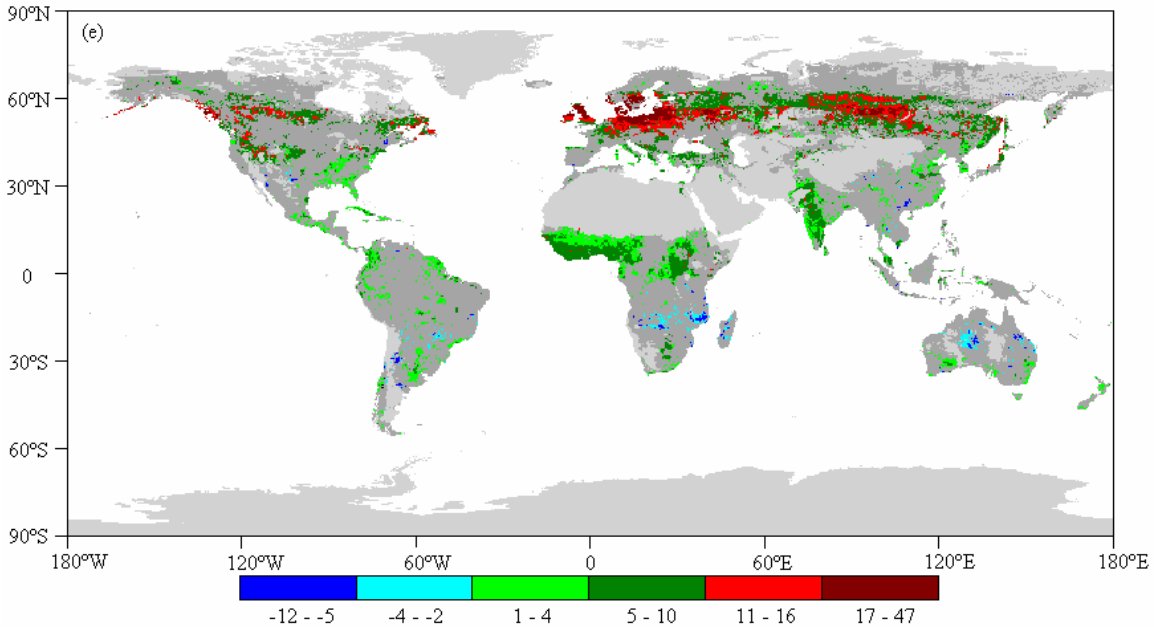

Fig. 2.2 Linear trends of NDVI that are statistically significant ($p < 0.05$) from 1982 to 1998 at both annual and seasonal scales pixel by pixel: (a) trends of annual NDVI averages; (b) trends of NDVI averages over spring (March-May); (c) trends of NDVI averages over summer (June-August); (d) trends of NDVI averages over autumn (September-November); (e) trends of NDVI averages over winter (December-February). The colored pixels represent those vegetated pixels with significant NDVI trends; the grayed pixels represent non-vegetated areas; the dark-grayed pixels represent those vegetated pixels without significant NDVI trends. The trends are given in percentages (%).

Table 2.3 Percentages of pixels with statistically significant ($p < 0.05$) linear trends of NDVI over all vegetated pixels for different geographical regions.

Region	Annual	March-May	June-August	September-November	December-February
Northern high latitudes	52.99	24.61	33.67	21.96	29.73
Northern middle latitudes	48.06	42.14	24.57	18.62	18.69
Tropics	32.84	23.48	17.05	12.57	20.13
Conterminous U.S.	51.67	31.07	27.83	15.45	20.30
China	53.39	48.63	18.00	20.14	16.55

2.4.3 Climatic correlates of NDVI trends

2.4.3.1 Northern high latitudes

In the northern high latitudes, 41.60% of the vegetated pixels with greening trends (Fig. 2.2 (a)) exhibited significant correlations between annual NDVI and annual mean temperature (Fig. 2.3 (a), table 2.4). These pixels are mainly distributed in Alaska, Canada, Europe, Russia, and northeastern China (Fig. 2.3 (a)). By contrast, only 6.44% of the vegetated pixels with greening trends (Fig. 2.2 (a)) showed significant correlations between annual NDVI and annual precipitation (Fig. 2.3 (b), table 2.5). These pixels are only observed in sparse areas in the northern high latitudes.

In the northern high latitudes, positive NDVI-temperature correlations are most prevalent over March-May (Fig. 2.3 (c), table 2.4). Positive NDVI-temperature correlations over September-November were only observed in Canada and eastern Russia (Fig. 2.3 (g)). Negative correlations between NDVI and spring precipitation were observed in western Canada and western Europe (Fig. 2.3 (d)).

2.4.3.2 Northern middle latitudes

In the northern middle latitudes, the positive correlations between annual NDVI averages and annual mean temperature are most prevalent in China (Fig. 2.3 (a), table 2.4). In contrast, the positive correlations between annual NDVI averages and annual precipitation were only observed in sparse areas in China (Fig. 2.3 (b), table 2.5). At the seasonal scale, the NDVI-temperature correlation was more prevalent over spring (Fig. 2.3 (c)) and winter (Fig. 2.3 (i)) than over summer (Fig. 2.3 (e)) and autumn (Fig. 2.3 (g), table 2.4).

NDVI-temperature and NDVI-precipitation correlations show spatially fragmented patterns in the conterminous U.S. (Fig. 2.3, tables 2.4-2.5). Positive NDVI-temperature correlations are mainly observed over March-May (Fig. 2.3 (c)) and winter (Fig. 2.3 (i)). Positive NDVI-precipitation correlations are most prevalent over September-November (Fig. 2.3 (h)).

Northern Mexico shows negative NDVI-temperature and positive NDVI-precipitation correlations (Fig. 2.3). However, no prevalent greening trend was observed in northern Mexico (Fig. 2.2). Thus, the effects of temperature and precipitation on vegetation activity may be self-canceling in northern Mexico.

2.4.3.3 Tropical regions

Positive correlations between annual NDVI averages and annual precipitation were observed in tropical Africa, and southern India, although the pattern is spatially fragmented (Fig. 2.3, tables 2.4-2.5). In tropical Africa, positive NDVI-precipitation correlations were primarily observed in the Sahel region (Fig. 2.3 (b)); positive NDVI-temperature correlations were observed in southern tropical Africa to the south of the Sahel (Fig. 2.3 (a)).

Decreasing trends of vegetation activity were observed in some regions in South America (e.g., Argentina), southern Africa, and Australia from 1982 to 1998 (Fig. 2.2). These regions show negative correlations between NDVI and temperature and positive correlations between NDVI and precipitation (Fig. 2.3).

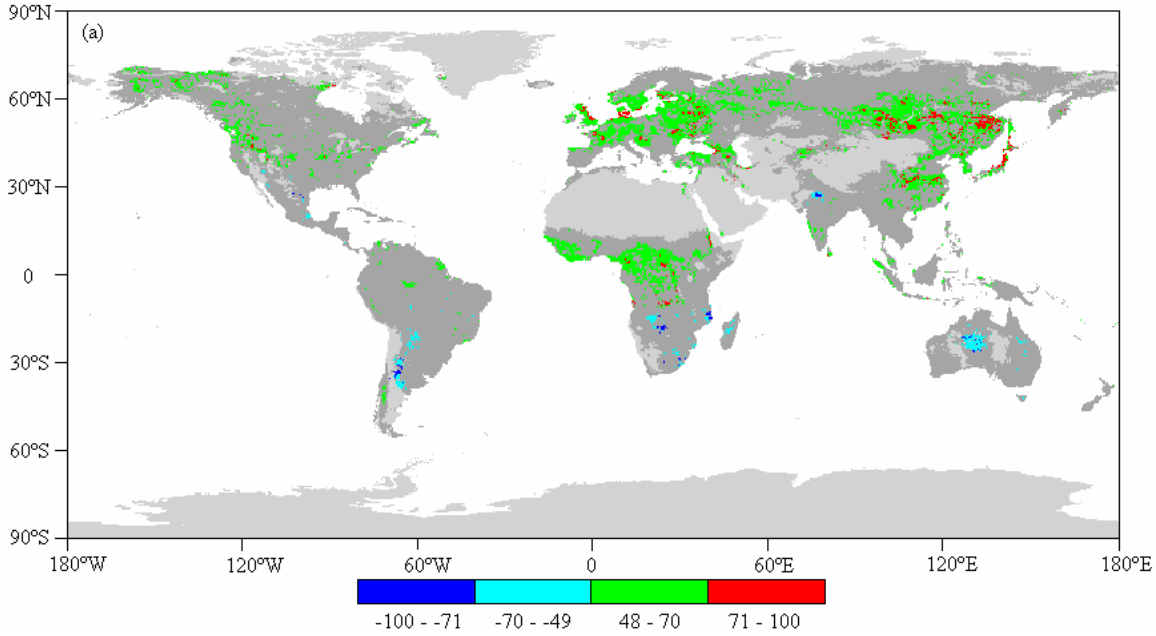
(a)
90°N
60°N
30°N
0
30°S
60°S
90°S
180°W
120°W
60°W
0
60°E
120°E
180°E
-100 - -71
-70 - -49
48 - 70
71 - 100

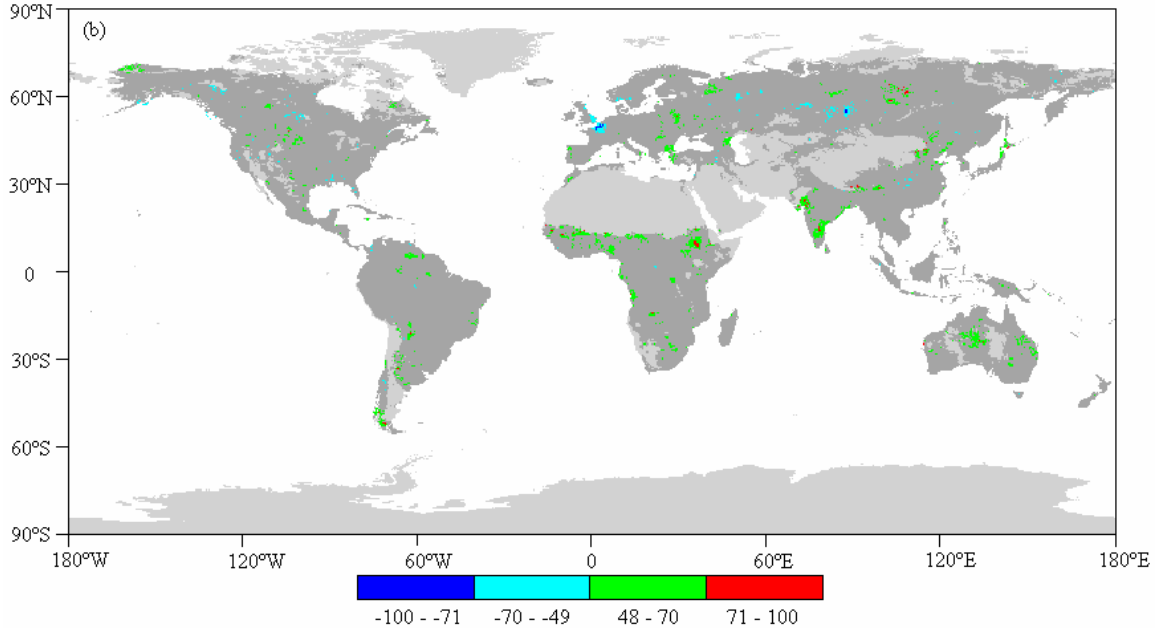
(b)
90°N
60°N
30°N
0
30°S
60°S
90°S
180°W
120°W
60°W
0
60°E
120°E
180°E
-100 - -71
-70 - -49
48 - 70
71 - 100

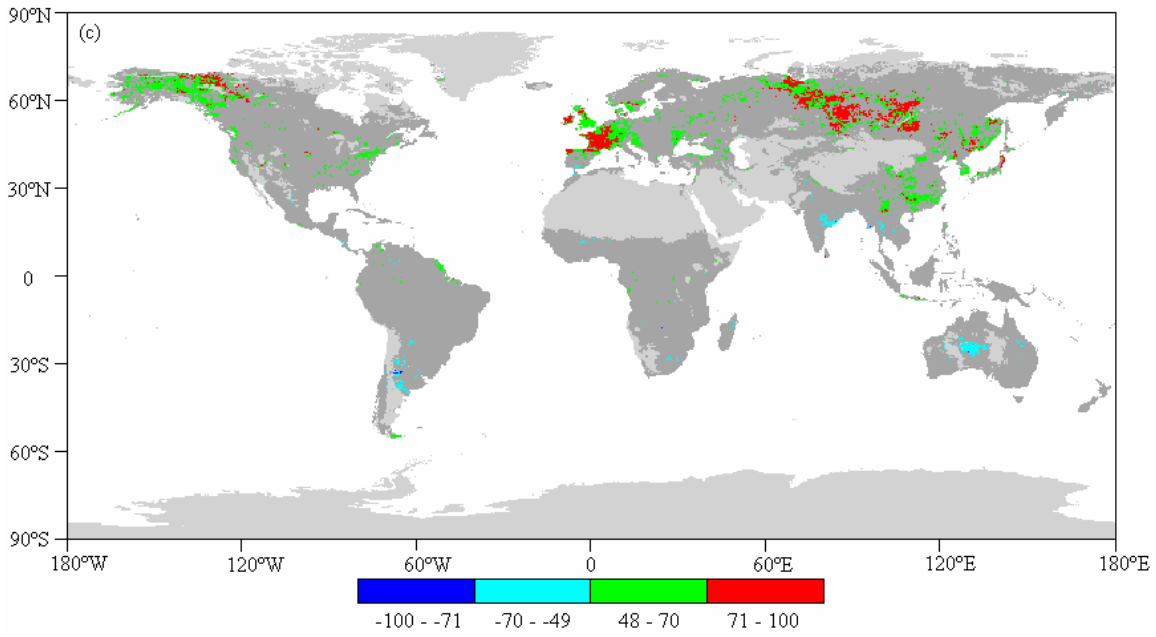
(c)
90°N
60°N
30°N
0
30°S
60°S
90°S
180°W
120°W
60°W
0
60°E
120°E
180°E
-100 - -71
-70 - -49
48 - 70
71 - 100

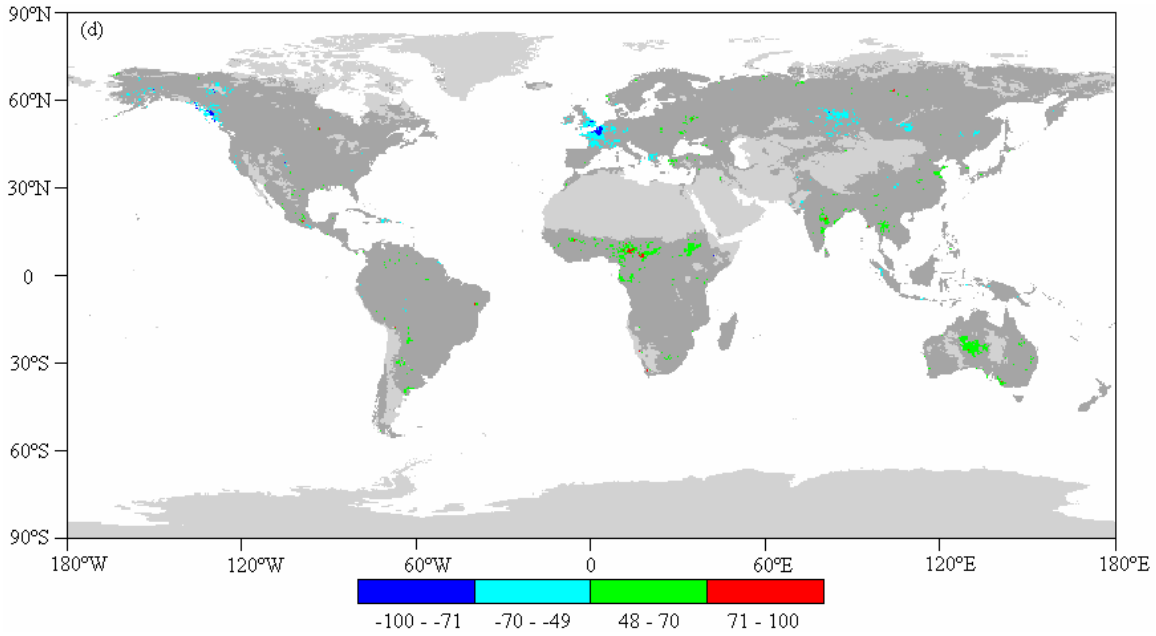
(d)
90°N
60°N
30°N
0
30°S
60°S
90°S
180°W
120°W
60°W
0
60°E
120°E
180°E
-100 - -71
-70 - -49
48 - 70
71 - 100

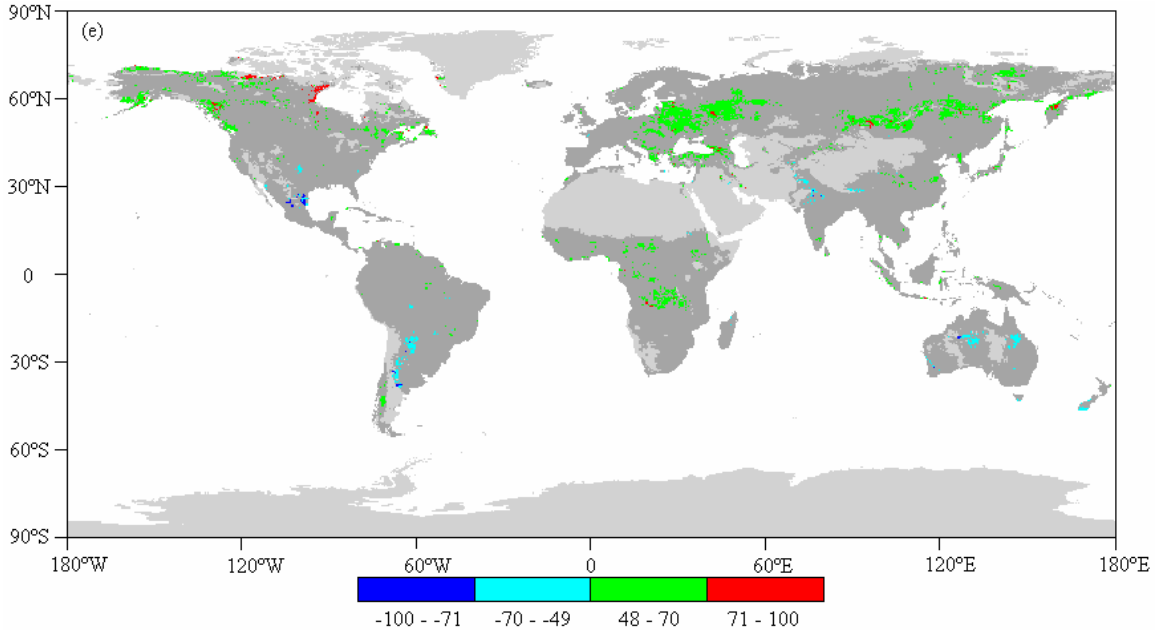
(e)
90°N
60°N
30°N
0
30°S
60°S
90°S
180°W
120°W
60°W
0
60°E
120°E
180°E
-100 - -71
-70 - -49
48 - 70
71 - 100

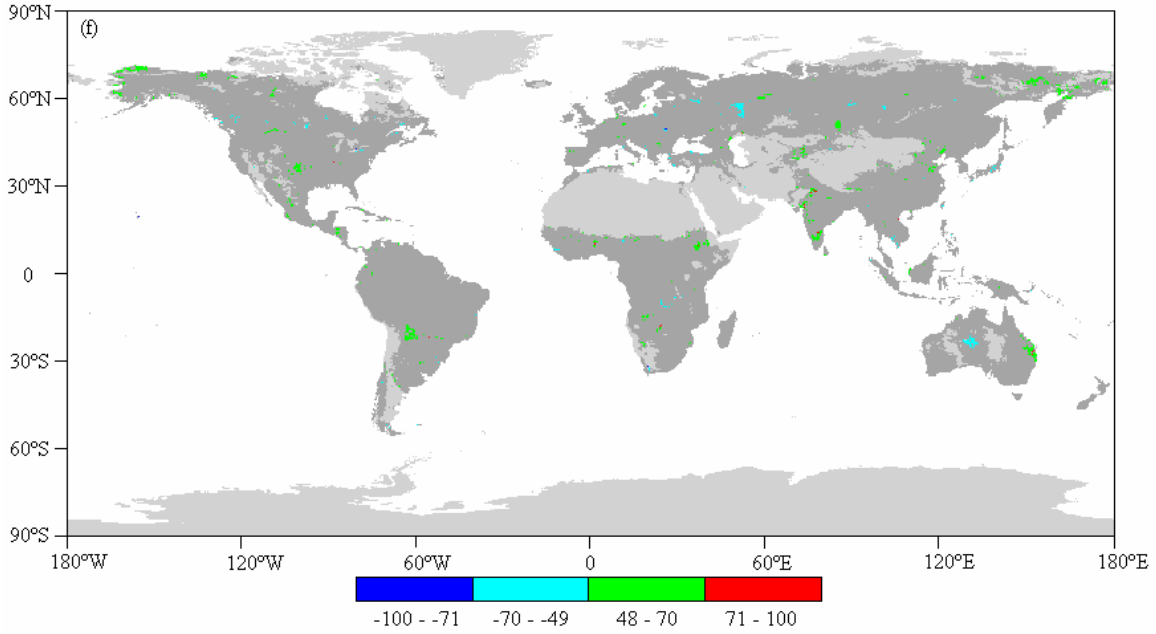
(f)
90°N
60°N
30°N
0
30°S
60°S
90°S
180°W
120°W
60°W
0
60°E
120°E
180°E
-100 - -71
-70 - -49
48 - 70
71 - 100

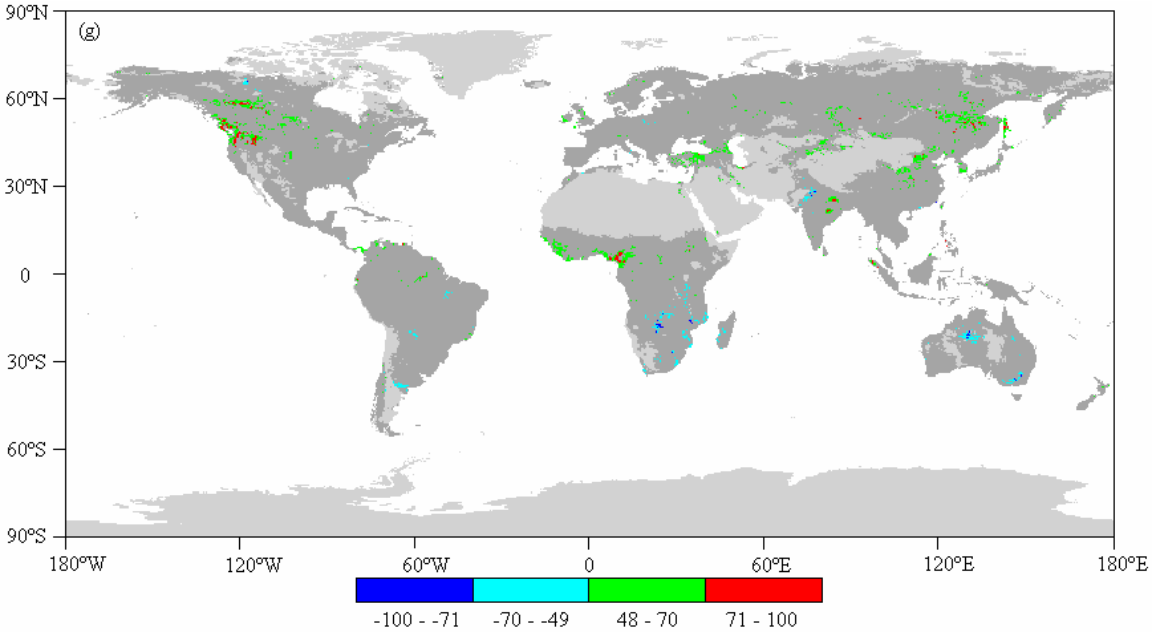
(g)
90°N
60°N
30°N
0
30°S
60°S
90°S
180°W
120°W
60°W
0
60°E
120°E
180°E
-100 - -71
-70 - -49
48 - 70
71 - 100

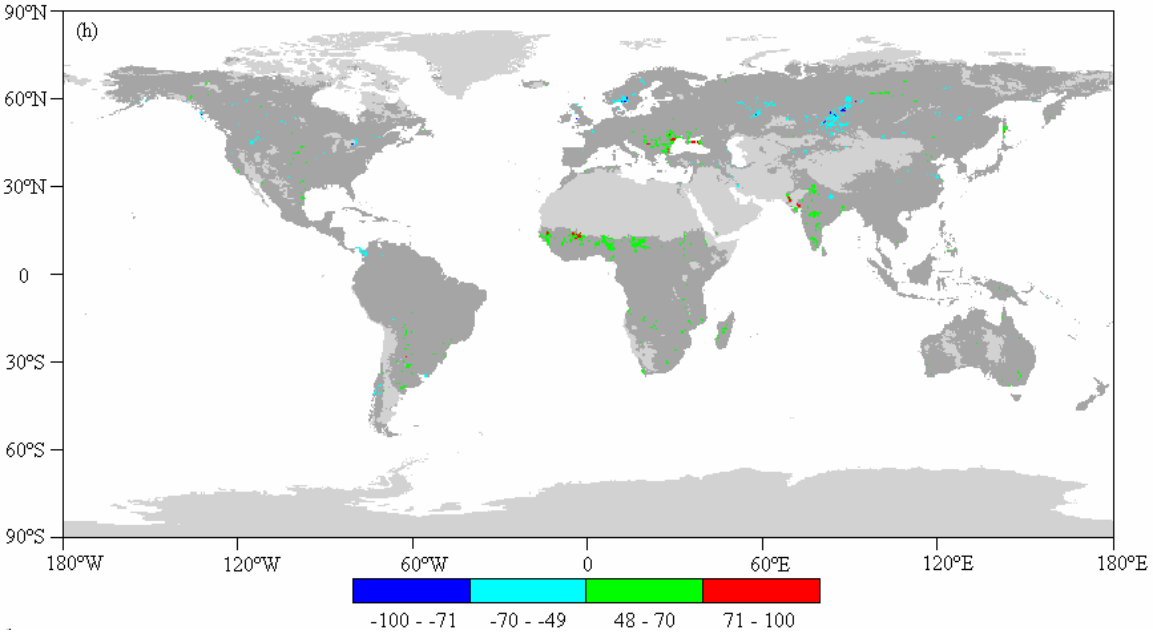
(h)
90°N
60°N
30°N
0
30°S
60°S
90°S
180°W
120°W
60°W
0
60°E
120°E
180°E
-100 - -71
-70 - -49
48 - 70
71 - 100

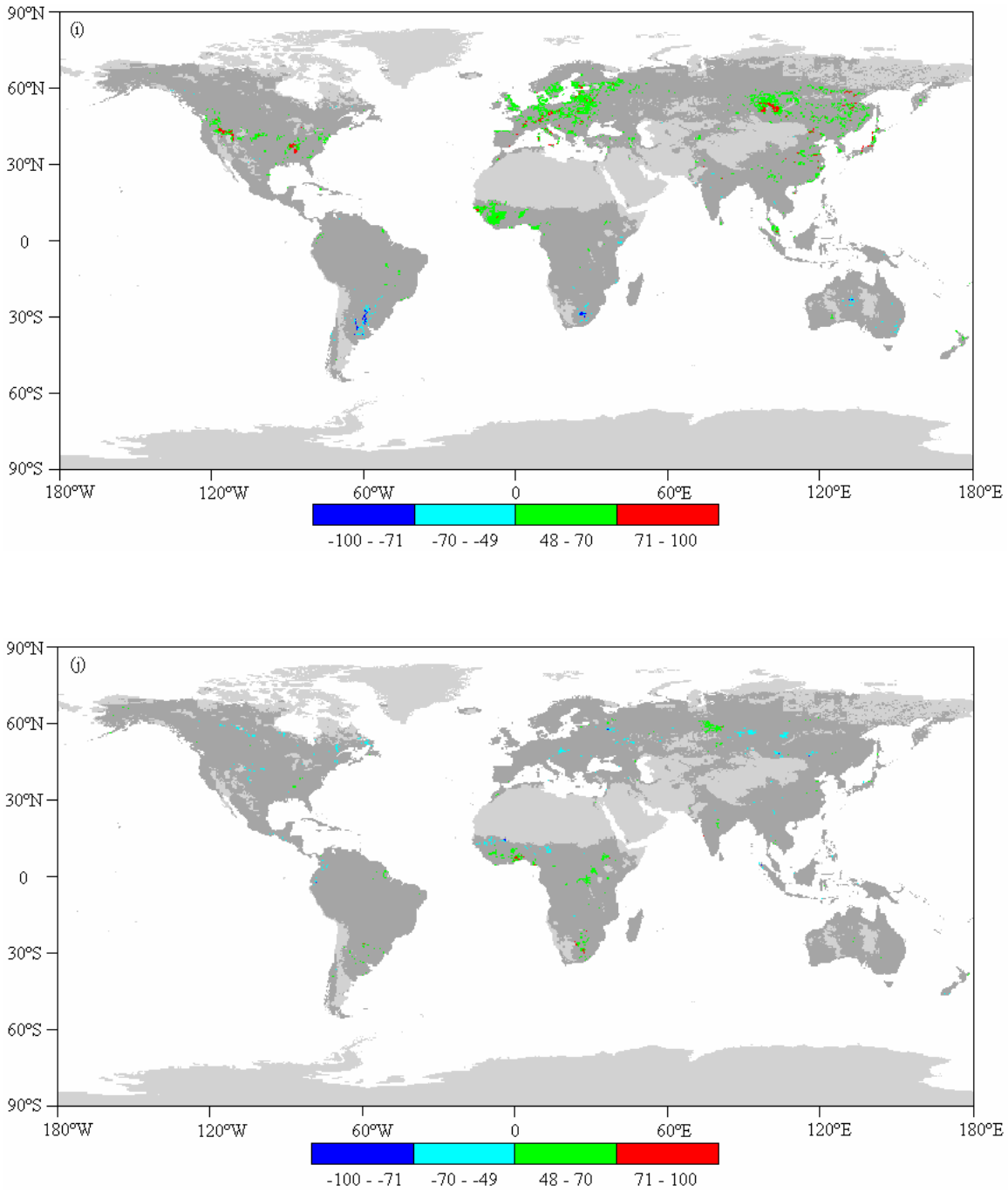

Fig. 2.3 Correlations between NDVI averages and temperature and correlations between NDVI averages and precipitation that are statistically significant ($p < 0.05$) from 1982 to 1998: (a) annual NDVI averages versus annual mean temperature; (b) annual NDVI averages versus annual precipitation; (c) NDVI averages versus temperature over March-May; (d) NDVI averages versus precipitation over spring (March-May); (e) NDVI averages versus temperature over summer (June-August); (f) NDVI averages versus precipitation over summer (June-August); (g) NDVI averages versus temperature over

autumn (September-November); (h) NDVI averages versus precipitation over autumn (September-November); (i) NDVI averages versus temperature over winter (December-February); (j) NDVI averages versus precipitation over winter (December-February). The colored pixels represent those pixels that have significant NDVI trends as well as significant NDVI-climate correlations; the grayed pixels represent non-vegetated areas; the dark-grayed pixels represent those vegetated pixels either with significant NDVI trends but no significant NDVI-climate correlations or with significant NDVI-climate correlations but no significant NDVI trends. The correlation coefficients are given in percentages (%).

Table 2.4 Percentages of pixels with statistically significant ($p < 0.05$) correlations between NDVI and temperature among vegetated pixels with a significant ($p < 0.05$) linear trends in NDVI for different geographical regions.

Region	Annual	March-May	June-August	September-November	December-February
Northern high latitudes	41.60	64.78	33.90	19.42	26.26
Northern middle latitudes	27.28	20.45	17.70	19.12	24.80
Tropic regions	31.06	7.94	17.76	21.83	11.68
Conterminous U.S.	21.57	34.82	16.13	21.10	30.42
China	54.58	40.02	15.64	26.96	46.99

Table 2.5 Percentages of pixels with statistically significant ($p < 0.05$) correlations between NDVI and precipitation among vegetated pixels with significant ($p < 0.05$) linear trends in NDVI for different geographical regions.

Region	Annual	March-May	June-August	September-November	December-February
Northern high latitudes	6.44	11.62	6.17	10.47	4.69
Northern middle latitudes	7.30	4.04	9.29	9.25	3.79
Tropic regions	14.12	15.67	9.30	15.84	8.48
Conterminous U.S.	6.37	6.89	10.34	7.09	3.82
China	8.71	3.65	10.99	3.44	4.40

2.5 Discussion

2.5.1 Northern high latitudes

Our results showed an overall greening trend from 1982 to 1998 for the northern high latitudes. The greening trend was distributed over a broad contiguous swath of land from Alaska and western Canada through central Europe to Russia and northeastern China. This greening pattern is roughly consistent with patterns reported elsewhere (Zhou et al. 2001, Tucker et al. 2001, Slayback et al. 2003).

Our results suggest that, compared with precipitation, temperature is a more important climatic correlate of the greening trend in the northern high latitudes and Western Europe between 1982 and 1998. In other studies that focused solely on high latitude greening trends, Zhou et al. (2001), Tucker et al. (2001), and Lucht et al. (2002) also argued that temperature is the leading climatic factor. Precipitation was assumed to play a minor role in increasing vegetation activity and was not fully considered by Zhou et al. (2001). Lucht et al. (2002) suggested that precipitation contributes only marginally to the greening trend. Our results support the assumption of Zhou et al. (2001) and the conclusion of Lucht et al. (2002).

Myneni et al. (1997) and Zhou et al. (2001) attributed the overall high-latitude greening trend to an advance of spring budburst and a delay of autumn leaf-fall. Our results suggest that, compared with autumn temperature, spring warming makes a greater contribution to the high-latitude greening trend than autumn temperature does, especially in Alaska.

2.5.2 Northern middle latitudes

Our results suggest that the northern middle latitudes (23.5°N-40°N) also exhibited an overall greening trend from 1982 to 1998. The greening trend was mainly observed in northeastern and southeastern North America, northern India, and China. The observed greening pattern is stronger and more contiguous than that shown by Kawabata et al. (2001) over a much shorter period (1982-1990). Our results suggest that the greening trend in the northern middle latitudes is partly due to temperature rises, as also suggested by Ichii et al. (2002).

Interestingly, the greening trends in eastern U.S. and much of India were not related to changes in either temperature or precipitation. The greening trend in these regions may be due to continuing forest regrowth following the abandonment of agricultural lands or plantations.

The greening pattern observed in the conterminous U.S. may suggest increasing carbon accumulation in U.S. forests. Nemani et al. (2002) suggested that precipitation is the leading climatic factor enhancing the terrestrial carbon sink in the conterminous U.S. By contrast, Caspersen et al. (2000) indicated that land-use change is the dominant factor controlling the rate of carbon accumulation in U.S. forests, with growth enhancement due to climate change, CO_2 fertilization, and N deposition only making minor contributions. Our results suggest that temperature makes a greater contribution to the increased vegetation activity in the conterminous U.S. than precipitation does (tables 2.4-2.5). Our results further suggest that climatic factors only explain a fraction of the greening trend in the conterminous U.S. Thus, the increased rate of carbon accumulation in U.S. forests

may be due to combined effect of forest regrowth and growth enhancement due to elevated temperature.

The greening trend in China is consistent with increasing vegetation activity suggested by Xiao and Moody (2004a) based on a satellite-derived LAI dataset and a gridded climate dataset. The prevalent greening pattern in China may suggest an increasing terrestrial carbon stock in vegetation biomass during the past two decades. This is consistent with the reported increase of carbon stock in forest biomass in China over this period (Goodale et al. 2002). Temperature makes a greater contribution to the increased vegetation activity than precipitation does. Moreover, the overall greening trend in China is mainly attributed to the greening in spring. These results suggest that the overall greening trend in China, as with the northern high latitudes, is partly brought about by earlier budburst due to spring warming.

However, the greening trend in China cannot be fully explained by elevated temperature or other climatic factors. The total forest coverage in China has increased from 5.2% in 1950 to 13.9% in 1995 primarily due to tree-planting projects (Liu 1996), although natural forest has declined to 30% of the total forest area due to extensive cutting of forests (Zhang et al. 1999). Thus, the greening pattern in China may result from land-use changes, such as afforestation and reforestation, and tree-growth enhancement due to temperature rises, especially in spring. Xiao and Moody (2004a) suggested that trends in agricultural practices, such as increased use of high-yield crops and application of chemical fertilizers, along with land-use changes such as afforestation and reforestation may have made a greater contribution to the greening trend than temperature.

2.5.3 Tropics

No greening trend was observed for the tropics as a whole from 1982 to 1998. This is not surprising, since the tropics provide a large carbon source due to extensive clearing of natural forests (Houghton et al. 2000). However, a greening trend was observed over large parts of the tropics, such as tropical Africa, India, the northern portion of South America, southern Mexico, and Indonesia. Nemani et al. (2003) suggested that the largest increase in NPP was in tropical ecosystems, Amazon rain forests in particular. They also showed increase in NPP in tropical Africa and other tropical areas. The greening pattern in tropical Africa shown by our analysis is generally consistent with the increase in NPP in this region suggested by Nemani et al. (2003).

Kawabata et al. (2001) suggested contiguous greening patterns in Southeast Asia for a short period (1982-1990). By contrast, our results suggest spatially-fragmented greening pattern in these regions from 1982-1998. The patchiness of the greening pattern may be associated with deforestation and forest regrowth after fires since forests account for a large fraction of the greenness in these regions (Fuller 1994). Ichii et al. (2002) suggested that tropical regions with NDVI increases such as central Africa did not exhibit significant NDVI-climate correlations, and attributed increased vegetation activity to CO_2 fertilization and N deposition. However, our results suggest positive correlations between NDVI and precipitation in the southern edge of Sahel, and positive correlations between NDVI and temperature for tropical Africa to the south of the Sahel. Thus, climate changes may also contribute to the increases in vegetation activity in tropical Africa.

The vegetation greening trend in parts of tropical Africa may suggest a regional terrestrial carbon sink, although tropical Africa as a whole is a large carbon source

primarily due to deforestation (Watson et al. 2000). Greening trends may be attributed to the combined effect of increased precipitation and elevated temperature. Precipitation may shift vegetation from grasses to shrubs and thus result in a larger fraction of woody component in this region (Fuller and Prince 1996). In addition to climatic effects, overgrazing by cattle may also shift vegetation from grasses to shrubs in the Sahelian region (Kerr 1998). CO_2 fertilization (Cao and Woodward 1998, Smith et al. 2000) and N deposition (Nadelhoffer et al. 1999) may also contribute to the increased vegetation activity in parts of tropical Africa.

Decreased vegetation activity was observed in some regions in southern South America, southern Africa, and Australia from 1982 to 1998. Ichii et al. (2002) suggested that NDVI decreases in these regions resulted from decreases in precipitation. However, our results suggest that the declined vegetation activity in these arid and semiarid regions may be due to combined effect of elevated temperature and decreased precipitation.

2.6 Conclusions

The results of this study document the geographic distribution of trends in vegetation greenness using a high quality long-term database. In areas that exhibited strongly significant trends, the correlation of these trends with changes in temperature and precipitation were evaluated. Our results suggest that:

1) Greening trends exhibit substantial latitudinal and longitudinal variability, with the strongest greening taking place in the northern high latitudes, much of the tropics, southeastern North America and eastern China.
2) Over large areas, these greening trends are strongly correlated with trends in temperature, especially in Europe, eastern Eurasia, and tropical Africa.

3) Precipitation does not appear to be a strong driver of increases in greenness, except for isolated and spatially fragmented regions.

4) Decreases in greenness occurred mainly in the southern hemisphere, in southern Africa, southern South America, and central Australia. These trends are strongly associated with both increases temperature and decreases in precipitation.

5) Vast regions of the globe, even in the northern high latitudes exhibit no trend in greenness.

6) Large areas that are undergoing strong greening trends show no associations with trends in temperature or precipitation.

Based on these results I conclude that, while greening trends are strong in many areas, these trends are only partially explained by climatic drivers. In large regions, other factors, such as CO_2 fertilization, reforestation, forest regrowth, woody plant proliferation, and trends in agricultural practices may be at play. Precipitation is generally not a significant driver of increasing greenness. Southern hemisphere decreases in greenness appear to be driven by changes in both temperature and precipitation, reflecting their joint control over soil water budgets.

2.7 Acknowledgements

The Version 3 Pathfinder NDVI data set was produced and kindly provided by Dr. Ranga B. Myneni at the Department of Geography, Boston University. This data set is available over the World Wide Web (http://cybele.bu.edu). The global monthly climatology data set was obtained from the Oak Ridge National Laboratory Distributed Active Archive Center (ORNL DAAC).

2.8 Chapter Synopsis

2.8.1 Background

Terrestrial vegetation plays an important role in the exchanges of C, water, and energy at the land surface (Hoffmann & Jackson 2000, Wu & Lynch 2000, Schimel et al. 2001). Changes in vegetation productivity at regional or larger scales have important implications for regulating the atmospheric CO_2 concentration and climate and affecting food production (Tans et al. 1990, Schimel et al. 1996). There is growing evidence that vegetation productivity has been increasing in the northern middle and high latitudes during the past two decades, suggesting that the earth has become greener due to natural factors and anthropogenic activities (Fan et al. 1998, Bousquet et al. 1999, Zhou et al. 2001, Goodale et al. 2002). This evidence has been obtained from analysis of atmospheric CO_2 data (Tans et al. 1990, Keeling et al. 1996), forest inventory data (Birdsey et al. 1993, Turner et al. 1995, Goodale et al. 2002), studies of land-use change (Houghton et al. 1999, Caspersen et al. 2000), ground-based phenological observations (Cayan et al. 2001, Fitter & Fitter 2002), analysis of satellite data (Myneni et al. 1997, 2001, Zhou et al. 2001), and simulations using biogeochemical models (Cao & Woodward 1998, Hicke et al. 2002, Lucht et al. 2002). Despite a number of studies on changes in vegetation productivity, the geographic distribution and patterns of the changes and their climatic correlates at the global scale are not well understood.

2.8.2 Synopsis

In Chapter 2, I presented a global-scale analysis of trends in vegetation productivity and their associations with climate variability over the period 1982-1998 using a recently developed satellite-derived NDVI data set (Nemani et al. 2003) in conjunction with a

gridded global climate data set (New et al. 2000). The NDVI was used as a proxy for vegetation productivity.

Vegetation productivity significantly increased in the northern high latitudes, the northern middle latitudes, and subtropical Asia. Temperature, and, in particular spring warming, was the primary climatic factor associated with greening in the northern high latitudes and Western Europe. Temperature trends also explained greening in the U.S. Pacific Northwest, tropical and subtropical Africa, and eastern China. Precipitation was a strong correlate of greening in fragmented regions only. Decreases in greenness in southern South America, southern Africa, and central Australia were strongly correlated to both increases in temperature and decreases in precipitation.

Over vast areas globally, strong positive trends in greenness exhibited no correlation with trends in either temperature or precipitation. These areas include the eastern United States, much of the African tropics and subtropics, most of the Indian subcontinent, and Southeast Asia. Thus, for large areas of land that are undergoing greening, there appears to be no climatic correlate. Globally, greening trends are a function of both climatic and non-climatic factors, such as forest regrowth, CO_2 enrichment, woody plant proliferation, and trends in agricultural practices.

2.8.3 Limitations

In this study I used NDVI as a proxy for vegetation productivity. The NDVI data came from the Version 3 Pathfinder NDVI data set (V3P-NDVI), which is probably the best long-term NDVI data set available. This NDVI data set was developed by Dr. Ranga B. Myneni's Climate and Vegetation Group, Boston University, and was referred to by Nemani et al. (2003). The V3P-NDVI has been subject to a series of corrections, and thus

the noise associated with residual atmospheric effects, orbital drift effects, intersensor variations, and stratospheric aerosol effects have been further reduced (Nemani et al. 2003). However, there is still residual noise remaining in the data, which may lead to uncertainties in the magnitudes of NDVI trends. I thus emphasize the statistically significant trends of NDVI rather than interpreting the magnitudes of changes in NDVI.

NDVI is sensitive to soil background reflectance in sparsely vegetated areas (Elvidge & Lyon 1985, Huete et al. 1985), and thus tends to exhibit a weak response to variation in plant productivity in arid and semiarid regions. NDVI also saturates in response to dense leaf canopies, e.g., the humid tropical forests and old growth forests (Myneni et al. 2001). Thus, the changes in NDVI may not well reflect small changes in vegetation productivity in very low or very high productivity regions.

The analysis of trends in NDVI could help identify the location of C sinks/sources. However, note that NDVI, while a reasonable proxy for photosynthetic activity or NPP of green vegetation, is not a good indicator for net ecosystem productivity (NEP). Thus, increases in vegetation productivity inferred from NDVI data indicate increases in photosynthetic activity or NPP, and do not necessarily indicate increases in NEP or increases in C stocks in ecosystems. For example, elevated temperature (Larcher 1983) and increased precipitation (Nemani et al. 2002) can increase NPP by lengthening the growing season and enhancing photosynthesis. At the same time, however, elevated temperatures can accelerate rates of plant and microbial respiration resulting in the release of C back into the atmosphere (Billings et al. 1984, Gorham 199, Woodwell & Mackenzie 1995, Houghton et al. 1998). Thus, my work does not directly address trends in carbon stocks in ecosystems, but only trends in vegetation productivity (GPP or NPP).

2.8.4 Future directions

The future characterization of increases in vegetation productivity at the global scale should be approached by combining multiple techniques and data sets including remote sensing, biogeochemical models, and a variety of ground-based measurements (e.g., flux tower measurements, forest inventory data, and field measurements).

Biogeochemical models have been widely used to simulate the changes in NPP and NEP in response to climate change and CO_2 enrichment at regional, continental or global scales (e.g., Cao & Woodward 1998, Hicke et al. 2002). However, most biogeochemical models are based on fixed parameterization of land use/land cover, and do not incorporate changes in land use and land cover in the simulations due to either the unavailability of time series of land use/land cover maps and/or the limitations of the models. Biogeochemical models are usually run at decadal scales. Substantial changes in land use/land cover may have occurred during the simulation period, including afforestation and reforestation, deforestation, selective logging, fire disturbances, and shifts of life forms.

Long-term NDVI data can be used to identify regions with changes in vegetation productivity as a starting point. Satellite data such as Landsat, ASTER, and IKONOS can be used to identify and monitor changes in land use/land cover. Ecosystems that are subject to substantial changes in land use/land cover may be separated from ecosystems that are not subject to changes in land use/land cover. For ecosystems without changes in land use/land cover, vegetation productivity (GPP, NPP, and NEP) can be simulated using biogeochemical models. Forest inventory data, biogeochemical models, and bookkeeping models can used to assess the changes in vegetation productivity in regions

experiencing deforestation, afforestation and reforestation. Dynamic global vegetation models (DGVMs) such as MC1 (Bachelet et al. 2001) and LPJ (Sitch et al. 2003) can be used to simulate the impacts of global climate change and fire disturbances on the distribution of vegetation and the associated changes in vegetation productivity and carbon fluxes.

The eddy covariance technique has emerged as an effective and popular way to assess ecosystem carbon exchange (Running et al. 1999, Baldocchi 2003). NEE measurements from the eddy flux tower network, FLUXNET (e.g., Ameriflux), can be used to calibrate and validate the estimates of GPP and NEP derived from biogeochemical models. On the other hand, biogeochemical models can help scale carbon fluxes measured from flux towers to the continental and global scales (Running et al. 1999).

The characterization of increases in vegetation productivity and the resulting C uptake in ecosystems at the global scale needs further collaboration among disciplines such as remote sensing, biogeochemistry, ecological modeling, and forestry. Multidisciplinary studies on the basis of satellite data, biogeochemical models, and ground-based measurements (e.g., LTER, FLUXNET, and forest inventory data) may lead to a better understanding of the increases in vegetation productivity and the associated changes in carbon fluxes at regional or global scales.

2.9 References

Asrar, G., Fuchs, M., Kanemasu, E.T., and Hatfield, J.L., 1984, Estimating of absorbed photosynthetic radiation and leaf area index from spectral reflecetance in wheat. *Agronomy Journal* **76**, 300-306.

Bachelet, D., Lenihan, J.M., Daly, C., Neilson, R.P., Ojima, D.S., & Parton, W.J., 2001. MC1: a dynamic vegetation model for estimating the distribution of vegetation and associated carbon, nutrients, and water—technical documentation. Version 1.0. Gen. Tech. Rep. PNW-GTR-508. Portland, OR: U.S. Department of Agriculture, Forest Service, Pacific Northwest Research Station. 95 p.

Baldocchi, D.D., 2003. Assessing the eddy covariance techniques for evaluating carbon dioxide exchange rates of ecosystems: past, present, and future. *Global Change Biology*, **9**, 479-492.

Billings, W.D., Peterson, K.M., Luken, J.O., & Mortensen, D.A., 1984. Interaction of increasing atmosphere carbon-dioxide and soil-nitrogen on the carbon balance of Tundra microcosms. *Oecologia*, **65**, 26-29.

Bogaert, J., Zhou, L., Tucker, C.J., Myneni, R.B., and Ceulemans, R., 2002, Evidence for a persistent and extensive greening trend in Eurasia inferred from satellite vegetation index data. *Journal of Geophysical Research,* **107**, art. no. 4119.

Cao, M., and Woodward, F.I., 1998, Dynamic responses of terrestrial ecosystem carbon cycling to global climate change. *Nature,* **393**, 249-252.

Caspersen, J.P., Pacala, S.W., Jenkins, J.C., Hurtt, G.C., Moorcroft, P.R., and Birdsey, R.A., 2000, Contributions of land-use history to carbon accumulation in U.S. forests. *Science,* **290**, 1148-1151.

Cayan, R.C., Kammerdiener, S.A., Dettinger, M.D., Caprio, J.M., and Peterson, D.H., 2001, Changes in the onset of spring in the western United States. *Bulletin of the American Meteorological Society,* **82**, 399-415.

Colombo, S.J., 1998, Climatic warming and its effect on bud burst and risk of frost damage to white spruce in Canada. *Forestry Chronicle*,**74**, 567-577.

Doherty, R.M., Hulme, M., and Jones, C.G., 1999, A gridded reconstruction of land and ocean precipitation for the extended Tropics from 1974-1994. *International Journal of Climatology,* **19**, 119-142.

Elvidge, C. D., & Lyon, R. J. P. (1985). Influence of rock soil spectral variation on the assessment of green biomass. *Remote Sensing of Environment*, **17**, 265– 279.

Fan, S., Gloor, M., Mahlman, J., Pacala, S., Sarmiento, J., Takahashi, T., and Tans, P., 1998, A large terrestrial carbon sink in North America implied by atmospheric and oceanic carbon dioxide data and modes. *Science,* **282**, 442-446.

Fitter, A.H., and Fitter, R.S.R., 2002, Rapid changes in flowering time in British plants. *Science,* **296**, 1689.

Fuller, D.O., 1994, *Foliar phenology of savanna vegetation in South-Central Africa and its relevance to climatic change*, Ph.D. dissertation, College Park, University of Maryland, Maryland.

Fuller, D.O., and Prince, S.D., 1996, Rainfall and foliar dynamics in tropical southern Africa: potential impacts of global climatic change on savanna vegetation. *Climatic Change,* **33**, 69-96.

Goodale, C.L., Apps, M.J., Birdsey, R.A., Field, C.B., Heath, L.S., Houghton, R.A., Jenkins, J.C., Kohlmaier, G.H., Kurz, W., Liu, S., Nabuurs, G.-J., Nilsson, S., and Shvidenko, A.Z., 2002, Forest carbon sinks in the northern hemisphere. *Ecological Applications*, **12**, 891-899.

Gorham, E., 1991. Northern peatlands - role in the carbon-cycle and probable responses to climatic warming. *Ecological Applications*, **1**, 182-195.

Goulden, M.L., Munger, J.W., Fan, S.M., Daube, B.C., and Wofsy, S.C., 1996, Exchange of carbon dioxide by a deciduous forest: response to interannual climate variability. *Science,* **271**, 1576-1578.

Hansen, J., Ruedy, R., Glascoe, J., and Sato, M., 1999, GISS analysis of surface temperature change. *Journal of Geophysical Research,* **104**, 30997-31022.

Hicke, J.A., Asner, G.P., Randerson, J.T., Tucker, C., Los, S. et al., 2002. Satellite-derived increases in net primary productivity across North America, 1982-1998. *Geophysical Research Letters*, **29**, 1427, 10.1029/2001GL013578.

Hoffmann, W.A., & Jackson, R.B., 2000. Vegetation-climate feedbacks in the conversion of tropical savanna to grassland. *Journal of Climate*, **13**, 1593-1602.

Houghton, R.A., Davidson, E.A., & Woodwell, G.M., 1998. Missing sinks, feedbacks, and understanding the role of terrestrial ecosystems in the global carbon balance. *Global Biogeochemical Cycles*, **12**, 25-34.

Houghton, R.A., Skole, D.L., Nobre, C.A., Hackler, J.L., Lawrence, K.T., and Chomentowski, W.H., 2000, Annual fluxes of carbon from deforestation and regrowth in the Brazilian Amazon. *Nature,* **403**, 301-304.

Huete, A. R., Jackson, R. D., & Post, D. F. (1985). Spectral response of a plant canopy with different soil backgrounds. *Remote Sensing of Environment*, **17**, 37– 53.

Hulme, M., Osborn, T.J., and Johns, T.C., 1998, Precipitation sensitivity to global warming: Comparison of observations with HadCM2 simulations. *Geophysical Research Letters,* **25**, 3379-3382.

Ichii, K., Kawabata, A., and Yamaguchi, Y., 2002, Global correlation analysis for NDVI and climatic variables and NDVI trends: 1982-1990. *International Journal of Remote Sensing*, **23**, 3873-3878.

James, M.E., and Kalluri, S.N.V., 1994, The Pathfinder AVHRR land data set: An improved coarse-resolution data set for terrestrial monitoring. *International Journal of Remote Sensing,* **15**, 3347-3364.

Jones, P.D., and Hulme, M., 1996, Calculating regional climatic time series for temperature and precipitation: methods and illustrations. *International Journal of Climatology,* **16**, 361-377.

Karl, T.R., and Knight, R.W., 1998, Secular trends of precipitation amount, frequency, and intensity in the USA. *Bulletin of the American Meteorological Society,* **79**, 231-241.

Kaufmann, R.K., Zhou, L., Knyazikhin, Y., Shabanov, N.V., Myneni, R.B., and Tucker C.J., 2000, Effect of orbital drift and sensor changes on the time series of AVHRR vegetation index data. *IEEE Transactions on Geoscience and Remote Sensing,* 38: 2584-2597.

Kawabata, A., Ichii, K., and Yamaguchi, Y., 2001, Global monitoring of interannual changes in vegetation activities using NDVI and its relationships to temperature and precipitation. *International Journal of Remote Sensing,* **22**, 1377-1382.

Keeling, C.D., Chin, J.F.S., and Whorf, T.P., 1996, Increased activity of northern vegetation inferred from atmospheric CO_2 measurements. *Nature,* **382**, 146-149.

Kerr, R.A., 1998, The Sahara is not marching southward. *Science,* **281**, 633-634.

Larcher, W., Physiological and Plant Ecology. 2nd ed., Springer-Verlag, New York, 1983.

Liu, J., A Macro Inventory of China's Environments and Resources and Their Dynamics (China's Scientific Publication House, Beijing, 1996), p. 353 (in Chinese).

Lucht, W., Prentice, I.C., Myneni, R.B., Sitch, S., Friedlingstein, P. et al., Cramer, W., Bousquet, P., Buermann, W., and Smith, B., 2002, Climatic control of the high-latitude vegetation greening trend and Pinatubo effect. *Science,* **296**, 1687-1689.

Mekis, E., and Hogg, W.D., 1999, Rehabilitation and analysis of Canadian daily precipitation time series. *Atmosphere,* **37**, 53-85.

Melillo, J.M., McGuire, A.D., Kicklighter, D.W., Moore, B., Vorosmarty, C.J., and Schloss, A.L., 1993, Global climate change and terrestrial net primary production. *Nature,* **363**, 234-240.

Myneni, R.B., Hall, F.G., Sellers, P.J., and Marshak, A.L., 1995, The interpretation of spectral vegetation indexes. *IEEE Transations on Geoscience and Remote Sensing,* **33**, 481-486.

Myneni, R.B., Keeling, C.D., Tucker, C.J., Asrar, G., and Nemani, R.R., 1997, Increased plant growth in the northern high latitudes from 1981 to 1991. *Nature* **386**, 698-702.

Myneni, R.B., Tucker, C.J., Asrar, G., and Keeling, C.D., 1998, Interannual variations in satellite-sensed vegetation index data from 1981 to 1991. *Journal of Geophysical Research,* **103**, 6145-6160.

Myneni, R.B., Dong, J., Tucker, C.J., Kaufmann, R.K., Kauppi, P.E., et al., 2001, A large carbon sink in the woody biomass of northern forests. *Proceedings of the National Academy of Sciences of the United States of America* **98**, 14784-14789.

Nadelhoffer, K.J., Emmett, B.A., Gundersen, P., KjØnaas, O.J, Koopmans, C.J. et al., 1999, Nitrogen deposition makes a minor contribution to carbon sequestration in temperate forests. *Nature,* **398**, 145-148.

Nemani, R., White, M., Thornton, P., Nishida, K., Reddy, S., Jenkins, J., and Running, S., 2002, Recent trends in hydrologic balance have enhanced the terrestrial carbon sink in the United States. *Geophysical Research Letters,* **29**, 10.1029/2002GL014867.

Nemani, R. R., Keeling, C. D., Hashimoto, H., Jolly, W. M., Piper, S.D., Tucker, C.J., Myneni, R.B., & Running, S.W., 2003, Climate-driven increases in global terrestrial net primary production from 1982 to 1999. *Science*, **300**, 1560-1563.

New, M., Hulme, M., and Jones, P.D., 2000, Global Monthly Climatology for the Twentieth Century (New et al.). Data set. Available on-line (http://www.daac.ornl.gov) from Oak Ridge National Laboratory Distributed Active Archive Center, Oak Ridge, Tennessee, U.S.A.

Pacala, S.W., Hurtt, G.C., Baker, D., Peylin, P., Houghton, R.A. et al., 2001. Consistent land- and atmosphere-based U.S. carbon sink estimates. *Science*, **292**, 2316-2320.

Randserson, J.T., Field, C.B., Fung, I.Y., and Tans, P.P., 1999, Increases in early season ecosystem uptake explain recent changes in the seasonal cycle of atmospheric CO2 at high northern latitudes. *Geophysical Research Letters,* **26**, 2765-2769.

Running, S.W., Baldocchi, D.D., Turner, D.P., Gower, S.T., Bakwin, P.S. & Hibbard, K.A., 1999. A global terrestrial monitoring network integrating tower fluxes, flask sampling, ecosystem modeling and EOS satellite data. *Remote Sensing of Environment*, **70**, 108-127.

Schimel, D.S., Alves, D., Enting, I., Himann, M., Joos, F., Raynaud, D., and Wigley, T., 1996, CO2 and the carbon cycle, in *Climate Change 1995: The Science of Climate Change*, edited by J. T. Houghton et al., pp. 76-86, Cambridge University Press, New York, 1996.

Schimel, D.S., House, J.I., Hibbard, K.A., Bousquet, P., Ciais, P. et al., 2001, Recent patterns and mechanisms of carbon exchange by terrestrial ecosystems. *Nature,* **414**, 169-172.

Sitch, S., et al., Evaluation of ecosystem dynamics, plant geography and terrestrial carbon cycling in the LPJ Dynamic Global Vegetation Model. *Global Change Biology*, **9**, 161-185.

Slayback, D.A., Pinzon, J.E., Los, S.O., and Tucker, C.J., 2003, Northern hemisphere photosynthetic trends 1982-99. *Global Change Biology,* **9**, 1-15.

Smith, S.D., Huxman, T.E., Zitzer, S.F., charlet, t.n., housman, d.c., coleman, J.S., Fenstermaker, L.K., Seemann, J.R., and Howak, R.S., 2000, Elevated CO_2 increases productivity and invasive species success in an arid ecosystem. *Nature,* **408**, 79-82.

Tans, P.P., Fung, I.Y., and Takahashi, T., 1990, Observation constraints on the global atmospheric CO2 budget. *Science,* **247**, 1431-1438.

Tucker, C.J., Fung, I.Y., Keeling, C.D., and Gammon, R.H., 1986, Relationship between atmospheric CO_2 variations and a satellite-derived vegetation index. *Nature,* **319**, 195-199.

Tucker, C.J., Slayback, D.A., Pinzon, J.E., Los, S.O., Myneni, R.B., and Taylor, M.G., 2001, Higher northern latitude normalized difference vegetation index and growing season trends from 1982 to 1999. *International Journal of Biometeorology,* **45**, 184-190.

Watson, R.T., Noble, I.R., Bolin, B., Ravindranath, N.H., Verardo, D.J., and Dokken, D.J., 2000, *Land Use, Land Use Change and Forestry*. Cambridge Univ. Press, Cambridge.

Woodwell, G.M., & Mackenzie, F.T., Biotic Feedbacks in the Global Climatic System, 416 pp., Oxford Univ. Press, New York, 1995.

Wu, W., & Lynch, A.H., 2000. Response of the seasonal carbon cycle in high latitudes to climate anomalies. *Journal of Geophysical Research*, **105**, 22897-22908.

Xiao, J., and Moody, A., 2004a, Trends in vegetation activity and their climatic correlates: China 1982 to 1998. *International Journal of Remote Sensing*, In Press.

Xiao, J., and Moody, A., 2004b, Photosynthetic activity of US biomes: responses to the spatial variability and seasonality of precipitation and temperature. *Global Change Biology*, **10**, 437-451.

Zhai, P.M., Sun, A., Ren, F., Liu, X., Gao, B., and Zhang, Q., 1999, Changes of climate extremes in China. *Climatic Change,* **42**, 203-218.

Zhang, P. Zhou, X., Wang, F., Introduction to Natural Forest Conservation Program (China's Forestry Publishing House, Beijing, 1999), p. 388 (in Chinese).

Zhou, L., Tucker, C.J., Kaufmann, R.K., Slayback, D., Shabanov, N.V., and Myneni, R.B., 2001, Variations in northern vegetation activity inferred from satellite data of vegetation index during 1981 to 1999. *Journal of Geophysical Research,* **106**, 20069-20083.

Chapter 3

Photosynthetic activity of U.S. biomes: Responses to precipitation and temperature

3.1 Introduction

There is strong evidence of directional trends in temperature and precipitation at regional and global scales (IPCC 1996; IPCC 2001; Hulme and Viner 1998). Moreover, changes in temperature and precipitation dynamics, largely through their control over water balance and growing-season length, have been identified as probable drivers of change in terrestrial productivity (Woodward 1987; Myneni et al. 1997; Wang et al. 2001; Nemani et al. 2002) and in the distribution of vegetation functional types (Neilson 1986; Brown et al. 1997; Allen and Breshears 1998). Thus, regional- to global-scale changes in climate patterns could have substantial consequences for terrestrial productivity and carbon dynamics (IPCC 1996; Jackson et al. 2002;).

Spatial variation in productivity, both within and across biomes, derives from gradients in moisture, temperature, and energy that occur within, or cross over limits defining the suitability range for given biomes. Given that such climatic limits interact seasonally, and are often keyed to certain phenological stages, I can expect that the seasonality of climate changes will play a significant role in determining ecosystem

response (Neilson 1986; White et al. 2000; Nemani et al. 2002) and these responses will differ by biome type (VEMAP Members 1995; Kramer et al. 2000).

Large-scale, empirical studies of vegetation/climate coupling have often concentrated on associations between productivity and climate through time, either at specific locations, or averaged over regions (e.g. Le Houerou et al. 1988; Goward and Prince 1995; Los et al. 2001; Myneni et al. 1997; Sala et al. 1988). For example, positive associations have been found between year-to-year changes in precipitation and both NDVI (Paruelo and Lauenroth 1998; Kawabata et al. 2001) and ANPP (Le Houerou et al. 1988) in arid and semi-arid ecosystems.

The seasonality of precipitation, an important determinant of soil-water budgets (Dingman 1994) has also been shown to influence productivity through interaction with the physiology, physiognomy, or life-history of different vegetation types (Stephenson 1990; Shinoda 1995; Richard and Poccard 1998; Kramer et al. 2000). For example, Epstein et al. (1999) reported that field-measured ANPP is related to the seasonality of precipitation for shrublands and grasslands. This finding is consistent with other work illustrating the role of the annual course of water-balance in structuring the geographic distribution of major vegetation formations (Walter 1971; Neilson et al. 1992; Prentice et al. 1992; Paruelo and Lauenroth 1996).

Studies on NDVI-temperature relationships (Braswell et al. 1997; Yang et al. 1997; 1998; Potter and Brooks 1998) have emphasized the importance of growing-season length in controlling annual productivity. However, there is little large-scale empirical work on the differential responses of vegetation activity to maximum temperature, minimum temperature, or seasonal maxima and minima for different biomes (Alward et

al. 1999). Potter and Brooks (1998) and Wang et al. (2001) both examined the response of NDVI to maximum and minimum temperatures, but restricted their analyses to intra-annual time scales. Alward et al. (1999) reported that productivity in some grassland types is more responsive to elevated minimum temperatures, but did not consider other biome types.

In this study, I used satellite and climate data to assess the degree to which spatial gradients in productivity are driven by gradients in long-term average climate characteristics, both within and across major biomes (e.g. Lauenroth and Sala 1992; Paruelo et al. 1999). Specifically, I examined spatial associations between average annual photosynthetic activity and long-term averages of annual and seasonal precipitation, temperature minima (Tmin) and temperature maxima (Tmax) within the period 1990 to 2000 for the conterminous U.S. The normalized difference vegetation index, integrated over the growing season (gNDVI) was used as a proxy for annual photosynthetic activity due to its consistent availability over broad spatial and temporal scales (Asrar et al. 1984; Sellers et al. 1992; Myneni et al. 1997). Our primary goal was to evaluate the relative contribution of seasonal climate characteristics in governing spatial gradients in productivity within and across biomes.

3.2 Materials & Methods

3.2.1 NDVI data

I acquired AVHRR data for the conterminous U.S. from the USGS EROS Data Center. This data set contains biweekly-composited NDVI images at approximately 1 km spatial resolution (Eidenshink 1992). The data are georeferenced to the Lambert Azimuthal Equal Area map projection. I produced monthly NDVI composites for January

1990 to December 2000 by selecting the maximum NDVI value for each successive pair of biweekly composites. Monthly maximum value compositing further reduces atmospheric and sensor scan angle effects on NDVI (Spanner et al. 1990; Moody and Strahler 1994).

NDVI is based on the contrast between red (R) and near-infrared (NIR) reflectance of solar irradiance by vegetation (Holben 1986):

$$NDVI = (NIR - R) / (NIR + R). \quad (1)$$

The red and near-infrared detectors on the AVHRR sensors record radiance in the 0.58µm-0.68µm and 0.725µm-1.1µm wavelength regions, respectively. NDVI varies theoretically between –1.0 and +1.0 (Holben 1986), and increases from about 0.1 to 0.75 for progressively increasing amounts of vegetation (Myneni et al. 2001). The NDVI is most directly related to the fraction of photosynthetically active radiation (fPAR) absorbed by vegetation canopies (Asrar et al. 1984; Choudhury 1987), and hence to photosynthetic activity of terrestrial vegetation (Sellers et al. 1992; Myneni et al. 1995).

Although NDVI only approximates terrestrial vegetation activity, and despite sources of variance related to atmospheric conditions, calibration discrepancies, and variability in illumination/view geometry (Moody and Strahler 1994) AVHRR data currently provide our best empirical device for approximating spatio-temporal variability in terrestrial plant productivity at large scales.

3.2.2 Temperature and precipitation data

For the period 1990-2000, I obtained monthly precipitation totals and monthly averages of mean, minimum, and maximum temperature from the U.S. Historical

Climatology Network (USHCN) for 249 meteorological stations distributed throughout the conterminous U.S. (Karl et al. 1990) (Fig. 3.1). These data are subject to quality control assessment and adjustment procedures described by Karl et al. (1990).

3.2.3 Land-cover map

I used the 1-km land-cover map of North America from the USGS-NASA Distributed Active Archive Center. This map is derived from 1-km AVHRR data spanning April 1992 - March 1993 (Loveland et al. 1999). In this study, I adopted the IGBP (International Geosphere-Biosphere Programme) land-cover taxonomy, from which 17 classes are identified within the conterminous U.S. (Loveland et al. 1999).

3.2.4 Analysis

The climate data, land-cover data and monthly NDVI composites were all georeferenced to the Lambert Azimuthal projection and co-located. Thus, for the single pixel containing each climate station, I extracted land-cover type, monthly NDVI, and monthly climate data for the 11-year study period. Six IGBP vegetation types were represented among the 249 stations (Table 3.1; Fig. 3.1). I used a single AVHRR pixel for each station in order to avoid smoothing out the variability in the NDVI data. Of the 249 climate stations used, 93% had the same land-cover class as the majority of surrounding pixels within a 3 x 3 window.

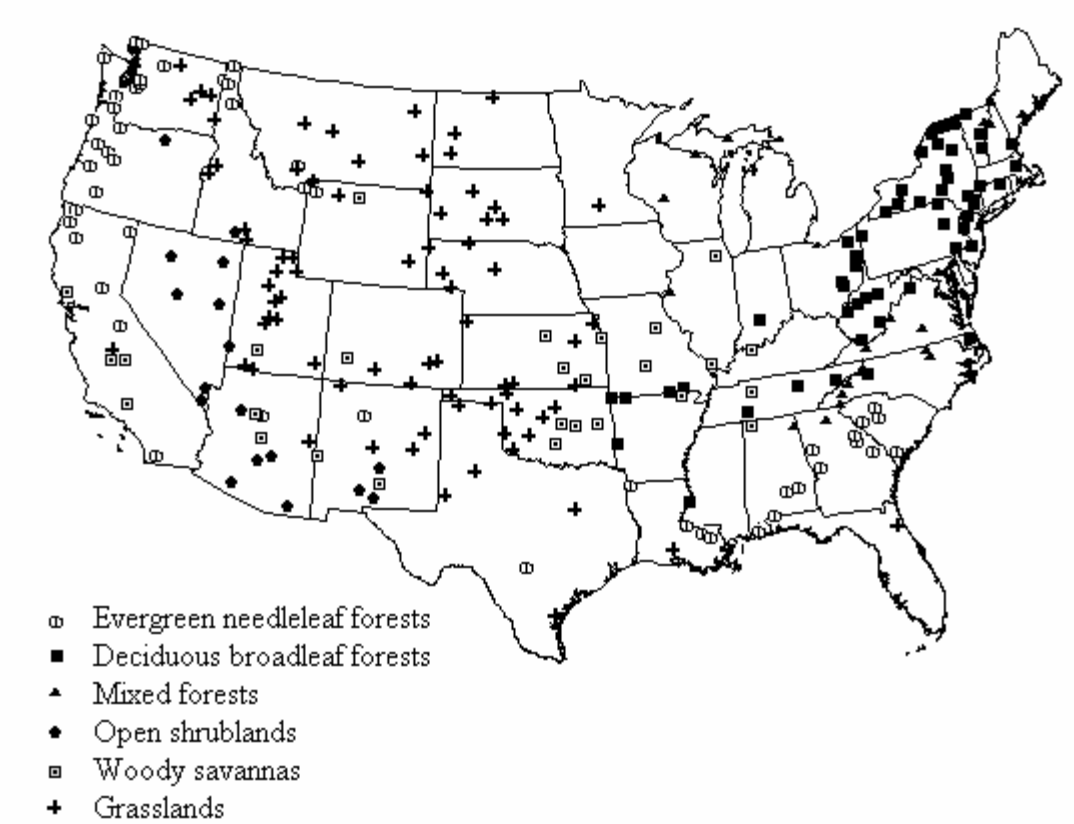

Fig. 3.1 Distribution of the 249 meteorological station locations used in this study, and the dominant biome type at each station.

Table 3.1 The biome types identified for the 249 meteorological stations and the number of stations for each biome. The number of stations for which the class labels from the AVHRR and MODIS land-cover maps agreed are given in parentheses.

IGBP Class	Biome type	Number of Stations	Definition (Belward and Loveland 1996)
1	Evergreen needleleaf forest (ENF)	50 (28)	Canopy cover > 60% & height > 2 m. Most of the canopy remains green all year.
4	Deciduous broadleaf forest (DBF)	55 (32)	Canopy cover > 60% & height > 2 m. Most of the canopy is deciduous.
5	Mixed forest (MF)	22 (6)	Canopy cover > 60% & height > 2 m. Mixed evergreen and deciduous canopy.
7	Open shrubland (OSH)	17 (11)	Woody vegetation cover between 10% and 60%, > 2 m. Evergreen or deciduous canopy.
8	Woody savanna (WS)	27 (7)	Canopy cover between 30% and 60%, & height > 2 m. Deciduous or evergreen canopy. Herbaceous or other understory vegetation.
10	Grassland (Gr)	78 (42)	Herbaceous cover. Woody cover <10%.
	Total	249 (126)	

I calculated the growing season NDVI totals (gNDVI) to approximate the annual photosynthetic activity of vegetation at each station (Asrar et al. 1984; Myneni et al. 1995). I defined the growing season as the period during which monthly NDVI values were greater than or equal to 0.1, after Myneni et al. (2001). Annual and seasonal precipitation totals, and annual and seasonal averages of mean-monthly Tmax and Tmin were calculated from the climate records at each station. All variables were averaged over the 11-year study period so that I could examine the relationships between gradients in long-term means of gNDVI and climate.

I used the coefficient of variation (CV) to characterize interannual variability in gNDVI and each climate variable at each station. The CV provides a standardized temporal variance of a given variable (x) at a particular location (i) relative to the long-term mean at that location ($\overline{x}_i$):

$$CVx_i = \sigma_{xi} / \overline{x}_i \bullet 100\ \% \qquad (2)$$

where σ_{xi} is the standard deviation of variable x at i. The CV values for each variable were used to examine whether temporal variability in gNDVI and temporal variability in climate were related across stations. The CV has been used extensively as an index of variability for both climatic and ecological data (Le Houerou et al. 1988; Lauenroth and Sala 1992; Frank and Inouye 1994) and has been demonstrated to reflect the differential capacity of different ecosystems to buffer interannual climatic variations (Paruelo and Lauenroth 1998).

For within-biome analysis, I examined gNDVI-climate associations across all the individual stations within each biome, thus treating within-biome observations as independent samples. Linear and nonlinear regression models were developed using

gNDVI and climate data for the stations within each biome (Fig. 3.1; Table 3.1). For across-biome analysis, I averaged the values of gNDVI and climate over all of the individual stations for each biome, thus treating each biome as independent from the others, and ignoring within-biome variability. I used linear regression and correlation analysis to examine relationships between biome-level means of gNDVI and climate variables. Given the substantial distances between them, I assumed spatial independence of the stations, both within and across biomes.

3.3 Results

3.3.1 Within-biome relationships between gNDVI and climate

3.3.1.1 Long-term means of gNDVI and precipitation

Within each biome, 11-year mean annual gNDVI was positively associated with mean annual precipitation (MAP) (Table 3.2, Fig. 3.2). The strength of this relationship varied across biomes. For example, *Mixed Forest* and *Woody Savanna* produced much stronger r^2 values than *Deciduous Broadleaf Forest* or *Grassland* (Table 3.2).

Associations between 11-year means of gNDVI and seasonal precipitation also varied by biome, as well as by season (Table 3.2). For all vegetation types except *Open Shrubland*, gNDVI was more strongly related to spring precipitation than to precipitation for any other season. This was especially notable for *Deciduous Broadleaf Forest*, *Grassland*, and *Woody Savanna* (Fig. 3.3). In general, gNDVI was also associated with fall precipitation, except for *Deciduous Broadleaf Forest* and *Mixed Forest*, which were the only two biomes to exhibit strong associations between gNDVI and winter precipitation (Table 3.2). Overall, the weakest seasonal relationships were between gNDVI and summer precipitation (Table 3.2).

I identified two statistical groupings of *Grassland* stations (Fig. 3.2f) and reanalyzed these subgroups separately (Fig. 3.4a). The association between gNDVI and precipitation was much stronger for the less productive subgroup ($r^2 = 0.53$, $P < 0.0001$) than for the more productive subgroup ($r^2 = 0.20$; $P < 0.003$). In both cases, gNDVI was most closely associated with spring precipitation (less productive group: $r^2 = 0.42$, $P < 0.0001$; more productive group: $r^2 = 0.35$, $P < 0.0001$).

I compared the geographic distribution of the two subgroups within the *Grassland* class (Fig. 3.4a) with published distributions of grassland functional type (Paruelo and Lauenroth 1996; Still et al. 2003) and morpohological and compositional characteristics (Ricketts et al. 1999). Based on these comparisons, the less productive subgroup appearing in the data (Fig. 3.2f, Fig. 3.4a) exhibited closest spatial correspondence to northern and northwestern mixed grasslands, western short grasslands, palouse grasslands, and grassland/shrubland transition zones on the Colorado Plateau (Ricketts et al. 1999). The more productive subgroup generally corresponded to central and southern mixed grasslands, and grasslands transitioning to forest, particularly in the central forest/grassland transition zone through Oklahoma, shrub steppe/montane forest transitions around the periphery of the Great Basin in Utah and Idaho, and montane valley and foothill grasslands in western Montana.

Table 3.2 R^2 and p-values of relationships between 11-year means of gNDVI and means of annual and seasonal precipitation (MAP) within each biome. Cells with $R^2 \geq 0.2$ *and* significant at $p \leq 0.05$ shown in bold.

IGBP Class	MAP	Spring	Summer	Fall	Winter
ENF	**0.42**	**0.35**	0.16	**0.20**	0.14
	<0.001	**<0.001**	0.004	**0.001**	0.006
DBF	**0.25**	**0.36**	0.00	0.03	**0.26**
	<0.001	**<0.001**	>0.10	>0.10	**<0.001**
MF	**0.59**	**0.59**	0.15	0.14	**0.54**
	<0.001	**<0.001**	0.07	0.09	**<0.001**
OSH	**0.41**	**0.28**	0.02	**0.36**	0.15
	0.006	**0.029**	>0.10	**0.01**	>0.10
WS	**0.62**	**0.65**	**0.28**	**0.57**	0.15
	<0.001	**<0.001**	**0.005**	**<0.001**	0.048
Gr	**0.28**	**0.42**	0.11	**0.25**	0.10
	<0.001	**<0.001**	0.003	**<0.001**	0.004

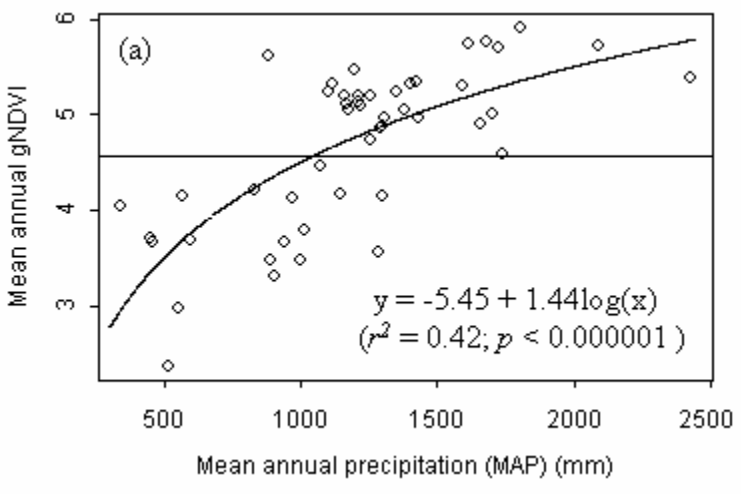
(a)
Mean annual gNDVI
3
4
5
6
500
1000
1500
2000
2500
Mean annual precipitation (MAP) (mm)
y = -5.45 + 1.441og(x)
($r^2 = 0.42$; $p < 0.000001$)

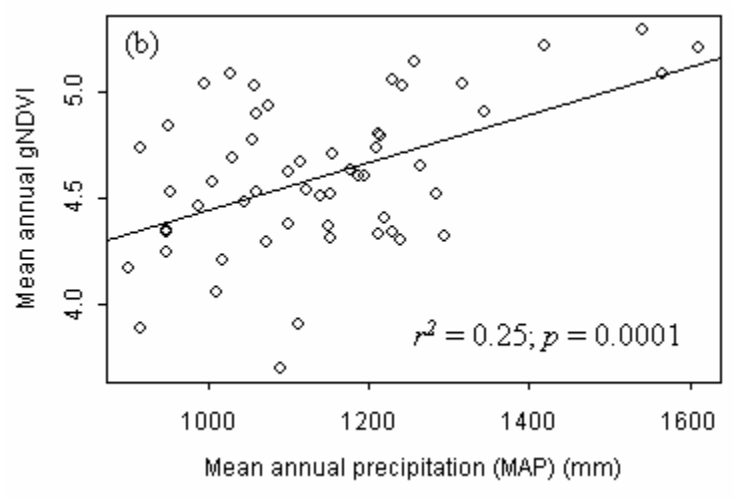
(b)
Mean annual gNDVI
4.0
4.5
5.0
1000
1200
1400
1600
Mean annual precipitation (MAP) (mm)
$r^2 = 0.25$; $p = 0.0001$

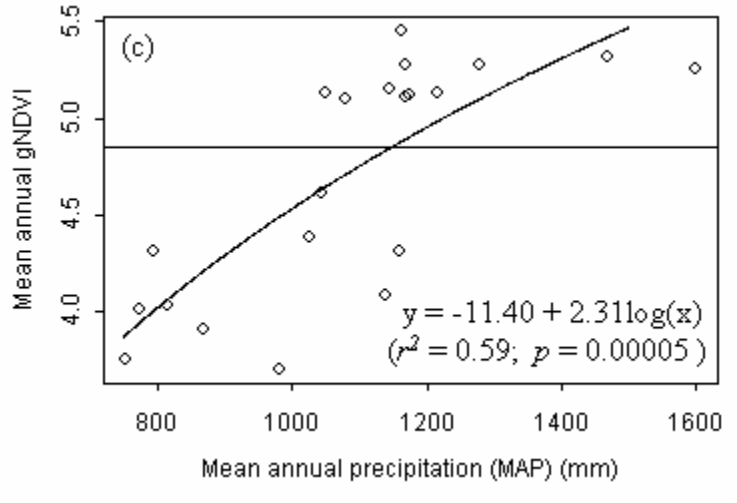
(c)
Mean annual gNDVI
4.0
4.5
5.0
5.5
800
1000
1200
1400
1600
Mean annual precipitation (MAP) (mm)
y = -11.40 + 2.311og(x)
($r^2 = 0.59$; $p = 0.00005$)

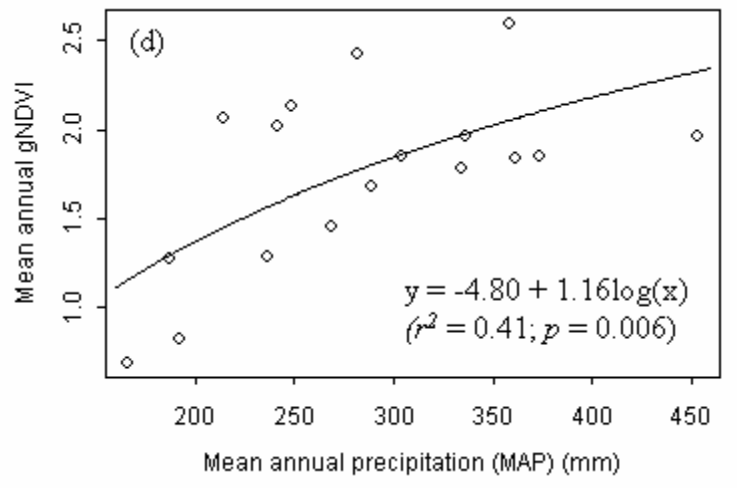
(d)
Mean annual gNDVI
1.0
1.5
2.0
2.5
200
250
300
350
400
450
Mean annual precipitation (MAP) (mm)
y = -4.80 + 1.161og(x)
($r^2 = 0.41$; $p = 0.006$)

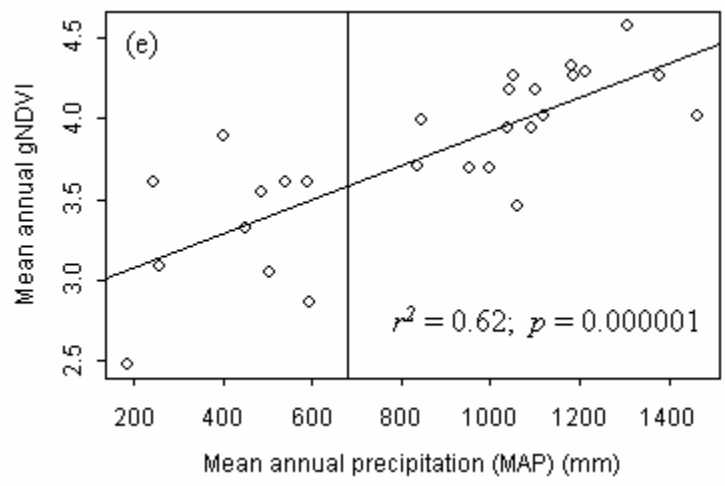

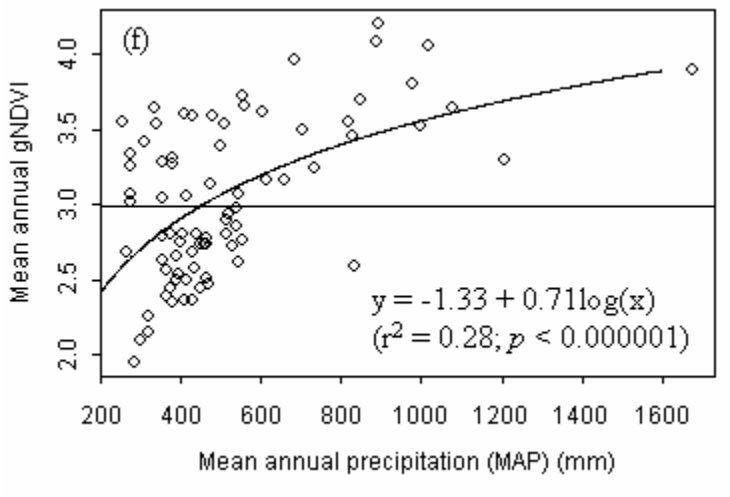

Fig. 3.2 Relationships between 11-year means of gNDVI and annual precipitation for each biome: (a) ENF; (b) DBF; (c) MF; (d) OSH; (e) WS; (f) Gr. Horizontal lines in a, c, and f, and the vertical line in e represent divisions between subgroups within these biomes. These subgroups are mapped in Fig. 3.4.

A closer investigation of *Mixed Forest* also revealed two distinct groups that are fundamentally different in their productivity and climatic characteristics. One group, characterized by higher gNDVI and higher MAP (Fig. 3.2c) is restricted to the Appalachian/Blue Ridge province in the southeastern U.S. (Fig. 3.4b) with a few stations on the mid-Atlantic piedmont. The other group is mostly restricted to the northeastern hardwood/boreal transition. Taken separately, gNDVI for these two groups was not significantly associated with MAP or any seasonal precipitation variables.

As with *Mixed Forest*, gNDVI/precipitation relationships for *Evergreen Needleleaf Forest* and *Woody Savanna* were also driven by two subgroups within their respective biomes (Fig. 3.2a, Fig 3.2e). The most productive and wettest *Evergreen Needleleaf Forest* stations were restricted to the U.S. southeast, and the coastal margin of the Pacific Northwest. The less productive stations were mostly located in the interior of the Pacific Northwest (Fig. 3.2a, Fig. 3.4c). The wetter, more productive *Woody Savanna* stations were distributed through the lower Great Plains and upper Mississippi Valley, and the drier, less productive stations were scattered about the U.S. southwest (Fig. 3.2e, Fig. 3.4d).

3.3.1.2 Interannual variability in gNDVI and precipitation

Open Shrubland exhibited a significant (positive) relationship between the CV of gNDVI and CV of annual precipitation ($r^2 = 0.26$, $p = 0.037$) and summer precipitation ($r^2 = 0.56$, $p = 0.0006$). For *Grassland*, the CV values of gNDVI and fall precipitation were also positively correlated ($r^2 = 0.36$, $p < 0.0001$).

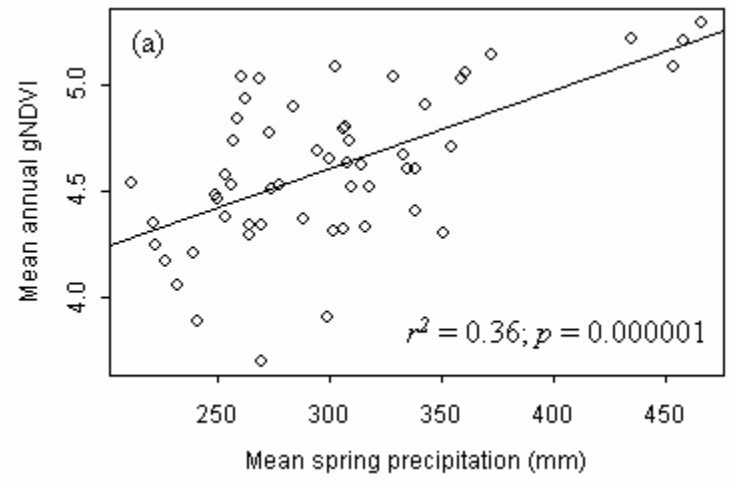
(a)
Mean annual gNDVI
4.0
4.5
5.0
250
300
350
400
450
Mean spring precipitation (mm)
$r^2 = 0.36; p = 0.000001$

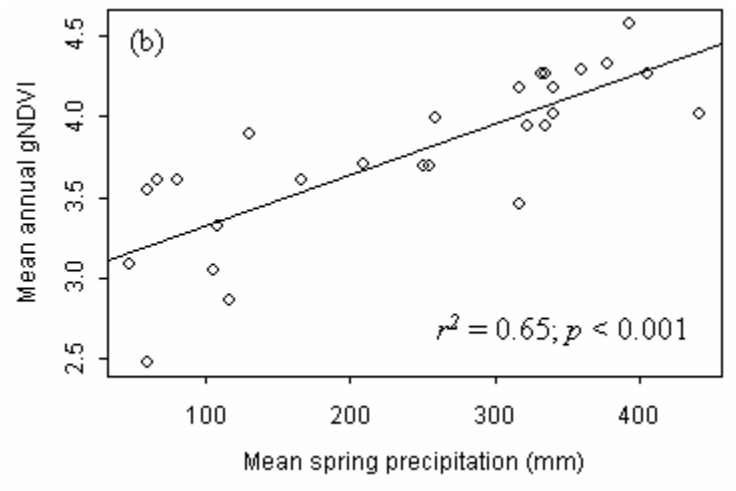
(b)
Mean annual gNDVI
2.5
3.0
3.5
4.0
4.5
100
200
300
400
Mean spring precipitation (mm)
$r^2 = 0.65; p < 0.001$

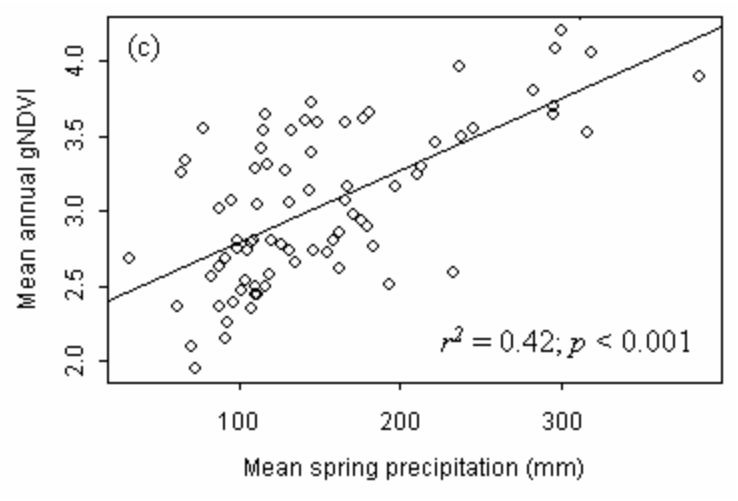

Fig. 3.3 Relationships between 11-year means of gNDVI and spring precipitation for three biomes: (a) DBF; (b) WS; (c) Gr.

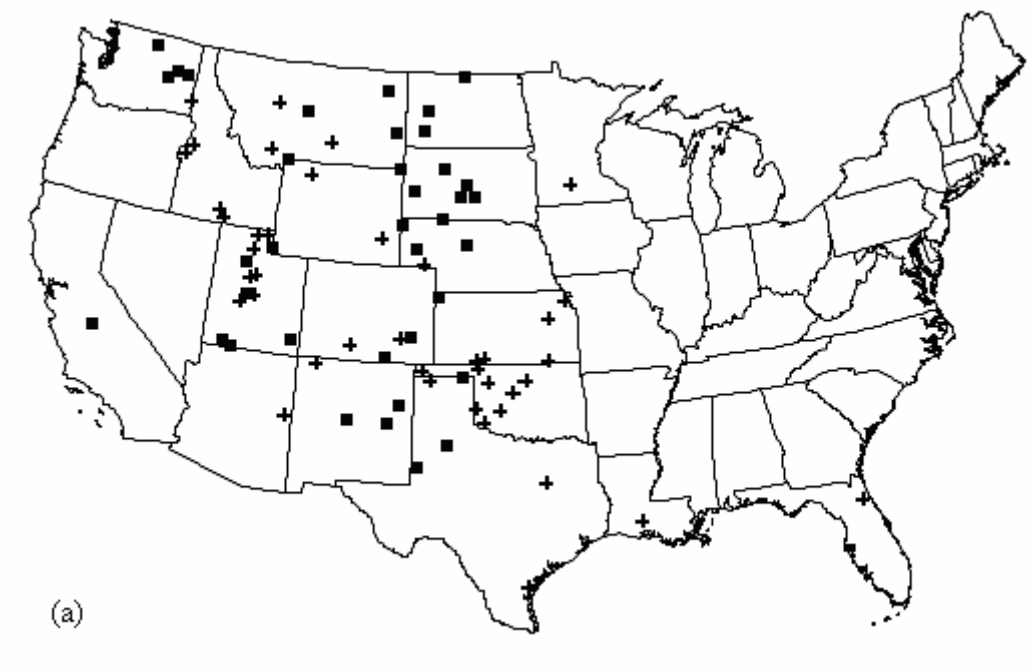

(a)

(b)

Fig. 3.4 Spatial distributions of the within-biome subgroups identified in Fig. 3.2: (a) Gr; (b) MF; (c) ENF; (d) WS. In each case, square symbols represent the less productive subgroup and cross symbols represent the more productive subgroup seen in Fig. 3.2.

Table 3.3 R^2 and p-values of relationships between 11-year mean annual gNDVI and means of annual and seasonal averages of Tmax and Tmin within each biome. For each biome, the first row indicates the relationships of gNDVI with Tmax, and the second row indicates the relationships of gNDVI with Tmin; in each row, the top and bottom numbers are R^2 and p-value, respectively. Cells with $R^2 \geq 0.2$ *and* significant at $p \leq 0.05$ shown in bold.

IGBP Class	Annual	Spring	Summer	Fall	Winter
ENF	0.17	**0.29**	0.11	**0.29**	**0.41**
	0.003	**<0.001**	0.02	**<0.001**	**<0.001**
	0.41	**0.39**	**0.25**	**0.41**	**0.51**
	<0.001	**<0.001**	**<0.001**	**<0.001**	**<0.001**
DBF	**0.32**	**0.33**	**0.30**	**0.31**	**0.33**
	<0.001	**<0.001**	**<0.001**	**<0.001**	**<0.001**
	0.29	**0.32**	**0.25**	**0.23**	**0.31**
	<0.001	**<0.001**	**<0.001**	**<0.001**	**<0.001**
MF	**0.60**	**0.61**	**0.26**	**0.58**	**0.73**
	<0.001	**<0.001**	**0.02**	**<0.001**	**<0.001**
	0.63	**0.66**	**0.38**	**0.48**	**0.74**
	<0.001	**<0.001**	**0.002**	**0.004**	**<0.001**
OSH	0.01	0.00	0.03	0.01	0.00
	>0.10	>0.10	>0.10	>0.10	>0.10
	0.05	0.05	0.08	0.06	0.02
	>0.10	>0.10	>0.10	>0.10	>0.10
WS	**0.23**	0.10	0.046	0.08	0.05
	0.01	>0.10	>0.10	>0.10	>0.10
	0.28	**0.31**	**0.34**	**0.27**	0.14
	0.004	**0.003**	**0.001**	**0.005**	0.05
Gr	0.04	0.03	0.04	0.06	0.03
	0.08	>0.10	0.07	0.05	>0.10
	0.07	0.08	0.08	0.07	0.05
	0.02	0.013	0.01	0.02	0.06

3.3.1.3 Long-term means of gNDVI, Tmin and Tmax

For the three forest biomes, gNDVI had significant positive associations with all long-term averages (annual and seasonal) of both Tmin and Tmax (Table 3.3, Fig 5a-c, 6a-c). In comparison, gNDVI for the most arid biomes, *Open Shrubland* and *Grassland*, was not associated with any temperature variable. *Woody Savanna* produced weak-to-moderate associations with Tmin for spring, summer, and fall (Table 3.3). For *Evergreen Needleleaf Forest*, gNDVI was more strongly associated with Tmin than Tmax, and was most strongly associated with winter, followed by spring and fall temperatures. As with annual precipitation, these results may actually reflect relationships across subgroups within *Woody Savanna* and *Evergreen Needleleaf Forest*; and most certainly for *Mixed Forest*.

3.3.1.4 Interannual variability in gNDVI, Tmin and Tmax

Overall, CV of gNDVI for *Mixed Forest* and *Woody Savanna* were more strongly associated (positive) with CV of temperature means than other biomes (Table 3.4). These associations for *Mixed Forest* were significant for the CV of annual, winter and spring temperature means for both Tmax and Tmin. In contrast, CV of gNDVI for *Woody Savanna* was associated with CV of annual, summer and fall Tmin (and only spring Tmax).

3.3.2 Across-biome relationships between gNDVI and climate

Mean annual gNDVI was greatest for the three forest biomes (4.61-4.72), intermediate for *Woody Savanna* and *Grassland* (3.77 and 3.04, respectively) and low for *Open Shrubland* (1.75) (Table 3.5). Likewise mean annual precipitation was high and

roughly equal for the forest biomes (1142 to 1269 mm/yr), intermediate for *Woody Savanna* and *Grassland* (857 and 523mm/yr, respectively), and low for *Open Shrubland* (285 mm/yr). Mean annual gNDVI was, thus, strongly correlated with mean annual precipitation across the six biomes (Fig. 3.7a), as well as with mean precipitation for each season, especially spring and fall (Fig. 3.7b and d).

The mean CV of gNDVI was similar across biomes, ranging from roughly 10.0% for the forest biomes, to 13.4% for *Grassland*. The exception was *Open Shrubland*, with a mean CV of 28.04%. Open Shrubland also exhibited substantially higher interannual variability in MAP and in precipitation for each season.

Across biomes, mean CV of gNDVI was significantly associated with mean CV of annual and seasonal precipitation totals. However, these relationships were driven by *Open Shrubland*. When this class was removed there were no significant relationships between interannual variability of gNDVI and precipitation.

The three forest biomes had the lowest mean Tmax values for both summer and winter, except for *Evergreen Needleleaf Forest*, which had a high mean winter Tmax due to the effect of averaging values from southeast and northwest conifer forests. The three non-forest biomes had relatively high Tmax, and *Open Shrubland* was always the highest. *Evergreen Needleleaf Forest* had the highest mean winter Tmin, followed by *Open Shrubland* and *Woody Savanna*. The other three biomes had relatively low winter Tmin (Table 3.5).

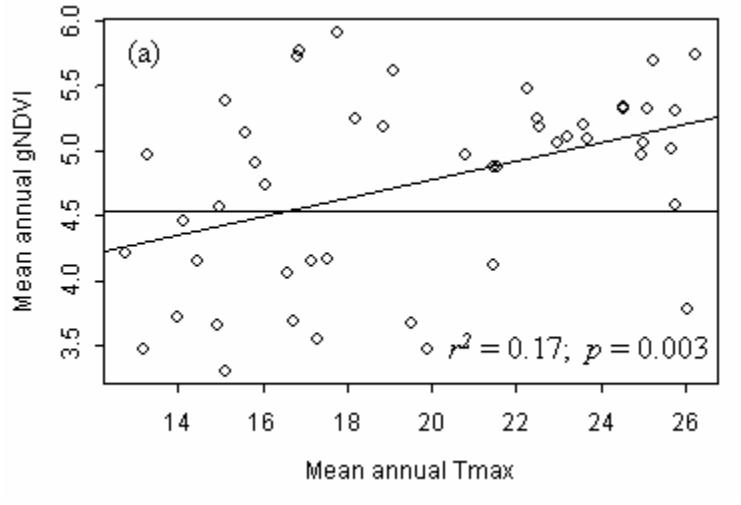
(a)
Mean annual gNDVI
Mean annual Tmax
$r^2 = 0.17;\ p = 0.003$

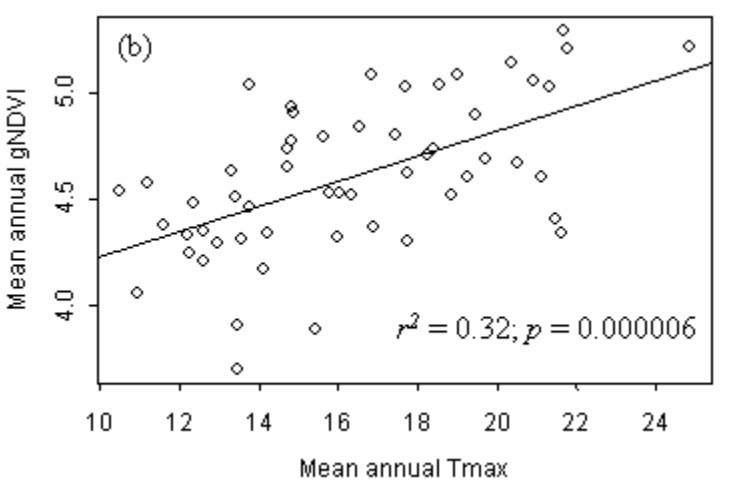
(b)
Mean annual gNDVI
Mean annual Tmax
$r^2 = 0.32; p = 0.000006$

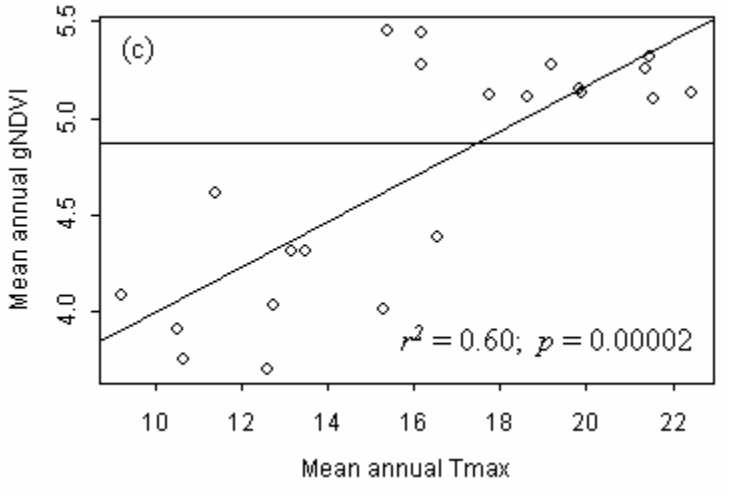
(c)
Mean annual gNDVI
Mean annual Tmax
$r^2 = 0.60;\ p = 0.00002$

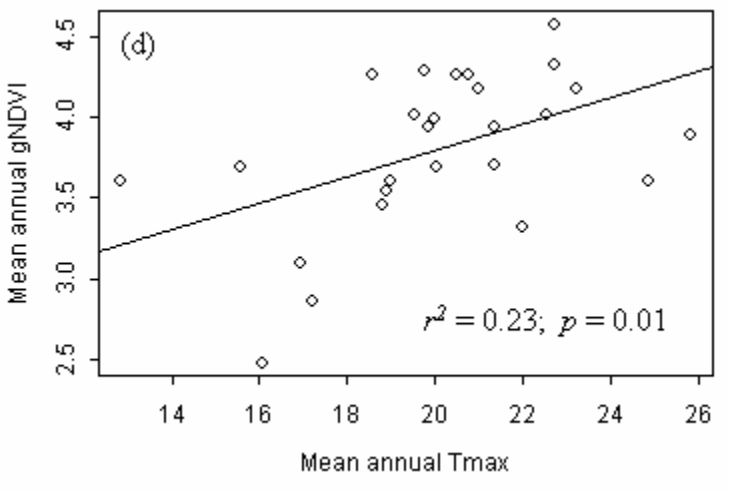

Fig. 3.5 Relationships between 11-year means of gNDVI and annual average Tmax for four biomes: (a) ENF; (b) DBF; (c) MF; (d) WS. Horizontal and vertical lines within plots correspond with Figs. 2 and 4.

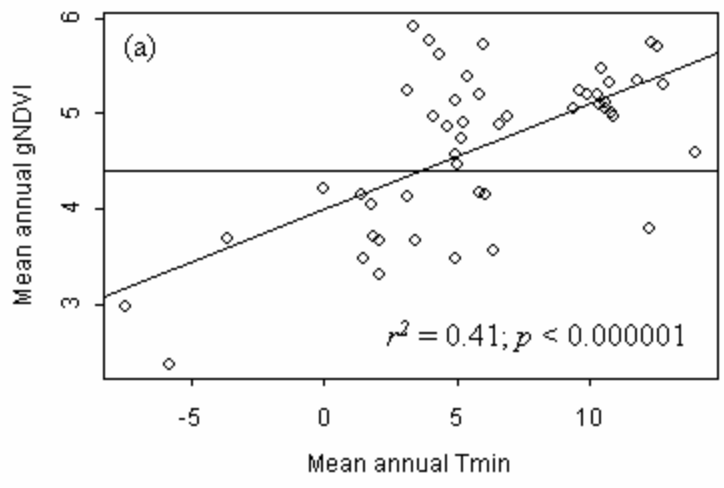
(a)
Mean annual gNDVI
Mean annual Tmin
$r^2 = 0.41; p < 0.000001$
3
4
5
6
-5
0
5
10

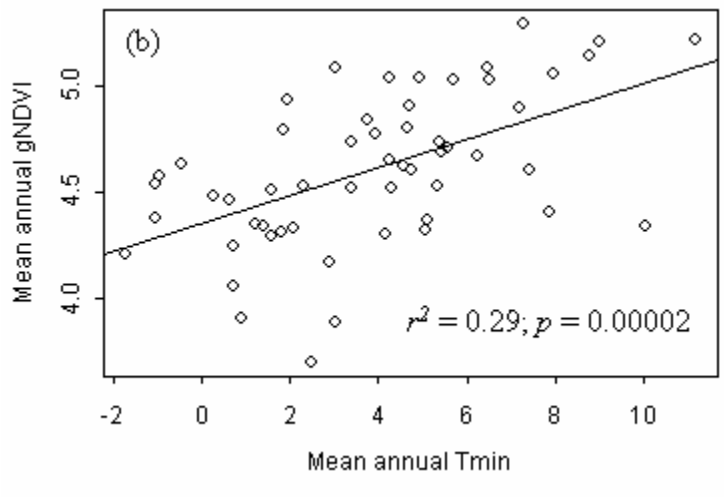
(b)
Mean annual gNDVI
Mean annual Tmin
$r^2 = 0.29; p = 0.00002$
4.0
4.5
5.0
-2
0
2
4
6
8
10

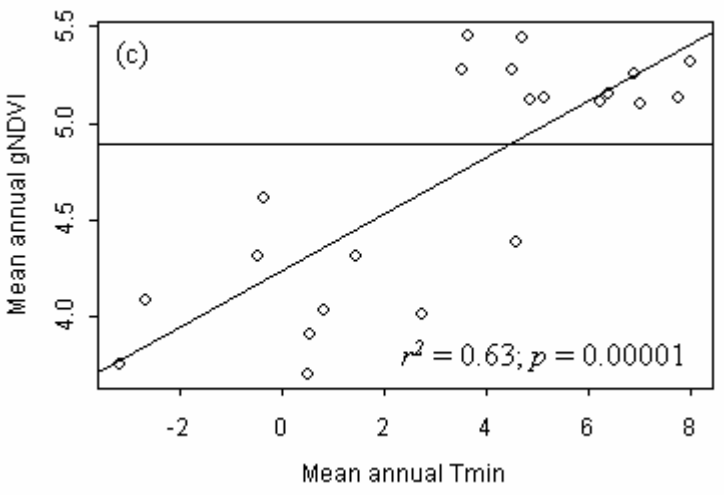
(c)
Mean annual gNDVI
Mean annual Tmin
$r^2 = 0.63; p = 0.00001$
4.0
4.5
5.0
5.5
-2
0
2
4
6
8

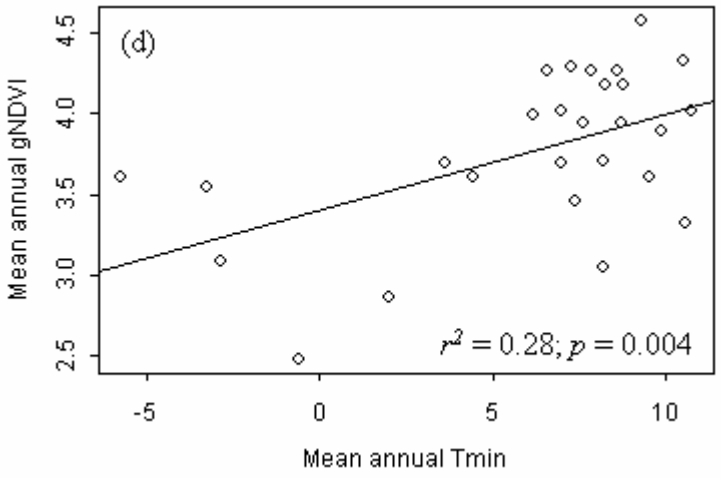

Fig. 3.6 Relationships between 11-year means of gNDVI and annual average Tmin for four biomes: (a) ENF; (b) DBF; (c) MF; (d) WS. Horizontal lines correspond with Figs. 2, 4, and 5.

Across biomes, mean annual gNDVI was negatively correlated with mean summer Tmax (Fig. 3.8). Mean annual gNDVI was not related to any other Tmax variable, or to mean annual or seasonal Tmin values. The CV values of gNDVI were not significantly associated with CV of annual or seasonal means of Tmax or Tmin. A significant relationship between mean CV of gNDVI and CV of summer average Tmin ($r^2 = 0.65$, $p < 0.02$) was heavily influenced by *Open Shrubland*, which exhibited high interannual variability in both gNDVI and average summer Tmin.

3.4 Discussion

3.4.1 Within-biome relationships between gNDVI and climate

3.4.1.1 Long-term means of gNDVI and precipitation

Strong association between gNDVI and MAP observed for all biomes considered here are consistent with other studies based on both NDVI (Davenport and Nicholson 1993; Paruelo and Lauenroth 1995) and ANPP measurements (Sala et al. 1988; Knapp and Smith 2001). These findings suggest that geographic reorganization of long-term averages in precipitation may influence the spatial distribution of productivity within biomes.

Although summer rainfall can be critical to plant life-cycles in arid regions (Pake and Venable 1995, 1996) spatial gradients in late-season rainfall were not responsible for geographic patterns of annual productivity within any biome. Precipitation was far more important in spring, fall, and winter, periods when evapotranspirative demand is low, and ground-water recharge is most efficient (Webb et al. 1978; Neilson et al. 1992; Paruelo and Sala 1995). This pattern was especially apparent for spring, when precipitation

provides near-surface soil moisture early in the growing season, and also replenishes ground water.

For deeply-rooted vegetation types in particular, ground-water provides a buffer against soil-water deficits during the growing season (Webb et al. 1978; Woodward 1987; Stephenson 1990; Jobaggy and Sala 2000). Our findings reinforce the importance of water-balance as a primary determinant of spatial gradients in productivity (e.g. Walker and Noy-Meir 1982; Eagleson and Segarra 1985; Neilson 1995) and further suggest that these processes are important for both deep- and shallow-rooted vegetation types.

The dominance of spring precipitation in explaining *Grassland* productivity reflects the reliance of shallow-rooted life-forms on water from the upper soil horizons where early season soil moisture can sufficiently maintained by precipitation (Walter 1971; Jobaggy and Sala 2000). Further, inputs to surface soil water are most critical during early life stages of germination and root development, especially for annual grasses and herbs common to many grasslands ecosystems (Neilson et al. 1992; Pake and Venable 1995, 1996). The geographic distributions of the two subgroups within the *Grassland* biome largely reflect changes in grassland productivity along orographic precipitation gradients (e.g. Great Basin steppe to montane forests) as well as synoptic-scale precipitation gradients (e.g. central forest/grassland transition zone) (Ricketts et al. 1999).

Table 3.4 R^2 and p-values of relationships between CV of gNDVI and CV of annual and seasonal averages of Tmax and Tmin. For each biome, the first row indicates the relationships of gNDVI with Tmax, and the second row indicates the relationships of gNDVI with Tmin; in each row, the top and bottom numbers are R^2 and p-value, respectively. Cells that are significant at $p \leq 0.05$ shown in bold.

IGBP Class	Annual	Spring	Summer	Fall	Winter
ENF	0.00	0.04	0.01	0.00	0.05
	>0.10	*>0.10*	*>0.10*	*>0.10*	*>0.10*
	0.04	0.02	0.01	**0.16**	0.06
	>0.10	*>0.10*	*>0.10*	***0.004***	*0.09*
DBF	0.05	**0.12**	0.04	**0.17**	**0.15**
	>0.10	***0.006***	*>0.10*	***0.001***	***0.002***
	0.10	0.03	0.03	0.02	0.02
	0.017	*>0.10*	*>0.10*	*>0.10*	*>0.10*
MF	0.20	**0.32**	0.04	0.04	**0.43**
	0.037	***0.007***	*>0.10*	*>0.10*	***0.0009***
	0.49	**0.45**	0.06	0.17	**0.30**
	0.0003	***0.0007***	*>0.10*	*0.06*	***0.008***
OSH	0.00	0.01	0.04	0.00	0.02
	>0.10	*>0.10*	*>0.10*	*>0.10*	*>0.10*
	0.01	0.01	0.00	0.00	0.00
	>0.10	*>0.10*	*>0.10*	*>0.10*	*>0.10*
WS	0.01	**0.27**	0.09	0.07	0.09
	>0.10	***0.005***	*>0.10*	*>0.10*	*>0.10*
	0.28	0.12	**0.34**	**0.23**	0.07
	0.004	*0.08*	***0.001***	***0.01***	*>0.10*
Gr	0.01	0.00	0.00	0.00	0.04
	>0.10	*>0.10*	*>0.10*	*>0.10*	*>0.10*
	0.00	0.02	0.00	0.01	0.00
	>0.10	*>0.10*	*>0.10*	*>0.10*	*>0.10*

Table 3.5 Biome-level means of gNDVI (unitless), precipitation (mm), Tmax (ºC), and Tmin (ºC). Standard deviations are denoted in italics.

	ENF	**DBF**	**MF**	**OSH**	**WS**	**Gr**
GNDVI	4.67	4.61	4.72	1.75	3.77	3.04
	0.83	*0.36*	*0.61*	*0.51*	*0.50*	*0.52*
MAP	1268.88	1141.78	1143.44	284.98	856.72	522.71
	540.35	*159.57*	*332.01*	*77.42*	*372.42*	*248.05*
Annual Tmin	6.07	3.89	3.31	6.19	6.14	3.43
	4.74	*2.94*	*3.30*	*6.03*	*4.46*	*4.26*
Annual Tmax	19.29	16.35	16.16	22.10	20.36	18.19
	4.70	*3.41*	*4.05*	*4.89*	*3.20*	*4.08*
Summer Tmin	13.22	14.47	13.91	15.27	15.96	13.80
	5.39	*2.51*	*2.64*	*6.13*	*4.76*	*4.21*
Summer Tmax	28.32	27.52	26.96	32.87	30.89	29.95
	4.16	*2.44*	*2.73*	*4.14*	*3.08*	*3.10*
Winter Tmin	-0.28	-6.28	-6.84	-1.87	-3.11	-6.35
	4.77	*4.02*	*5.10*	*5.85*	*5.12*	*5.00*
Winter Tmax	10.14	4.63	4.70	11.53	9.47	6.40
	5.58	*4.44*	*5.69*	*5.39*	*4.06*	*5.53*

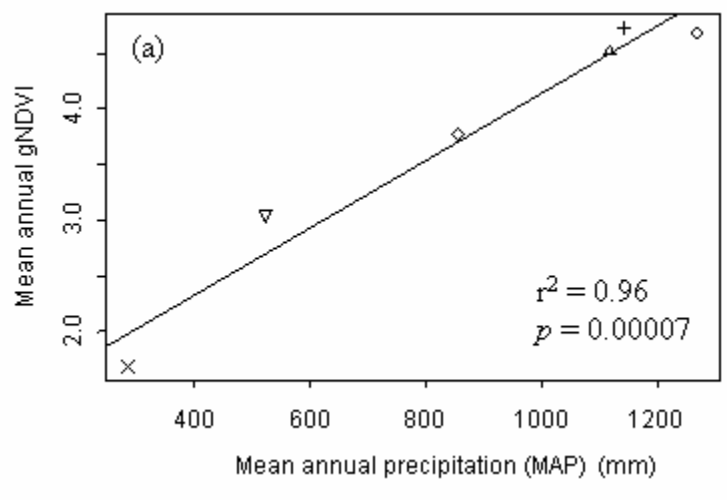
(a)
Mean annual gNDVI
2.0
3.0
4.0
400
600
800
1000
1200
Mean annual precipitation (MAP) (mm)
r² = 0.96
p = 0.00007

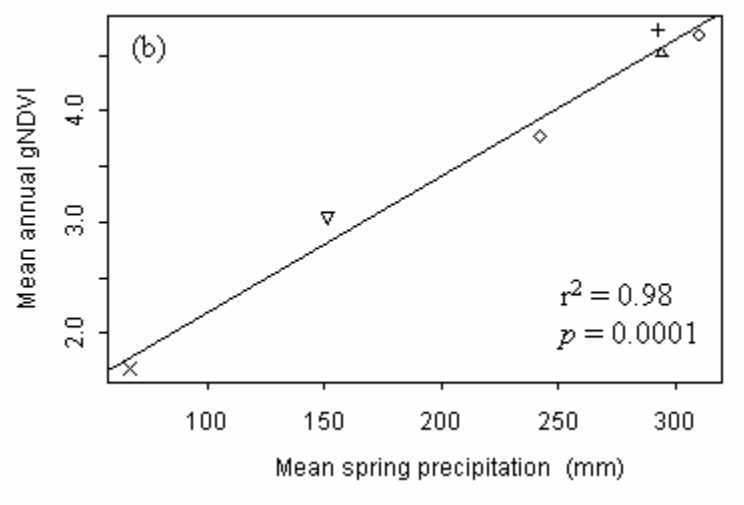
(b)
Mean annual gNDVI
2.0
3.0
4.0
100
150
200
250
300
Mean spring precipitation (mm)
r² = 0.98
p = 0.0001

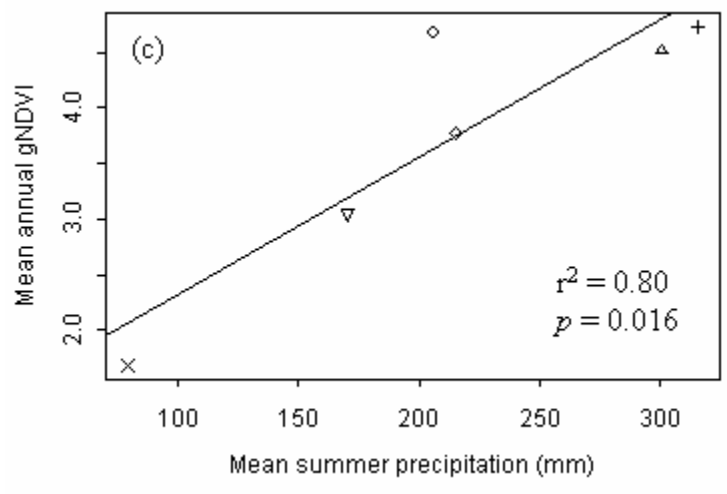
(c)
Mean annual gNDVI
2.0
3.0
4.0
100
150
200
250
300
Mean summer precipitation (mm)
r² = 0.80
p = 0.016

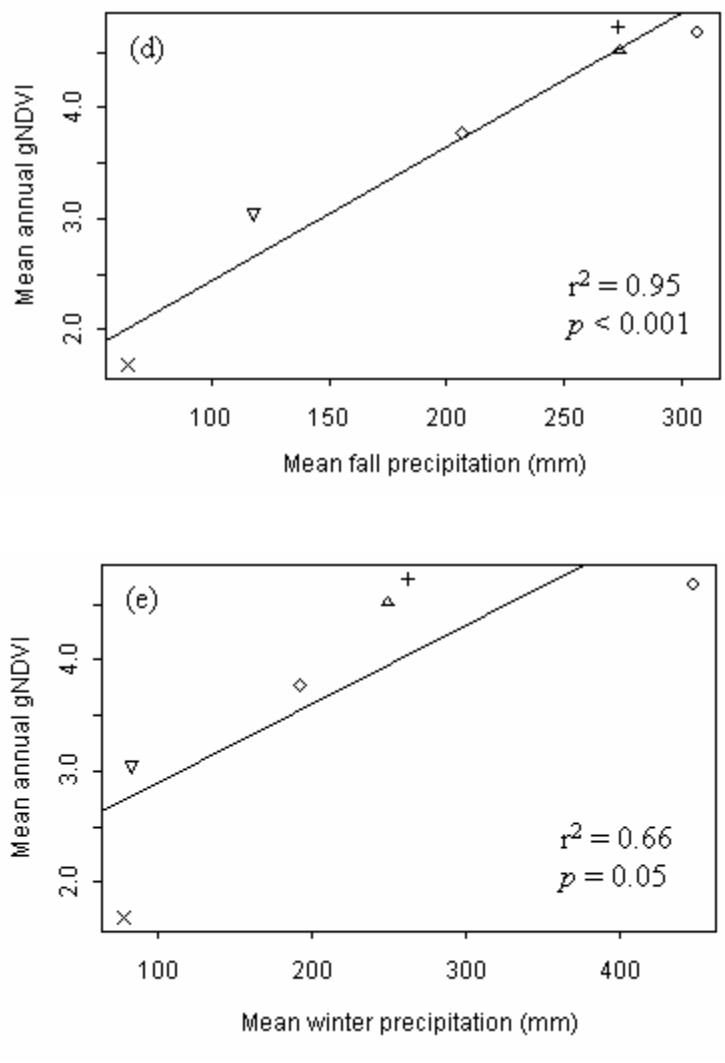

Fig. 3.7 Relationships between biome-level means of gNDVI and annual and seasonal precipitation across six biomes: (a) annual; (b) spring; (c) summer; (d) fall; (e) winter.

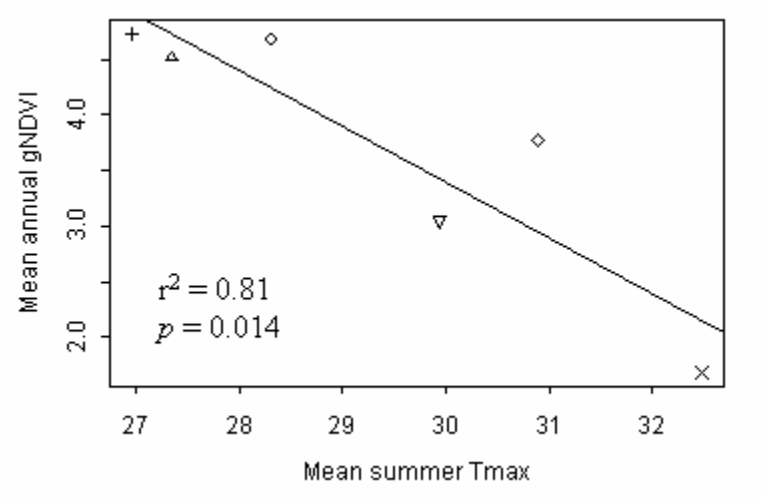

Fig. 3.8 Relationship between mean annual gNDVI and mean summer Tmax across six biomes.

In dry regions, where plants can develop and senesce rapidly in response to moisture availability, precipitation-driven pulses in productivity for *Grassland* may have occurred below the temporal resolution of the data used in this study. This could be the case for *Woody Savanna* and *Open Shrubland* as well, which can include substantial herbaceous components. Thus, summer precipitation is possibly more critical to plant productivity for these biomes than is suggested by our results.

The relationship between gNDVI of *Woody Savanna* and spatial gradients in precipitation supports the view of savannas as tree-grass complexes, with lateral and vertical competition for limited soil water determining tree cover (Walker and Noy-Meir 1982; Eagleson and Segarra 1985; Neilson et al. 1992; Pan et al. 2002). Such relationships have obvious implications for the productivity and distribution of savannas under changing precipitation regimes (Haxeltine et al. 1995; VEMAP Members 1995). However, the absence of associations between gNDVI and precipitation within geographic subgroups of *Woody Savanna* implies that overstory productivity is not limited by water in this biome type, at least at the regional scale. This suggests that factors other than water limitation, such as disturbance (Daly et al. 2000; Van Langevelde et al. 2003) are critical for the development and maintenance of certain savanna complexes. However, I note that gNDVI (and other remote sensing products) may be relatively insensitive to productivity of the shallow rooted, understory vegetation in *Woody Savanna*.

As with *Woody Savanna*, similar results for subgroups within *Mixed Forest* and *Evergreen Needleleaf Forest* also reflect the buffering effect of ground water for deep-rooted biomes (Neilson et al. 1992; Prentice et al. 1992; Paruelo and Lauenroth 1996).

These results reinforce the value of stratifying functional vegetation types by ecoregion, climate division or other strata, as an effective means to maintain within-class homogeneity for incorporating vegetation heterogeneity in climate models, and modeling vegetation response to climate changes (e.g. VEMAP members 1995; Bachelet et al. 2001).

3.4.1.2 Interannual variability in gNDVI and precipitation

Open Shrubland and some grasslands that exist in arid regions are often assumed to experience unusually high interannual variability in rainfall totals (Pake and Venable 1995, 1996; Davidowitz 2002). Our results show that, within these biomes, different stations experienced a wide range of interannual variability in precipitation, which was positively correlated to variability in gNDVI. Similar findings have been reported previously for arid biomes (Le Houerou et al. 1988; Kawabata et al. 2001) and for shrubland ecosystems in particular (Paruelo and Lauenroth 1998).

Variability in productivity for arid biomes was most sensitive to precipitation variability in summer and fall, when water is limiting, and when particularly wet periods may initiate or amplify productivity of late-season grasses and drought-dormant annuals. The potential impact of changes in precipitation variability on the distribution and function of arid vegetation types is most likely mediated by life-form. Thus, greater interannual variability in summer precipitation should favor more deeply-rooted shrubs that are capable of surviving and growing during dry periods. It is conceivable that, in the absence of fire or other events that suppress that development of shrublands, increasing interannual variability in precipitation may facilitate shrub proliferation in grasslands.

3.4.1.3 Long-term means of gNDVI, Tmin and Tmax

The sensitivity of gNDVI to long-term annual and seasonal averages of Tmax and Tmin decreased along a bioclimatic gradient, from forested to arid biomes. The lack of association between gNDVI and temperature for *Grassland* and *Open Shrubland*, in combination with the results discussed above indicates the dominance of water balance (Jobaggy and Sala 2000) as the limiting control on productivity in these biomes. For forested biomes, strong positive relationships between productivity and temperature emphasize the importance of growing-season length in controlling productivity. Our results most likely reflect the synchrony between latitudinal gradients in temperature and productivity, the strength of which increases with decreasing water limitation. The notable sensitivity of *Evergreen Needleleaf Forest* to winter temperatures, and Tmin in particular, may reflect a temperature control on photosynthetic rate, rather than growing season length. Our results clearly suggest that long-term temperature changes will differentially influence productivity for different biome types (Los et al. 2001) but response to the seasonal component of these changes are difficult to ascertain, potentially due to the strong multicollinearity between the temperature measures used.

Global mean surface air temperature has shown a narrowing of the diurnal temperature range (Karl et al. 1995; Easterling et al. 1997) with global minimum temperatures increasing at about twice the rate of maximum temperatures (IPCC 1996; IPCC 2001). However, the relative ecological consequences of changes in Tmin and Tmax are largely unexplored over large spatial scales (Alward et al. 1999; Mitchell and Csillag 2001). Our results suggest that productivity may respond more strongly to changes in Tmin for *Evergreen Needleleaf Forest* and *Woody Savanna*. Increases in Tmin

may thus contribute to increases in productivity within these biomes, which could potentially include increases in stem density.

3.4.2 Across-biome relationships between gNDVI and climate

Most of the variance in average gNDVI across biomes is explained by average annual or seasonal precipitation. Average gNDVI for *Evergreen Needleleaf Forest* was high given the average amount of summer precipitation (Fig. 3.7c) and summer Tmax (Fig. 3.8), and low given the amount of winter precipitation (Fig. 3.7e). These residuals suggest an especially strong reliance of *Evergreen Needleleaf Forest* on stored water supplies rather than growing-season precipitation, and identify water balance as a potentially limiting factor for this biome (Webb et al. 1978; Stephenson 1990).

The strong relationships between gNDVI and precipitation totals from spring and fall further emphasize the importance of rainfall during the beginning and end of the growing season in driving differences in productivity across biomes. In combination with the negative association between mean annual gNDVI and mean summer Tmax, our results reflect an interaction between the seasonality characteristics of precipitation and temperature in governing the distributions of biomes, presumably due to their joint control over annual soil-water budgets (Stephenson 1990).

3.4.3 Sources of Uncertainty

There are several uncertainties related to the data and methods used in this analysis that may influence the results presented here. First, NDVI is not as effective an indicator of photosynthetic activity for sites with sparse vegetation. Second, despite corrections for most known, systematic sources of error (Eidenshink 1992) the satellite data used in this

study contain variability in radiometry that is related to instrument, orbital, or atmospheric characteristics. Moreover, uncertainties in the geolocation of AVHRR pixels can result in mismatches between the locations of climate stations and their enclosing pixels. By using a large number of stations, and averaging over a number of years, I have attempted to limit the impact of this effect on the results. Finally, the approach used to derive the growing season will have overestimated productivity in cases where NDVI never drops below 0.1. Such cases are most likely to occur for *Evergreen Needleleaf Forest* or *Mixed Forest*, and could influence the across biome results by elevating the points for these two class types along the y-axis in Fig. 3.7.

Because there is a large amount of structural and compositional variability within biomes, the degree to which pixels are consistently classified using satellite data is difficult to determine over large areas. For example, a comparison of the 1993 AVHRR-based map used in this analysis with the 2000/2001 MODIS-based map that also uses the IGBP land-cover taxonomy (Friedl et al. 2000) produces an agreement rate of only 50.1% (Table 3.1) (unpublished results). Confusions are particularly common between *Deciduous Broadleaf Forest* and *Mixed Forest*; and between *Open Shrubland* and *Grassland.* These disagreements can result from land-cover changes, misclassification in one or both maps, or misregistration between them. I reran our analyses using only stations for which the two maps agreed. The results changed marginally in magnitude, with no changes in sign. However, with loss in degrees of freedom (Table 3.1) some of the resulting statistics became insignificant.

3.5 Conclusion

Our results reflect the seasonal climatic control over large-scale spatial gradients in plant productivity, both within and across biomes. Correlations between precipitation and approximated plant productivity differed across biomes in a manner consistent with their expected sensitivity to soil water limitation. For example, productivity of relatively shallow-rooted, drought-prone ecosystems, such as *Grassland* and *Open Shrubland*, varied strongly with gradients in spring precipitation. Conversely, winter precipitation, presumably due to a greater contribution to stored water, was more important for deep-rooted forest biomes, especially *Evergreen Needleleaf Forest*, which is more typically water limited.

In contrast to water balance, which influenced productivity for all biomes, the effect of seasonal Tmax and Tmin was only apparent for forested biomes, which are less likely to be water limited. The seasonality of temperature relations, and the relatively greater importance of Tmin for some biomes, suggest that the dominant effect of temperature is through its influence on growing-season length.

Historically, the increase in U.S. annual precipitation is due largely to increases during fall (September to November) (Groisman and Easterling 1994; IPCC 1996) which is related to gNDVI for the more arid biomes considered here. As with spring precipitation, late season contributions to soil moisture can extend the growing season for water-limited biomes, such as *Open Shrubland* and *Grassland*. These sensitivities may lead to changes in the density or extent of woody vegetation in arid and semi-arid regions, with consequent implications for ecosystem productivity and carbon storage (Brown et al. 1997; Goodale and Davidson 2002; Jackson et al. 2002).

Our results indicate that the greatest climate-change impacts on biome distributions and productivity would result from changes in spring, winter and fall precipitation, and changes in fall and spring temperature, especially Tmin, which has historically increased at roughly twice the rate of Tmax (IPCC 2000). These effects differ by biome type, and also vary within biomes.

3.6 Acknowledgements

We thank David Greenland and three anonymous referees for their constructive critique of this report.

3.7 Chapter Synopsis

3.7.1 Background

Increases in temperature and moisture could increase vegetation activity by lengthening the period of carbon uptake (Nemani et al. 2002), enhancing photosynthesis (Keeling et al. 1996, Randerson et al. 1999), and changing nutrient availability by accelerating decomposition or mineralization (Melillo et al. 1993). Temperature is thought to be the leading climatic factor controlling the high-latitude greening trend, and precipitation is assumed to play a minor role in increasing vegetation productivity (Myneni et al. 1997, Zhou et al. 2001, Tucker et al. 2001, Lucht et al. 2002). By contrast, Nemani et al. (2002) showed that increases in precipitation and humidity are the most important factors enhancing vegetation activity for the conterminous US. In addition, Global minimum temperatures have been increasing at about twice the rate of maximum temperatures (IPCC 1996, 2001), but the ecological consequences of the differential

increases in maximum and minimum temperatures are largely unexplored (Alward et al. 1999).

3.7.2 Synopsis

I examined the response of vegetation productivity to mean precipitation, maximum temperature (Tmax), and minimum temperature (Tmin) over an 11-year period (1990-2000) for six biomes in the conterminous United States. I focused on within- and across-biome variance in long-term average vegetation productivity, emphasizing the degree to which this variance is explained by spatial gradients in long-term average seasonal climate. Since direct measurements of vegetation productivity are unavailable at the spatial and temporal scales studied, I used the satellite-based normalized difference vegetation index (NDVI) as a proxy for net photosynthetic activity. Annual productivity was approximated by NDVI integrated over the growing season (gNDVI).

Forested and non-forested biomes differed sharply in their response to spatial gradients in temperature and precipitation. Gradients in mean spring and fall precipitation totals explained much of the variance in mean annual gNDVI within arid biomes. For forested biomes, mean annual gNDVI was positively associated with mean annual and seasonal Tmin and Tmax. These trends highlight the importance of the seasonal components of precipitation and temperature regimes in controlling productivity, and reflect the influence of these climatic components on water balance and growing-season length. According to the International Panel on Climate Change (IPCC) (2001) increases in temperature minima and fall precipitation have contributed the dominant components of U.S. increases in temperature and precipitation, respectively.

Within the range of conditions observed over the study region, our results suggest that these trends have particularly significant consequences for above-ground plant productivity, especially for *Grassland*, *Open Shrubland*, and *Evergreen Needleleaf Forest*. If historical climatic trends and the biotic responses suggested in this analysis continue to hold, I can anticipate further increases in productivity for both forested and nonforested ecoregions in the conterminous U.S., with associated implications for carbon budgets and woody proliferation.

3.7.3 Limitations

I used the biweekly NDVI product (1km) obtained from the USGS EROS Data Center (EDC) in this study. This product has been subject to a series of processing, but there is still noise in the data set. The residual noise remaining in the NDVI data may lead to uncertainties in the analysis. In addition, the data set that I used was the period from 1990 to 2000, which is not be ideally long for examining relationships between vegetation activity and climate. Now, this AVHRR NDVI data has been extended to 2005.

NDVI is a good proxy for photosynthetic activity or NPP of green vegetation. However, net carbon accumulation by ecosystems is measured by NEP. As mentioned earlier, elevated temperature (Larcher 1983) and increased precipitation (Nemani et al. 2002) can increase NPP by lengthening the growing season and enhancing photosynthesis, but elevated temperatures can also accelerate the rates of plant and microbial respiration and release more C back into the atmosphere (Billings et al. 1984, Gorham 199, Woodwell & Mackenzie 1995, Houghton et al. 1998). Thus, influences of temperature or precipitation on NDVI indicate the influences of climate variability on vegetation productivity (GPP or NPP), not necessarily on carbon stocks in ecosystems.

The analysis of this study was based on individual stations because high-resolution gridded climate data at the kilometer scale was not available. When this study was conducted, the highest spatial resolution of the gridded climate data sets available was 0.5˚×0.5˚. Thus, I used climate data obtained from meteorological stations to ensure that climate data were as accurate as possible. The spatial analysis of the relationships between vegetation productivity and climate variability has been recently made possible by the availability of high-resolution gridded climate data (1km or 4km), which will be discussed below.

3.7.4 Future directions

High-resolution gridded climate data have been available, including Daymet (Thornton et al. 1997) and PRISM (Daly et al. 2001). The Daymet data consists of gridded temperature, precipitation, humidity, and radiation over the period 1980-1997 at a 1km spatial resolution (Thornton et al. 1997). Moreover, century-long gridded climate data with 4km spatial resolution (Daly et al. 2001) have been available for the conterminous US. The development of this high-quality data set was made possible through the use of PRISM, a climate analysis system that use point climate data, a digital elevation model, and other spatial datasets to generate gridded climate data (Daly et al. 2001).

The USGS EROS Data Center (EDC) has been producing biweekly NDVI composites (greenness information) of the conterminous U.S. and Alaska using AVHRR data for over 10 years. I used this product (1990-2000) for this study. In 2001, EDC began to produce greenness products with improved atmospheric correction for the effects of water vapor, ozone, and Rayleigh scattering. This improved product is

available now. The spatial analysis of the relationships between vegetation productivity and climate variables is made possible by the recent availability of the improved NDVI product and high-resolution gridded climate data (Daymet or PRISM).

In contrast to satellite-derived NDVI data, field measurements can provide direct measurements of NPP or NEP. The long Term Ecological Research (LTER) Network established by the National Science Foundation consists of 24 sites located throughout the climates and habitats of North America and Antarctica (Hobbie 2003). Annual measurements of aboveground NPP are available from at least at 11 LTER sites across North America (Knapp & Smith 2001). The analysis of relationships between vegetation productivity and climate variability is made possible by the availability of reliable measurements of NPP and climate variables (Knapp & Smith 2001).

In addition, the eddy covariance technique has emerged as an effective and popular way to assess ecosystem carbon exchange (Running et al. 1999, Baldocchi 2003). The eddy flux tower network, FLUXNET (e.g., AmeriFlux), provides continuous observations of ecosystem level exchanges of CO_2, water, energy and momentum spanning seasonal and interannual time scales. Accurate measurements of NEE, climate variables and/or soil moisture are available from FLUXNET. These are valuable data sets for examining relationships between vegetation activity and climate variability and influences of climate variability on carbon stocks in ecosystems.

AVHRR on board the NOAA series of polar-orbiting meteorological satellites (NOAA 7, 9, 11 and 14) provides observations of terrestrial vegetation with spatially and temporally consistent coverage. Satellite observations of vegetation cover the full range of vegetation types, climate zones, and disturbance (e.g., harvest, fire, logging, and insect

outbreaks) and management regimes in contrast to measurements provided by LTER sites and eddy-covariance networks. Satellite data and biogeochemical models can scale measurements to regional or larger scales so that the spatial analysis of the relationships between vegetation productivity and climate variability can be examined at regional or global scales.

3.8 References

Allen CD, Breshears DD (1998) Drought-induced shift of a forest-woodland ecotone: Rapid landscape response to climate variation. *Proceedings of the National Academy of Science*, **95**, 14839-14842.

Alward RD, Detling JK, Milchunas DG (1999) Grassland vegetation changes and nocturnal global warming. *Science*, **283**, 229-231.

Asrar G, Fuchs M, Kanemasu ET, Hatfield JL (1984) Estimating absorbed photosynthetic radiation and leaf area index from spectral reflectance in wheat. *Agronomy Journal*, **76**, 300-306.

Bachelet D, Neilson RP, Lenihan JM, Drapek RJ (2001) Climate change effects on vegetation distribution and carbon budget in the United States. *Ecosystems*, **4**, 164-185.

Baldocchi, D.D., 2003. Assessing the eddy covariance techniques for evaluating carbon dioxide exchange rates of ecosystems: past, present, and future. *Global Change Biology*, **9**, 479-492.

Billings, W.D., Peterson, K.M., Luken, J.O., & Mortensen, D.A., 1984. Interaction of increasing atmosphere carbon-dioxide and soil-nitrogen on the carbon balance of Tundra microcosms. *Oecologia*, **65**, 26-29.

Braswell BH, Schimel DS Linder E Moore III B (1997) The response of global terrestrial ecosystems to interannual temperature variability. *Science*, **278**, 870-872.

Brown JH, Valone TJ, Curtin CG (1997) Reorganization of an arid ecosystem in response to recent climate change. *Proceedings of the National Academy of Science*, **94**, 9729-9733.

Choudhury BJ (1987) Relationships between vegetation indices, radiation, absorption, and net photosynthesis evaluated by a sensitivity analysis. *Remote Sensing of Environment*, **22**, 209-233.

Daly F, Bachelet D, Lenihan JM, Neilson RP, Parton W, Ojima D (2000) Dynamic simulation of tree-grass interactions for global change studies. *Ecological Applications*, **10**, 449-469.

Daly, C., G.H. Taylor, W. P. Gibson, T.W. Parzybok, G. L. Johnson, P. Pasteris. 2001. High-quality spatial climate data sets for the United States and beyond. *Transactions of the American Society of Agricultural Engineers*, **43**, 1957-1962.

Davenport ML, Nicholson SE (1993) On the relation between rainfall and the normalized difference vegetation index for diverse vegetation types in East Africa. *International Journal of Remote Sensing*, **14**, 2369-2389.

Davidowitz G (2002) Does precipitation variability increase from mesic to xeric biomes? *Global Ecology & Biogeography*. **11**, 143-154.

Dingman SL (1994) *Physical Hydrology*. Prentice Hall, Englewood Cliffs, N.J.

Eagleson PS, Segarra RI (1985) Water-limited equilibrium of savanna vegetation systems. *Water Resources Research*, **21**, 1483-1493.

Easterling DR, Horton B, Jones PD, et al. (1997) Maximum and minimum temperature trends for the globe. *Science*, **277**, 364-367.

Eidenshink JC (1992) The 1990 conterminous US AVHRR data set. *Photogrammetric Engineering & Remote Sensing*, **58**, 809-813.

Epstein HE, Burke IC, Lauenroth WK (1999) Response of the shortgrass steppe to changes in rainfall seasonality. *Ecosystems*, **2**, 139-150.

Frank DA, Inouye RS (1994) Temporal variation in actual evapotranspiration of terrestrial ecosystems – Patterns and ecological implications. *Journal of Biogeography*, **21**, 401-411.

Friedl MA, Muchoney D, McVicar D, Gao F, Hodges J, Strahler A (2000). Characterization of North American land cover from NOAA-AVHRR data using the EOS-MODIS classification algorithm. *Geophysical Research Letters*, **27**, 977-980.

Goodale CL, Davidson EA (2002) Uncertain sinks in the shrubs. *Nature*, **418**, 593-594.

Gorham, E., 1991. Northern peatlands - role in the carbon-cycle and probable responses to climatic warming. *Ecological Applications*, **1**, 182-195.

Goward SN, Prince SD (1995) Transient effects of climate on vegetation dynamics: satellite observations. *Journal of Biogeography*, **22**, 549-563.

Groisman PY, Easterling DR (1994) Variability and trends of precipitation and snowfall over the United States and Canada. *Journal of Climate*, **7**, 184-205.

Haxeltine A, Prentice I, Cresswell I (1995) A coupled carbon and water flux model to predict vegetation structure. *Journal of Vegetation Science*, **7**, 651-666.

Hobbie, J.E., 2003. Scientific accomplishments of the long term ecological research program: an introduction. *BioScience*, **53**, 17-20.

Holben BN (1986) Characteristics of maximum-value composite images from temporal AVHRR data. *International Journal of Remote Sensing*, **7**, 3473-3491.

Houghton, R.A., Davidson, E.A., & Woodwell, G.M., 1998. Missing sinks, feedbacks, and understanding the role of terrestrial ecosystems in the global carbon balance. *Global Biogeochemical Cycles*, **12**, 25-34.

Hulme M, Viner D (1998) A climate change scenario for the tropics, *Climatic Change*, **39**, 145-176.

Intergovernmental Panel on Climate Change (1996) *Climate Change 1995: The Science of Climate Change. Contribution of Working Group I to the Second Assessment Report of the IPCC*, Cambridge University Press, New York.

Intergovernmental Panel on Climate Change (2001), *Climate Change 2001: The Scientific Basis*. *IPCC Third Assessment Report*, Cambridge University Press, New York.

Jackson RB, Banner JL, Jobbagy EG, Pockman WT, Wall DH (2002) Ecosystem carbon loss with woody plant invasion of grasslands. *Nature*, **418**, 623-626.

Jobbagy EG, Sala OE (2000) Controls of grass and shrubs aboveground production in the Patagonian steppe. *Ecological Applications*, **10**, 541-549.

Karl TR, Williams CN, Quinlan FT, Boden TA (1990) *United States Historical Climatology Network (HCN) Serial Temperature and Precipitation Data*, Environmental Science Division, Publication No. 3404, Carbon Dioxide Information and Analysis Center, Oak Ridge National Laboratory, Oak Ridge, TN, 389 pp.

Karl TR, Knight RW, Plummer N (1995) Trends in high-frequency climate variability in the twentieth century. *Nature*, **377**, 217-220.

Kawabata A, Ichii K, Yamaguchi Y (2001) Global monitoring of interannual changes in vegetation activities using NDVI and its relationships to temperature and precipitation. *International Journal of Remote Sensing*, **22**, 1377-1382.

Keeling, C.D., Chin, J.F.S., & Whorf, T.P., 1996. Increased activity of northern vegetation inferred from atmospheric CO_2 measurements. *Nature*, **382**, 146-149.

Knapp AK, Smith MD (2001) Variation among biomes in temporal dynamics of aboveground primary production. *Science*, **291**, 481-484.

Kramer K, Leinonen I, Loustau D (2000) The importance of phenology for the evaluation of impact of climate change on growth of boreal, temperate, and Mediterranean forest ecosystems: An overview. *International Journal of Biometeorology*, **44**, 67-75.

Larcher, W., Physiological and Plant Ecology. 2nd ed., Springer-Verlag, New York, 1983.

Lauenroth WK, Sala OE (1992) Long-term forage production of North American shortgrass steppe. *Ecological Applications*, **2**, 397-403.

Le Houerou HN, Bingham RL, Skerbek W (1988) Relationship between the variability of production and the variability of annual precipitation in world arid lands. *Journal of Arid Environments*, **15**, 1-18.

Los SE, Collatz GJ, Bounoua L, Sellers PJ, Tucker CJ (2001) Global interannual variations in sea-surface temperature and land surface vegetation, air temperature, and precipitation. *Journal of Climate*, **14**, 1535-1549.

Loveland TR, Zhu Z, Ohlen DO, Brown JF, Reed BC, Yang L (1999) An Analysis of the IGBP Global Land-Cover Characterization Process. *Photogrammetric Engineering and Remote Sensing*, **65**, 1021-1032.

Lucht, W., Prentice, I.C., Myneni, R.B., Sitch, S., Friedlingstein, P. et al., 2002, Climatic control of the high-latitude vegetation greening trend and Pinatubo effect. *Science,* **296**, 1687-1689.

Melillo, J.M., McGuire, A.D., Kicklighter, D.W., Moore, B., Vorosmarty, C.J., & Schloss, A.L., 1993. Global climate change and terrestrial net primary production. *Nature,* **363**, 234-240.

Mitchell SW, Csillag F (2001) Assessing the stability and uncertainty of predicted vegetation growth under climatic variability: northern mixed grass prairie. *Ecological Modelling*, **139**, 101-121.

Moody A, Strahler AH (1994) Characteristics of composited AVHRR data and problems in their classification. *International Journal of Remote Sensing*, **15**, 3473-3491.

Myneni RB, Hall FG, Sellers PJ, Marshak AL (1995) The interpretation of spectral vegetation indexes. *IEEE Transactions on Geoscience and Remote Sensing*, **33**, 481-486.

Myneni RB, Keeling CD, Tucker CJ, Asrar G, Nemani RR (1997) Increased plant growth in the northern high latitudes from 1981-1991. *Nature*, **386**, 698-702.

Myneni RB, Dong J, Tucker CJ, et al. (2001) A large carbon sink in the woody biomass of northern forests. *Proceedings of the National Academy of Sciences of the United States of America*, **98**, 14784-14789.

Neilson RB (1986) High resolution climatic analysis and southwest biogeography. *Science*, **232**, 27-34.

Neilson RB, King GA, Koerper G (1992) Toward a rule-based biome model. *Landscape Ecology*, **7**, 27-43.

Neilson, RB (1995) A model for predicting continental-scale vegetation distribution and water balance. *Ecological Applications*, **5**, 363-385.

Nemani R, White M, Thornton P, Nishida K, Reddy S, Jenkins J, Running S (2002) Recent trends in hydrological balance have enhanced the terrestrial carbon sink in the United States. *Geophysical Research Letters*, **29**, 2002GLO14867.

Pake CE, Venable DL (1995) Is coesxistence of Sonoran desert annuals mediated by temporal variability in reproductive success? *Ecology*, **76**, 246-261.

Pake CE, Venable DL (1996) Seed bands in desert annuals: Implications for persistence and coexistence in variable environments. *Ecology*, **77**, 1427-1435.

Pan Y, McGuire AD, Melillo JM, Kicklighter DW, Sitch S, Prentice IC (2002) A biogeochemistry-based dynamic vegetation model and its application along a moisture gradient in the continental United States. *Journal of Vegetation Science*, **13**, 369-382.

Paruelo JM, Lauenroth WK (1995) Regional patterns of normalized difference vegetation index in North American shrublands and grasslands. *Ecology*, **76**, 1888-1898.

Paruelo JM, Lauenroth WK (1996) Relative abundance of plant functional types in grasslands and shrublands of North America. *Ecological Applications*, **6**, 1212-1224.

Paruelo JM, Lauenroth WK (1998) Interannual variability of NDVI and its relationship to climate for North American shrublands and grasslands. *Journal of Biogeography*, **25**, 721-733.

Paruelo JM, Lauenroth WK, Burke IC, Sala OE (1999) Grassland precipitation-use efficiency varies across a resource gradient. *Ecosystems*, **2**, 64-68.

Potter CS, Brooks V (1998) Global analysis of empirical relations between annual climate and seasonality of NDVI. *International Journal of Remote Sensing*, **19**, 2921-2948.

Prentice CI, Cramer W, Harrison SP, Leemans R, Monserud RA, Solomon AM (1992) A global biome model based on plant physiology and dominance, soil properties and climate. *Journal of Biogeography*, **19**, 117-134.

Randserson, J.T., Field, C.B., Fung, I.Y., & Tans, P.P., 1999. Increases in early season ecosystem uptake explain recent changes in the seasonal cycle of atmospheric CO2 at high northern latitudes. *Geophysical Research Letters,* **26**, 2765-2769.

Richard Y, Poccard I (1998) A statistical study of NDVI sensitivity to seasonal and interannual rainfall variations in Southern Africa. *International Journal of Remote Sensing*, **19**, 2907-2920.

Ricketts TH, Dinerstein E, Olson DM, et al. (1999) *Terrestrial ecoregions of North America: A Conservation Assessment*. Island Press, Covelo, CA.

Running, S.W., Baldocchi, D.D., Turner, D.P., Gower, S.T., Bakwin, P.S. & Hibbard, K.A., 1999. A global terrestrial monitoring network integrating tower fluxes, flask sampling, ecosystem modeling and EOS satellite data. *Remote Sensing of Environment*, **70**, 108-127.

Sala OE, Parton WJ, Joyce LA, Lauenroth WK (1988) Primary production of the Central Grassland region of the United States. *Ecology*, **69**, 40-45.

Sellers PJ, Berry JA, Collatz GJ, Field CB, Hall FG (1992) Canopy reflectance, photosynthesis, and transpiration. III. A reanalysis using improved leaf models and a new canopy integration scheme. *Remote Sensing of Environment*, **42**, 187-216.

Shinoda M (1995) Seasonal phase lag between rainfall and vegetation activity in tropical Africa as revealed by NOAA satellite data. *International Journal of Climatology*, **15**, 639-656.

Spanner MA, Pierce LL, Running SW, Peterson DL (1990) The seasonality of AVHRR data of temperate coniferous forests: relationship with leaf area index. *Remote Sensing of Environment*, **33**, 97-112.

Stephenson NL (1990) Climatic control of vegetation distribution: The role of water balance. *The American Naturalist*, **135**, 649-670.

Still CJ, Berry JA, Collatz GJ, DeFries RS (2003) Global distribution of C3 and C4 vegetation: Carbon cycle implications. *Global Biogeochemical Cycles*, **17**, 1006, doi:10.1029/2001GB001807.

Thornton, P.E., Running, S.W., & White, M.A., 1997. Generating surfaces of daily meteorological variables over large regions of complex terrain. *Journal of Hydrology*, **190,** 214-251.

Tucker, C.J., Slayback, D.A., Pinzon, J.E., Los, S.O., Myneni, R.B., and Taylor, M.G., 2001, Higher northern latitude normalized difference vegetation index and growing season trends from 1982 to 1999. *International Journal of Biometeorology,* **45**, 184-190.

Van Langevelde F, Van de Vijver CADM, Kumar L (2003) Effects of fire and herbivory on the stability of savanna ecosystems. *Ecology*, **84**, 337-350.

VEMAP Members (1995) Vegetation/ecosystem modeling and analysis project: comparing biogeography and biogeochemistry models in a continental-scale study of terrestrial ecosystem responses to climate change and CO_2 doubling. *Global Biogeochemical Cycles*, **9**, 407-437.

Walker BH, Noy-Meir I (1982) Aspects of the stability and resilience of savanna ecosystems. In: *Ecology of Tropical Savannas* (eds Huntley BJ, Walker BH), pp. 556-590. Springer-Verlag, Berlin.

Walter H (1971) *Natural savannas. Ecology of Tropical and Sub-Tropical Vegetation*. Oliver and Boyd, Edinburgh.

Wang J, Price KP, Rich PM (2001) Spatial patterns of NDVI in response to precipitation and temperature in the central Great Plains. *International Journal of Remote Sensing*, **22**, 3827-3844.

Webb W, Szarek S, Luenroth W, Kinerson R, Smith M (1978) Primary productivity and water use in native forest, grassland, and desert ecosystems. *Ecology*, **59**, 1239-1247.

White, MA, Thornton, PE, Running, SW, Nemani, RR (2000) Parameterization and sensitivity analysis of the BIOME-BGC terrestrial ecosystem process model: net primary production controls. *Earth Interactions*, **4**, 1-85.

Woodward FI (1987) *Climate and Plant Distribution*. Cambridge University Press, Cambridge, UK.

Woodwell, G.M., & Mackenzie, F.T., Biotic Feedbacks in the Global Climatic System, 416 pp., Oxford Univ. Press, New York, 1995.

Yang L, Wylie BK, Tieszen LL, Reed BC (1998) An analysis of relationships among climate forcing and time-integrated NDVI of grasslands over the U.S. northern and central Great Plains. *Remote Sensing of Environment*, **65**, 25-37.

Yang W, Yang L, Merchant JW (1997) An assessment of AVHRR/NDVI-ecoclimatological relations in Nebraska, U.S.A. *International Journal of Remote Sensing*, **18**, 2161-2180.

Zhou, L., Tucker, C.J., Kaufmann, R.K., Slayback, D., Shabanov, N.V., and Myneni, R.B., 2001, Variations in northern vegetation activity inferred from satellite data of vegetation index during 1981 to 1999. *Journal of Geophysical Research,* **106**, 20069-20083.

Chapter 4

Expansion of western juniper in central Oregon: rates and carbon consequences

4.1 Introduction

Arid and semiarid ecosystems characterized by the coexistence of herbaceous and woody vegetation cover roughly 45% of the global land surface (Burgess 1995, Bailey 1998). During the past 150 years, the balance between herbaceous and woody vegetation in arid and semiarid regions has shifted to favor trees and shrubs (Archer 1994). These regions have experienced woody plant proliferation in areas dominated by herbaceous vegetation and/or shrubs (Archer 1989, Van Auken 2000). This phenomenon has been attributed to climate change (Brown et al. 1997), atmospheric CO_2 enrichment (Polley et al. 2002), fire suppression (Houghton et al. 2000, Tilman et al. 2000), overgrazing (Archer 1989, Brown & Archer 1999), and nitrogen deposition (Köchy & Wilson 2001). Their relative contributions to the expansion of woody plant cover still remain uncertain (Van Auken 2000).

Western juniper woodlands in the Pacific Northwest have been expanding during the past century. The expansion of western juniper has been primarily documented at local scales (Burkhardt & Tisdale 1969, 1976, Caraher 1978, Eddleman 1987, Miller & Wigand 1994, Miller & Rose 1995, Knapp & Soulé 1998, Soulé & Knapp 1999, Soulé et

al. 2003). However, little research has examined western juniper expansion at regional scales. To date, the rates of change and geographical extent of western juniper expansion have not been systematically quantified, and the resulting changes in carbon (C) pools have not been quantitatively tracked or assessed at regional scales. Thus, we know little about changes in plant C pools that may have occurred in western juniper woodlands due to recent changes in climate and land use.

This study has four objectives: (1) to evaluate the feasibility of using Landsat data to examine the expansion of woody plant cover; (2) to estimate the rates of the expansion of western juniper in central Oregon; (3) to estimate the changes in C stocks in woody biomass caused by the expansion of western juniper; (4) to assess the potential impact of the expansion of western juniper on the regional C budget. I sought to quantify local and regional changes in woody plant cover and aboveground C pools across 650 km^2 of western juniper woodland in central Oregon from 1975 to 2000. I began by quantifying woody cover in 1975, 1989, and 2000, respectively using Landsat data. Spatially explicit changes in woody cover were then computed. Regional changes in aboveground C storage over the 25-year period were then estimated using allometric relationships between aboveground biomass and woody plant canopy cover. Finally, I assessed the potential impact of western juniper expansion on the regional C budget.

4.2 Background

The abundance of woody plants has increased substantially in savannas, shrublands, and grasslands worldwide during the last 150 years (Van Auken 2000). Woody plant proliferation has been attributed to climate change (Brown et al. 1997), atmospheric CO_2 enrichment (Polley et al. 2002), fire suppression (Houghton et al. 2000, Tilman et al.

2000), overgrazing (Archer 1989, Brown & Archer 1999), nitrogen deposition (Köchy & Wilson 2001), and a combination of two or more of these factors (Van Auken 2000). Fire suppression reduces the occurrences of fires that would have killed small trees/shrubs. Overgrazing by domestic livestock also reduces fuel load, which decreases the frequency of fires. This coupled with a warmer, wetter climate conducive to seedling establishment has created favorable conditions for juniper to establish and expand its range (Azuma et al. 2005). The relative importance of these mechanisms is still controversial (Van Auken 2000).

Woody plant proliferation in grasslands and savannas adversely affects herbaceous productivity and livestock handling, and thus has been a concern of land managers (Fisher 1950, Rappole et al. 1986). The expansion of woody plant cover can also lead to changes in the amount of C stored in plant biomass as well as in soils. A recent U.S. C budget reconciled land- and atmosphere-based estimates by incorporating a large sink (0.12-0.13 Pg C per year) to account for woody plant proliferation in non-forest areas in the western U.S. (Pacala et al. 2001).

Woody plant proliferation has been documented primarily at local scales in the US (Schlesinger et al. 1990, Miller & Rose 1995, Brown et al. 1997, Briggs et al. 2002a, b, Asner et al. 2003). Little research has examined the expansion of woody plant cover in arid and semiarid regions at regional scales (Asner et al. 2003). Neither the rates of change nor the geographical extent of the phenomenon have been systematically quantified (Anser et al. 2003), not to mention the resulting C consequences and the implications on regional C budgets. About 21%-40% of the US C sink was attributed to woody plant proliferation (Houghton et al. 1999, 2000, Pacala et al. 2001). However,

these studies emphasized the large uncertainty in their estimates, and regional-scale analysis of the rates and geographical extent of woody plant proliferation and the resulting C sequestration are needed.

Western juniper woodlands in Oregon have increased dramatically since the 1930s (Azuma et al. 2005). Western juniper (*Juniperus occidentalis* ssp. *occidentalis*) is a small to medium-statured native tree of the Pacific Northwest region (Karl & Leonard 1996). Western juniper is primarily distributed in California and Oregon, extending from Lassen County California northward across Oregon to the Columbia River and from just east of the Cascade Mountains to the Owyhee Plateau of southeastern Idaho (Eddleman et al. 1994). Scattered stands are also distributed in southeastern Washington and in northwestern Nevada. Juniper cover is generally lower than 50% (Azuma et al. 2005). Most juniper woodlands are privately owned. In eastern Oregon, for example, 52% is privately owned (Azuma et al. 2005).

The land area occupied by western juniper is uncertain. Eddleman et al. (1994) estimated that western juniper woodlands exist on a minimum of 932,000 hectares in Oregon based on several literature sources to produce these estimates. In 1936, Cowlin et al. (1942) estimated the area of juniper forest in eastern Oregon to be around 0.17 million hectares. In 1999, Gedney et al. (1999) estimated the area of juniper forest to be 0.89 million hectares using aerial photography. However, Azmua et al. (2005) suggested that juniper forest and savanna in Oregon have increased dramatically since the 1930s from about 0.61 million hectares to around 2.63 million hectares.

Western juniper is a native tree that reproduces by seed (Bedell et al. 1993). The germination of seeds requires a continuous period below a certain unknown maximum

cool or cold temperature. Seedlings establish primarily under big or low sagebrush plants, bitterbrush, rabbitbrush, aspen or juniper, and conifers, and this protected micro-environment appears conducive to germination and establishment of juniper seedlings (Bedell et al. 1993). Western juniper appears well adapted to all types of soils, ranging from shallow to deep, dry to sub-irrigated, and sandy to clay texture (Driscoll 1964a, 1964b, Green 1975, Dyksterhuis 1981, Josaitis 1991, Lentz & Simonson 1986, Pomerencing et al. 1983, Bedell et al. 1993). The climate that western juniper grows is typically semiarid with dry hot summers, cold winters, and precipitation ranges from 250 to 355 mm (Eddleman et al. 1994). Precipitation comes mostly in November-January and May-June, and July-September is particularly dry (Eddleman et al. 1994).

The best-documented ecological and environmental impacts of western juniper expansion include the alterations of herbaceous and woody plant cover (Eddleman 1987, Bedell et al. 1993, Knapp & Soulé 1998), phytomass production (Vaitkus & Eddleman 1991), species richness and abundance (Bedell et al. 1993), and nutrient cycles (Bedell et al. 1993). The effects of accelerated soil erosion, increased surface runoff, reduced infiltration, and decreased wildlife habitat have also been reported (Bedell et al. 1993), but are not supported by experimental evidence (Gifford 1987, Belsky 1996).

The expansion of western juniper has been attributed to overgrazing by domestic livestock, fire suppression, climate change, and CO_2 enrichment (Burkhardt & Tisdale 1976, Eddleman et al. 1994, Knapp & Soulé 1998). The relative contributions of these mechanisms remain uncertain. Many studies suggested that the invasion of western juniper was directly related to the cessation of fires (Burkhardt & Tisdale 1976). Fire occurrences were common in western juniper woodlands before Euro-American

settlement (Martin & Johnson 1979, Shinn 1980). These fires were usually caused by lighting and Native Americans, and resulted in a landscape characterized by a mosaic of scattered woodlands (Karl & Leonard 1996). Fires have been much less frequent during the past century due to active fire control, development of roads and other fire barriers, and reduced fuel because of heavy grazing and a shift towards decreased precipitation (Burkhardt & Tisdale 1976). Eddleman et al. (1994) suggested that the reduction in fuel load partly caused by livestock grazing may play a larger role in the reduction in fire frequency than did active suppression, whereas Martin (1978) and Martin & Johnson (1979) suggested that sagebrush-grass communities will be dominated by western juniper in the absence of fire regardless of grazing pressure. Some studies suggested the expansion was due to the combination of optimal climatic conditions, reduced fire return intervals, and the indirect of livestock through the reduction of fine fuels (Miller & Rose 1995).

The expansion of western juniper in the Pacific Northwest during the last century has been well documented at local scales (Burkhardt & Tisdale 1969, 1976, Caraher 1978, Eddleman 1987, Miller & Wigand 1994, Miller & Rose 1995, Knapp & Soulé 1998, Soulé & Knapp 1999, Soulé et al. 2003). For example, Knapp & Soulé (1998) examined the expansion of western juniper in the Horse Ridge Research Natural Area using aerial photography, and suggested that juniper cover had increased from 14.6% in 1951 to 34.5% in 1995. However, these studies are limited to the analysis of rates of western juniper expansion and driving factors (e.g., grazing, fire suppression, CO_2 enrichment) at local scales. Regional changes in western juniper cover and C stocks in woody biomass at regional scales have not been quantified.

4.3 Study region

This study was conducted over an area of approximately 650 km^2 located in central Oregon (Fig. 4.1). The elevation of this region ranges from 1046 to 1783 m. The climate of the region is semiarid. Annual precipitation at nearby Bend is winter-dominated and averages 303 mm (Williams et al. 2005). Annual average minimum and maximum temperatures at Bend are 31.7 ˚C and 59.8 ˚C, respectively (Williams et al. 2005).

This region is primarily dominated by western juniper woodland, ponderosa pine forest and woodland, and big sagebrush shrubland (Kiilsgaard 1999). Fig.1 shows the distribution of western juniper across the study region.

4.4 Data

4.4.1 Landsat data

The Landsat data used in this study included a MSS (Multispectral Scanner) image acquired in 1975, a TM (Thematic Mapper) image acquired in 1989, and a ETM+ (Enhanced Thematic Mapper Plus) image acquired in 2000 (Table 4.1). All the Landsat data were acquired from Global Land Cover Facility (http://www.landcover.org). The six reflective bands were used for either ETM+ or TM image.

The Landsat ETM+ image was georeferenced using seventy-three ground controls points (GCPs) selected with reference to 1m Digital Orthophoto Quadrangles (DOQs). The geometric correction was performed using a first-order transformation with an overall root-mean-squared error (RMSE) of less than 0.5 pixel. The Landsat TM and MSS images were geometrically corrected with reference to the georeferenced Landsat ETM+ image with RMSE of less than 0.5 pixel, respectively.

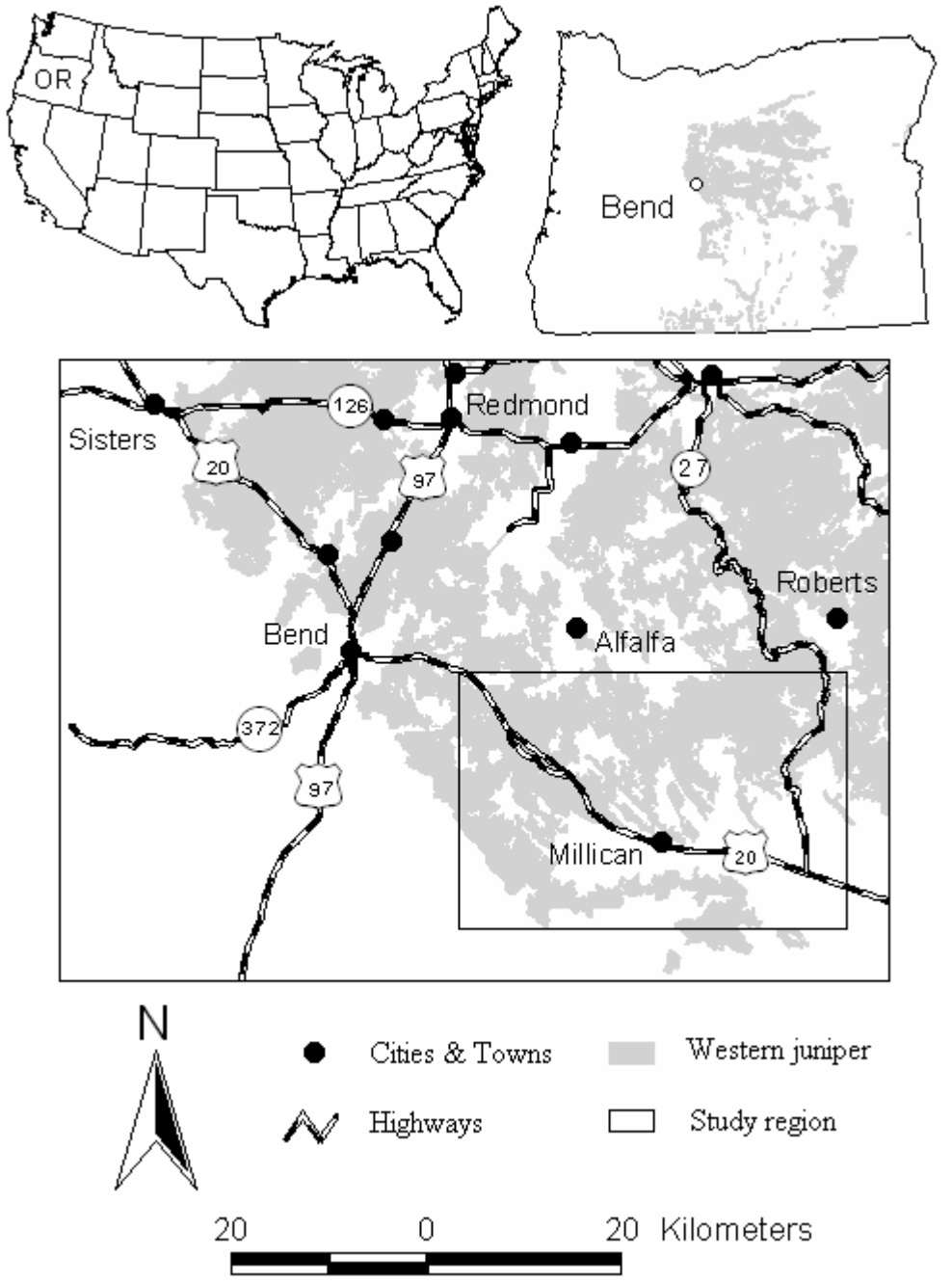

Fig. 4.1 Location of the study region (Millican, Oregon). The shaded area shows the distribution of western juniper woodland based on the Oregon Gap Analysis 1998 Land Cover for Oregon (Kiilsgaard 1999).

Table 4.1 Landsat data (MSS, TM, and ETM+) used in this study

Sensor	Path/Row	Acquisition Date	Bands	Resolution
ETM+	45/29 (WRS-2)	09/18/2000	1-5, 7	30m
TM	45/29 (WRS-2)	09/12/1989	1-5, 7	30m
MSS	48/29 (WRS-1)	10/01/1975	1-4	57m

The digital number (DN) values of the geometrically-corrected ETM+ data were converted to at-satellite radiance using the following equation (Markham & Barker, 1987; Price, 1987):

$$L_\lambda = ((LMAX_\lambda - LMIN_\lambda) / (QCALMAX-QCALMIN)) \times (QCAL-QCALMIN) + LMIN_\lambda \quad (1)$$

where L_λ is at-satellite radiance (W m^{-2} sr^{-1} μm^{-1}), QCAL = DN, $LMAX_\lambda$ and $LMIN_\lambda$ are the spectral radiances that are scaled to QCALMAX and QCALMIN in W m^{-2} sr^{-1} μm^{-1}, respectively, QCALMAX = 255, and QCALMIN = 1.

At-satellite radiances were then converted to surface reflectance by correcting for both solar and atmospheric effects. The general equation for converting at-satellite radiance to surface reflectance (Moran et al., 1992) is:

$$\rho = \frac{\pi(L_s - L_d)}{\tau_v(E_0 \cos\theta_z \tau_z + E_d)} \quad (2)$$

where ρ is the surface reflectance, L_s is the at-satellite radiance, L_d is the path radiance (W m^{-2} μm^{-1}), E_0 is the solar spectral irradiance (W m^{-2} μm^{-1}), θ_z is solar zenith angle, τ_v is the atmospheric transmittance along the path from the ground surface to the sensor, τ_z is the atmospheric transmittance along the path from the sun to the ground surface, and E_d is downward diffuse radiation (W m^{-2} μm^{-1}). I converted at-satellite radiance values to surface reflectance using a dark object subtraction (DOS) approach (Chavez, 1989) which assumes no atmospheric transmittance loss and no downward diffuse radiation (Song et al. 2001). The surface reflectance of the dark object was assumed to be 1%, and thus the path radiance was assumed to be the dark-object radiance minus the radiance contributed by 1% surface reflectance (Moran et al., 1992, Song et al. 2001). The DN of the dark object is often estimated from the ETM+ image using the lower bound of the histogram

derived from each band (Moran et al., 1992). The DN value of the dark object here was selected as the darkest DN with at least a thousand pixels over the entire scene (Teillet & Fedosejevs, 1995, McDonald et al., 1998, Song et al. 2001).

4.4.2 Aerial photographs

Aerial photographs were used to develop training and validation data for estimating percent woody cover from Landsat data. A DOQ (1m) was obtained from the Oregon Geospatial Enterprise Office for 2000. Two color-infrared aerial photographs were obtained from the USGS EarthExplorer for the study region for 1973 (1:300,000) and 1987 (1:30,000). Each color-infrared aerial photograph was georeferenced using GCPs selected with reference to the 1m DOQ.

4.4.3 Forest inventory data

Although I would have preferred using measurements of aboveground biomass from a large sample of trees representing the complete range of western juniper conditions found in the region, time and funding restrictions limited us to using available tree measurements data. I obtained the Pacific Northwest Forest Inventory and Analysis (PNW-FIA) Integrated Database (IDB) – Forest Inventory Data for California, Oregon, and Washington (Forest Inventory & Analysis Program 2004) from the Pacific Northwest Research Station. The PNW-FIA IDB database contains the most recent periodic inventory data collected by PNW-FIA, the National Forest System (NFS: Regions 5 and 6), and the Bureau of Land Management (BLM) in California, Oregon, and Washington. This database contains an extensive amount of measured and calculated information for

each inventory plot, and is the primary database used for summary and analysis of resource data in the Pacific Northwest (Forest Inventory & Analysis Program 2004).

The PNW-FIA IDB database contains measurements of aboveground biomass and crown width for a large number of tree species, including western juniper. The total aboveground wood biomass is the oven-dry weight of the woody components of the tree (tons). This biomass is the accumulated weight of the stem, bark, stump, top and live woody branches. It was calculated for all live trees >= 2.5 cm dbh. The biomass of foliage, cones, fruits and roots were not calculated in the IDB database and thus it was not included in this estimate of aboveground biomass.

Biomass of the stem was calculated from the cubic volume of the total stem which includes the stump and top. Tree bole biomass, regardless of whether it is merchantable bole or total stem, was calculated from the cubic volume estimate and the woody density factors as follows:

$$\text{Bole biomass in tons} = (\text{cubic volume} * \text{woody density}) / 2000 \quad (3)$$

Cubic volume (ground to tip, excluding all branches) (CVTS) is expressed as a function of DBH and total height. Available data were limited to measurements from 52 trees that well felled and sectioned for a western juniper site index study (Sauerwein 1982). The data were gathered in central, southern, and southeastern Oregon and from one plot in northeastern California, and the trees were believed to sample all site indexes throughout the range of western juniper – southwestern Idaho, eastern Oregon, northeastern California, and western Nevada (Chittester & MacLean 1984). The cubic volume (cubic feet) equation is (Chittester & MacLean 1984):

$$CVTS = BA*F*HT*(HT/(HT-4.5))^2 \quad (4)$$

$$F = 0.307 + 0.00086*HT - 0.0037*DBH*HT / (HT-4.5) \quad (5)$$

$$BA = 0.005454154 * DBH^2 \quad (6)$$

where F is the form factor, DBH is diameter at breast height outside bark (inches), and HT is total height including stump and tip (feet).

Biomass of the bark and live woody branches were calculated from published equations for western juniper using the following equations, respectively:

$$BB = \exp(-10.175 + 2.6333 \times \log(DBH \times \pi)) \quad (7)$$

$$BLB = \exp(-7.2775 + 2.3337 \times \log(DBH \times \pi)) \quad (8)$$

where BB is the biomass of the bark, and BLB is the biomass of live woody branches.

In addition to aboveground biomass data, crown width measurements were also used in this study. Crown width is the distance of the lowest part of the crown, from one side to the other. Crown widths are either field-measured or estimated in the office with equations based on DBH. The method used to determine crown width was identified for each measurement in the database.

Aboveground biomass and crown width data for western juniper obtained from this database were used to produce an empirical relationship between aboveground biomass and crown width. Only those trees that crown widths were directly measured in the field were used to establish this empirical relation. A total of 4467 western juniper trees were included in the analysis. This empirical relation in conjunction with field measurements was used to develop a pixel-level relationship between total aboveground biomass and percent woody cover.

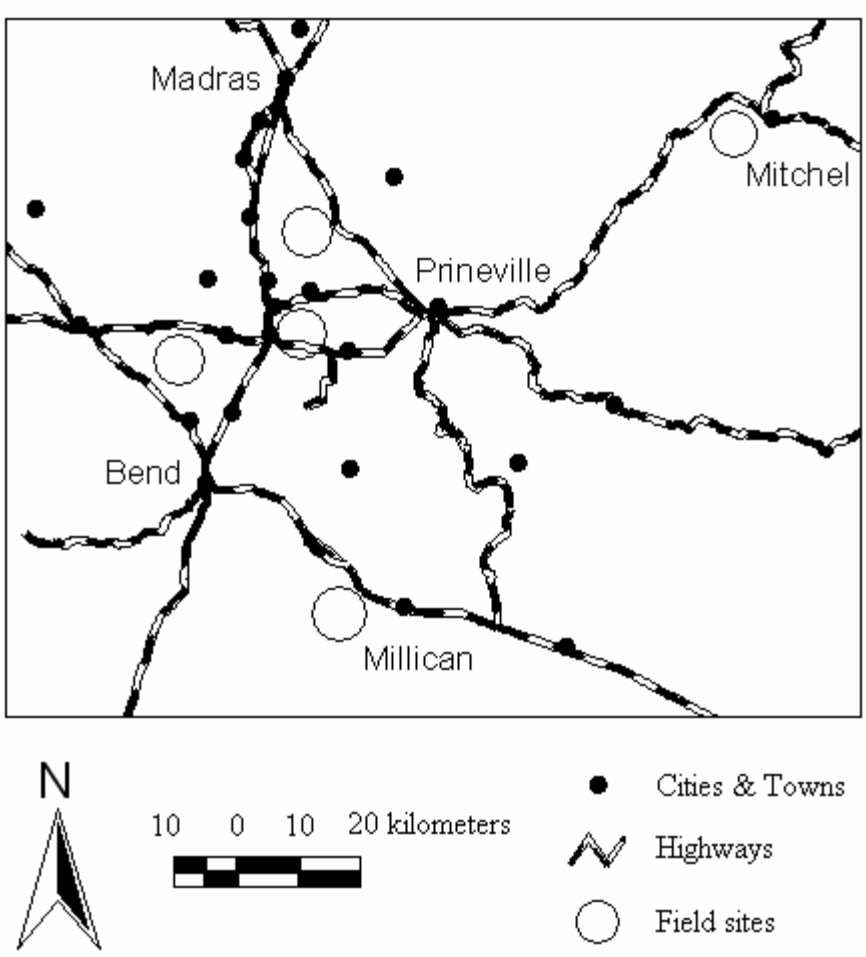

Fig. 4.2 Distribution of field sites in central Oregon. Each circle represents a field site. All sites were selected on public land. Five to six circular plots were selected at each site.

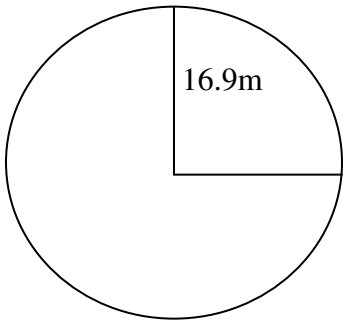

(a) Circular plot

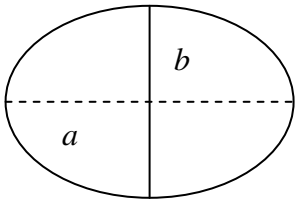

(b) Crown size

Fig. 4.3 A total of 33 circular plots were selected in the field: (a) Each plot has a radius of 16.9m, and thus has the same area as a Landsat TM/ETM+ pixel; (b) The projection of each crown is assumed to have a shape of an ellipse. *a* is the maximum crown width, and *b* is the minimum crown width.

4.4.4 Field measurements

The field work was conducted in the late July and early August, 2005. The majority of the juniper woodland in central Oregon is privately owned, which complicated the selection of field plots. Five sites were selected on public land (Fig. 4.2). At each site, 5 to 6 circular plots were selected (Fig. 4.3). Each plot has a radius of 16.9m, and thus each plot has the same area as a Landsat TM/ETM+ pixel.

For each plot, the crown size was measured for each individual tree within the plot. The projection of the crown is assumed to have a shape of an ellipse (Fig. 4.3). For each individual tree, the maximum crown width and minimum crown width were measured.

4.4.5 Digital elevation model (DEM)

The Shuttle Radar Topography Mission (SRTM) elevation data was obtained from the Global Land Cover Facility. SRTM is an international project in which agencies including the National Geospatial-Intelligence Agency (NGA) and the National Aeronautics and Space Administration (NASA) are involved. The mission of SRTM was to obtain elevation data on a near-global scale to generate the most complete high-resolution DEM database. The SRTM DEM obtained from the Global Land Cover Facility has 30m spatial resolution. Slope and aspect were calculated from the DEM in ERDAS IMAGINE (ERDAS, Inc.). Elevation along with slope and aspect were used as ancillary data to estimate percent woody cover from Landsat data.

4.5 Methods

4.5.1 Aerial photography analysis

Training and validation data were developed from aerial photographs. The three aerial photographs acquired in 1973, 1987, and 2000 were used for training and validation of the Landsat data acquired in 1975, 1989, and 2000, respectively. Each aerial photograph was classified into woody plant and 'other' categories using a combined texture analysis and unsupervised classifier. Three texture metrics, including mean, variance, and range (Anys et al. 1994), were calculated across the photograph based on a 3×3 moving window. These three metrics were a consistent indicator of woody plant presence or absence, because each tree/shrub crown produced a low pixel brightness value relative to surrounding soil and herbaceous vegetation (Asner et al. 2003).

For each aerial photograph, the brightness and the three texture metrics were combined together. An unsupervised classifier (ISODATA) was applied to the combined image. The classified image was aggregated to a woody/non-woody image. The 1m woody/non-woody map was degraded to 30m resolution. Each pixel on the degraded map corresponded to 30 pixel × 30 pixel on the 1m woody/non-woody map. The digital number of each pixel on the degraded map was the percentage of woody plant cover calculated from the 30 pixel × 30 pixel block on the woody/non-woody map.

The percent woody cover image was overlaid on the Landsat image. A number of pixels were randomly selected and were equally split into a training data set and a validation data set. For each pixel, the percent woody cover was extracted from the woody/non-woody map derived from the aerial photograph. Fig. 4.4 illustrates the process of developing training and validation data from aerial photographs.

4.5.2 Percent woody cover

Several methods have been used for estimating percent woody cover, including spectral mixture analysis (Adams et al. 1986, 1995, Smith et al. 1990, Xiao & Moody 2005), multiple linear regression model (Huang et al. 2001), and regression tree (Huang et al. 2001, Yang et al. 2003). Spectral mixture analysis assumes that the spectral signature of a given pixel is the linear combinations of contributions from unique surface materials, called endmembers (Adams et al. 1986, 1995, Smith et al. 1990). The fractions derived from spectral mixture analysis are sensitive to endmember signatures and endmember configurations, particularly in heterogeneous regions (Xiao & Moody 2005). Regression tree produces rule-based models for predictions of continuous variables based on training data (Yang et al. 2003). All these methods have proven effective for estimating percent woody cover. Huang et al. (2001) showed that linear regression model achieved comparable accuracy to regression tree for estimating percent canopy cover.

I used the stepwise linear regression model in this study. The development of the model was based on the training data derived from aerial photographs. The dependent variable was percent woody cover, and the independent variables included each spectral band, the variance of each band, normalized difference vegetation index (NDVI), TM5/NDVI, elevation, slope, and aspect. I used the backward stepwise model. A full model incorporating all the independent variables was developed first, and the best model was then developed by dropping a variable at a time. The resulting linear regression model was used to estimate percent woody cover for each pixel from each Landsat image. The estimates of percent woody cover were validated using the validation data derived from the aerial photographs.

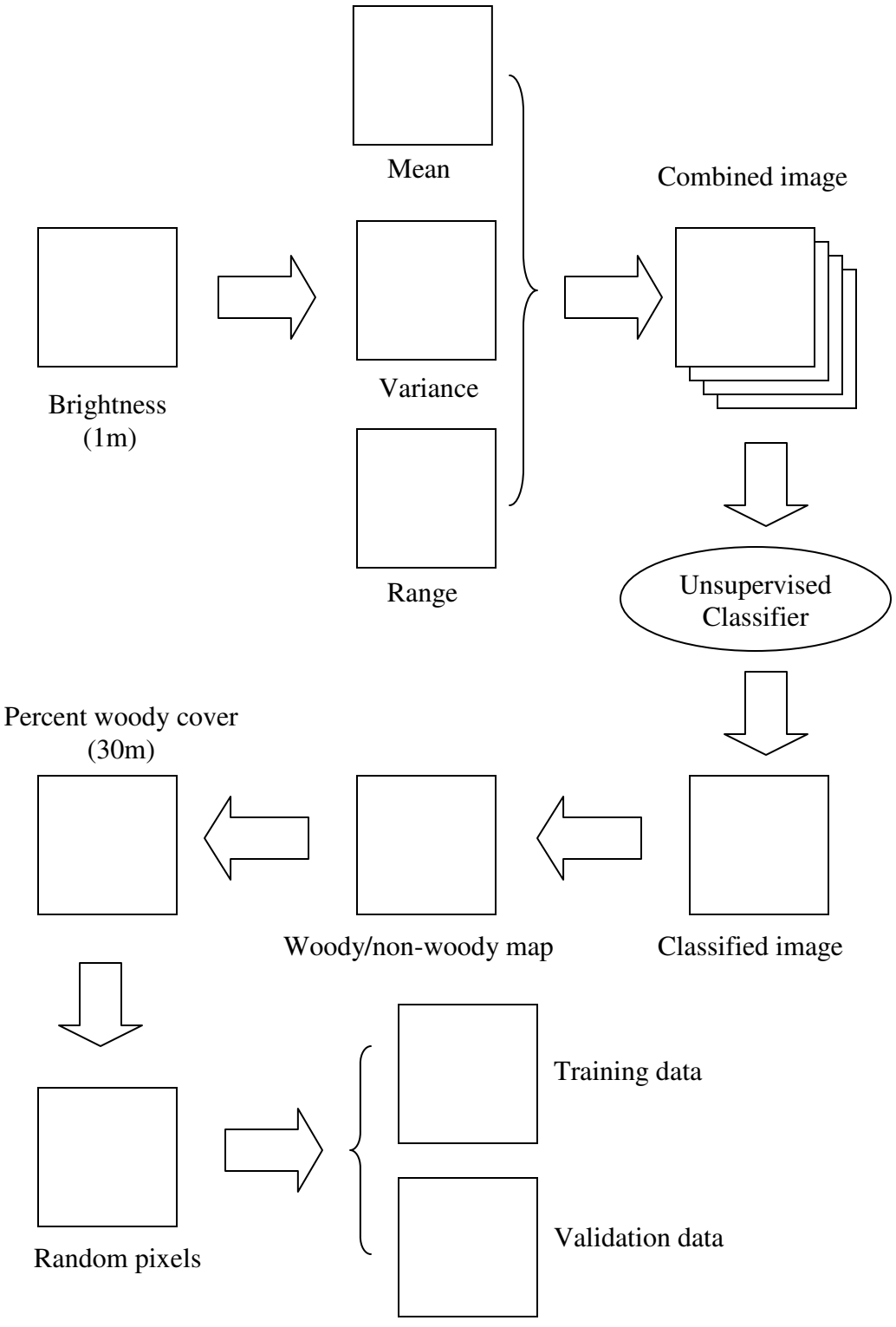

Fig. 4.4 Flow diagram of the development of training and validation data from aerial photographs.

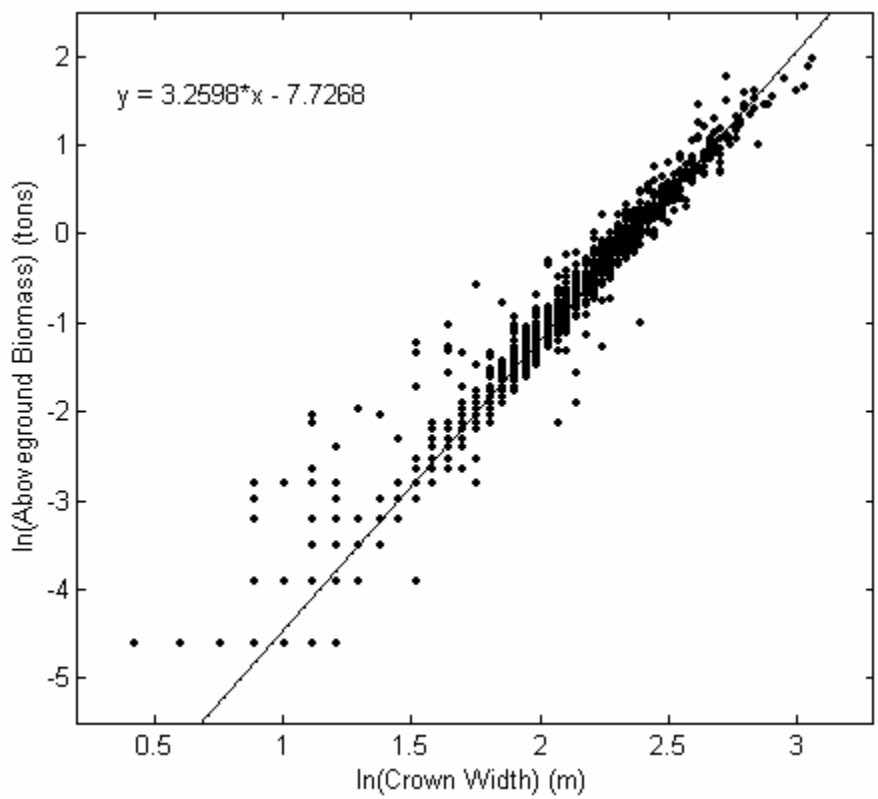

Fig. 4.5 Log-linear relationship between aboveground biomass and crown width for western juniper in the Pacific Northwest based on measurements from PNW-FIA IDB database.

4.5.3 Changes in carbon stocks in woody biomass

One of the objectives of this study was to estimate the changes in C stocks in woody biomass caused by the expansion of western juniper. In order to translate percent woody cover to C stocks in woody biomass, I developed a pixel-level relationship between total aboveground biomass and percent woody cover. This relationship was developed from forest inventory data and field measurements.

The PNW-FIA IDB database (Forest Inventory & Analysis Program 2004) contains measurements of aboveground biomass and crown width for a large number of western juniper trees. An empirical relation between aboveground biomass and crown width for western juniper was developed from the PNW-FIA IDB database (Fig. 4.5, $R^2 = 0.98$, $p < 0.001$):

$$\ln(ABD) = -7.7268 + 3.2598 \ln(CD) \quad (9)$$

where ABD is the aboveground biomass, and CD is the crown width. The aboveground biomass is the oven-dry weight of the woody components of the tree, including stem, bark, stump, top and live woody branches. The biomass of foliage, cones, fruits and roots was not calculated in the IDB and was not included in this estimate of aboveground biomass (Forest Inventory & Analysis Program 2004). Biomass of the stem was calculated from the cubic volume of the total stem which included the stump and top, and biomass of the bark and live woody branches were calculated from published equations (Forest Inventory & Analysis Program 2004). Thus, the aboveground biomass was not directly measured.

As mentioned above, the crown size of each individual tree was measured for each circular plot selected in the field. For each plot, the empirical relation (equation (9)) was

used to estimate the aboveground biomass for each individual tree from the measurements of crown width. The total aboveground biomass of each plot was simply the sum of aboveground biomass of all the individual trees within the plot.

For each plot, the crown area of each individual tree was calculated from the measurements of maximum and minimum crown width using the following equation assuming the projection of the crown has a shape of an ellipse:

$$CA = (\pi * a * b)/4 \quad (10)$$

where CA is the crown area, a is the maximum crown width, and b is the minimum crown width. The total crown area of each plot was simply the sum of the crown area of all individual trees in the plot. The canopy cover (CC, %) or percent woody cover of each plot was calculated as:

$$CC = (CA/900) * 100\% \quad (11)$$

The total aboveground biomass and percent woody cover were estimated for each plot, respectively. Then I examined the relationship between total aboveground biomass and canopy cover at the plot level. There was a log-linear relationship between total aboveground biomass and percent canopy cover (Fig. 4.6). Each dot on the graph represented a circular plot, and thus this empirical relation was a plot-level relation. This empirical relation was also a pixel-level relation because each plot had the same area as a Landsat TM/ETM+ pixel.

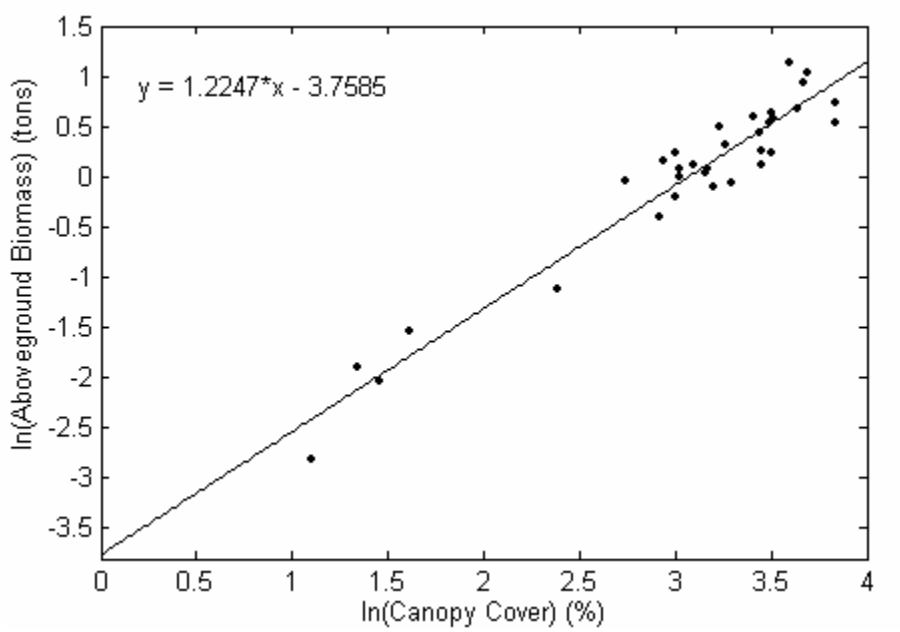

Fig. 4.6 Log-linear relationship between total aboveground biomass (tons) and percent canopy cover (%) based on estimates from the circular plots. Each dot represents a plot. This plot-level relationship is also a pixel-level relationship because each circular plot has the same area as a Landsat TM/ETM+ pixel.

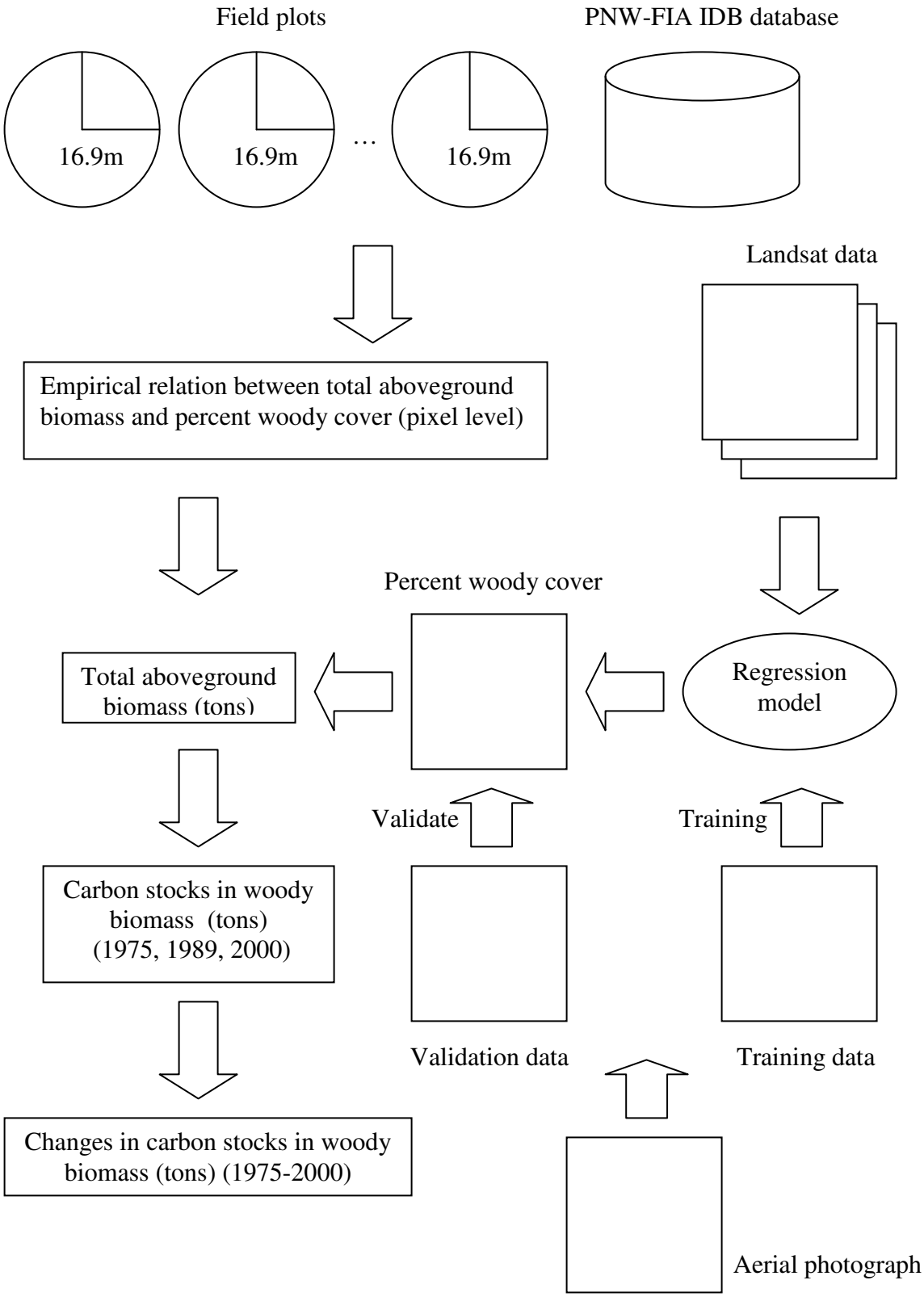

Fig. 4.7 Flow diagram of the methodology used in this study.

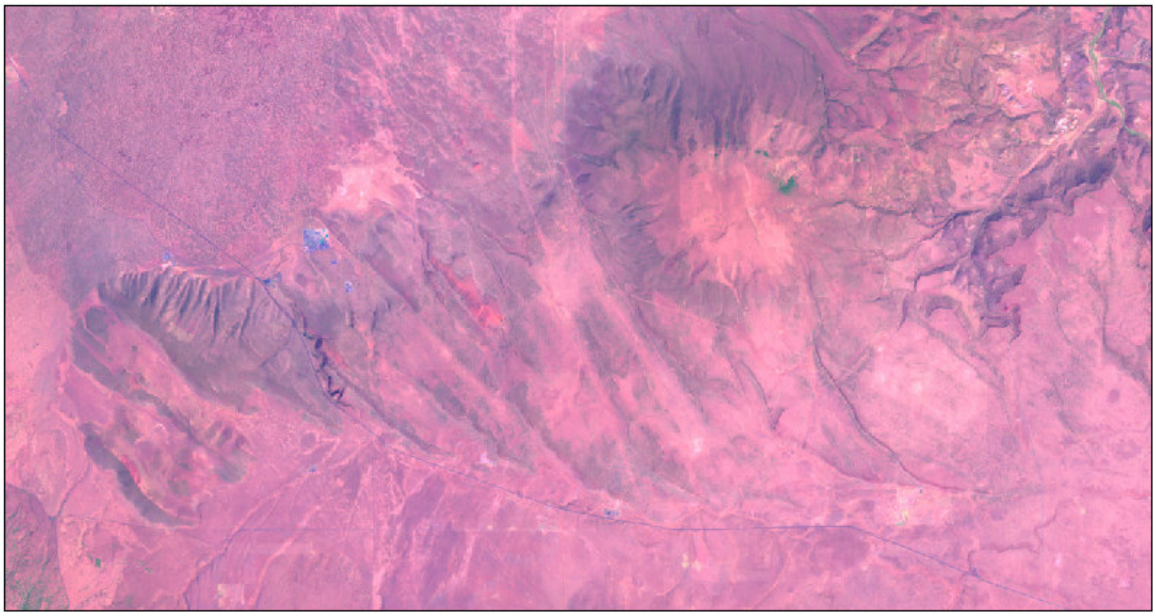

(a) Landsat ETM+

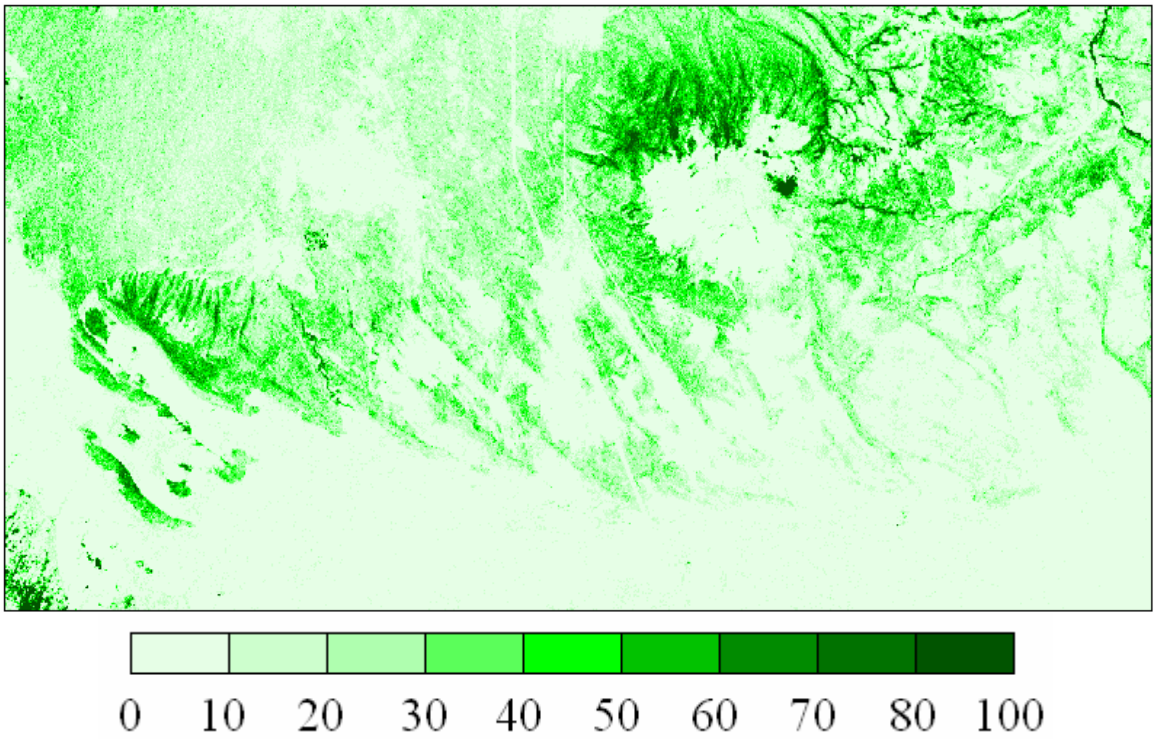

(b) Percent woody cover (%)

Fig. 4.8 Landsat image and percent woody cover estimated from the Landsat image: (a) Landsat ETM+ image acquired in 2000; (b) percent woody cover estimated from the Landsat ETM+ image.

This pixel-level empirical relation was used to estimate total aboveground biomass for each Landsat pixel from percent woody cover for 1975, 1989, and 2000, respectively. Aboveground biomass was converted to aboveground C stock using a conversion factor of 0.48 (Schlesinger 1997). Fig. 4.7 shows the methodology used in this study to estimate C stocks in woody biomass and changes in C stocks over the study period.

4.6 Results and Discussion

4.6.1 Percent woody cover

Percent woody cover was estimated from Landsat data for 1975, 1989, and 2000, respectively. Fig. 4.8 shows the Landsat ETM+ image and the estimated percent woody cover for 2000. Percent woody cover varies substantially over the landscape, and is typically less than 60%.

The estimates of percent woody cover were validated using the validation data derived from aerial photographs (Fig. 4.9). There was a strong, linear relationship between actual and predicted percent woody cover for 1975 ($R^2 = 0.61$, $p < 0.001$), 1989 ($R^2 = 0.84$, $p < 0.001$), and 2000 ($R^2 = 0.84$, $p < 0.001$), respectively. Overall, percent woody cover was estimated with reasonable accuracy. The accuracy of percent woody cover for 1975 was lower than that for 1989 or 2000. This is because that I used a MSS image for 1975, and TM/ETM+ images for 1989 and 2000. A MSS image has substantially lower spatial resolution (57m) and fewer spectral bands (4) than TM/ETM+ images (30m, 6 reflective bands).

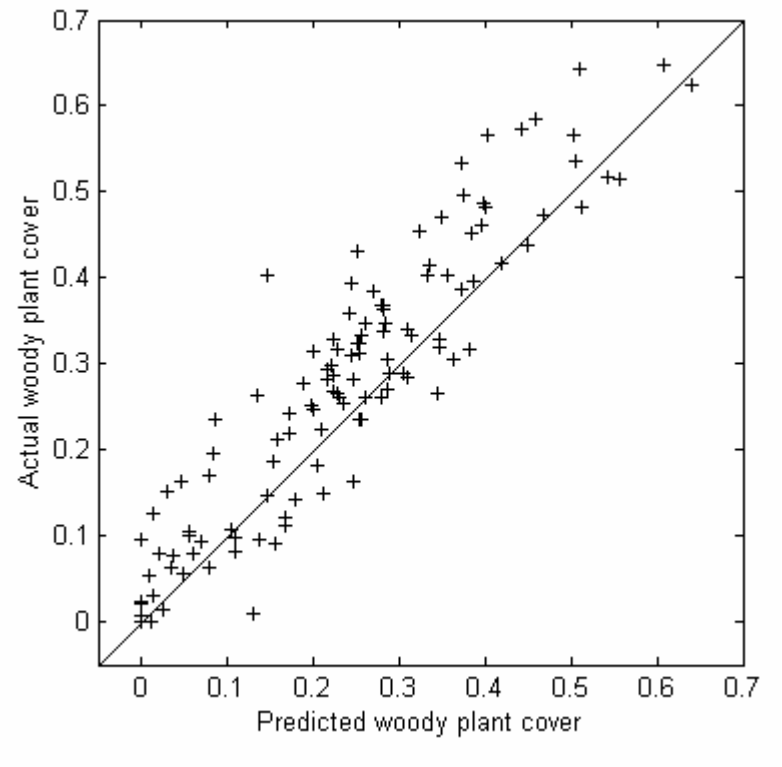

(a) Landsat ETM+ (2000)

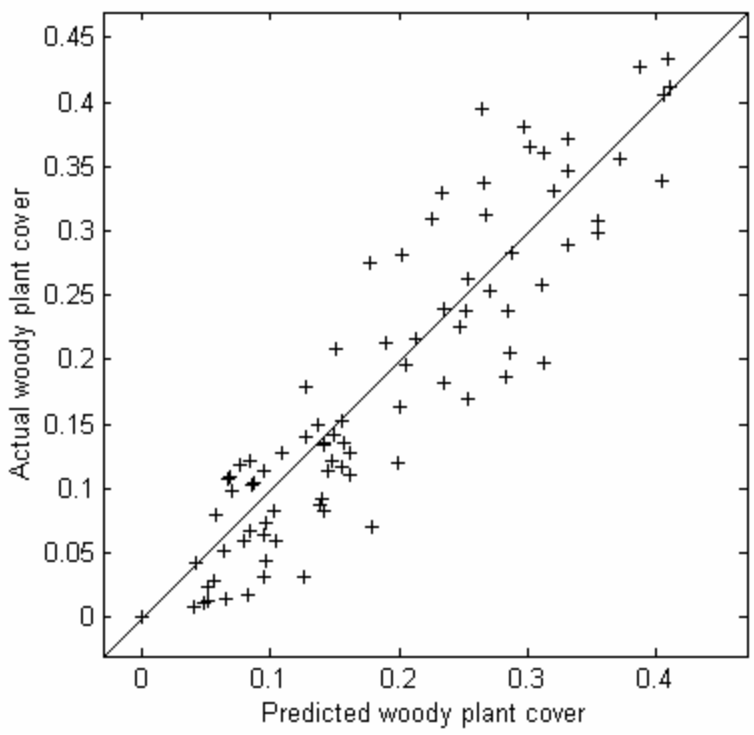

(b) Landsat TM (1989)

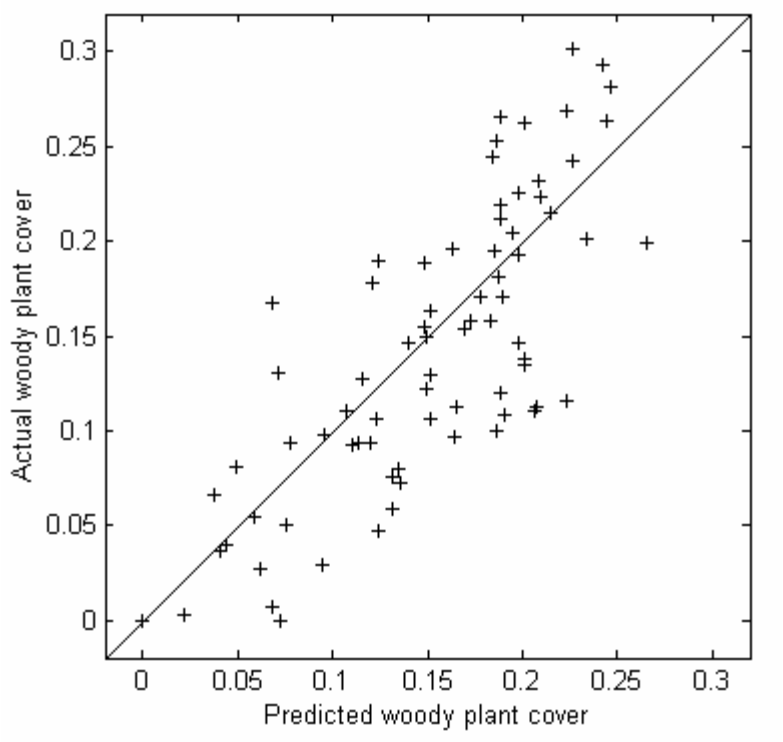

(c) Landsat MSS (1975)

Fig. 4.9 Validation of percent woody cover estimated from Landsat data: (a) Landsat ETM+ (2000) ($y = 0.9915x + 0.0433$, $R^2 = 0.84$, $p < 0.001$); (b) Landsat TM (1989) ($y = 1.0209x - 0.0117$, $R^2 = 0.84$, $p < 0.001$); (c) Landsat MSS (1975) ($y = 0.9793x – 0.0061$, $R^2 = 0.61$, $p < 0.001$).

Table 4.2 Woody plant cover (%) in the study region in 1975, 1989, and 2000 and changes in woody plant cover over the study period.

	1975 Cover (%)	1989 Cover (%)	2000 Cover (%)	Relative change (%)			Rate of change (% per year)		
				75-89	89-00	75-00	75-89	89-00	75-00
Study region	7.9	9.28	11.55	17.47	24.46	46.20	0.10	0.21	0.15

Over the study region, woody plant cover was estimated to be 7.9% in 1975, 9.28% in 1989, and 11.55% in 2000 (Table 4.2). This suggests that western juniper had expanded over the 25-year period. On average, the rate of change in woody plant cover was 0.10% per year for the period 1975-1989 and 0.21% for the period 1989-2000, indicating that the expansion of western juniper had increased throughout the entire study period. The average rate of change in woody plant cover was 0.15% per year.

4.6.2 Changes in carbon stocks

The C density in aboveground woody biomass had increased from 4.59 Mg C ha^{-1} in 1975 to 7.39 Mg C ha^{-1} in 2000 (Table 4.3). In the Oregon Transect Ecosystem Research (OTTER) Project, the team of researchers made standardized measurements required to initialize and to run a carbon-, water-, and nitrogen-cycling ecosystem model, and also took remotely sensed measurements seasonally from various platforms. In one study of the OTTER project, Runyon et al. (1994) measured biomass, NPP, and light use efficiency for selected sites across the Oregon transect including a western juniper site. Woody biomass of the western juniper site was 8 Mg ha^{-1}. The woody biomass reported by Runyon et al. (1994) is very close to that inferred from my estimates of aboveground woody biomass if aboveground woody biomass accounts for 80% of the total woody biomass.

The C accumulation rate was 0.112 Mg C ha^{-1} yr^{-1} over the study period. The C stocks in woody biomass had increased from 0.13 Tg C in 1975 to 0.21 Tg C in 2000. Thus, the expansion of western juniper had accumulated 0.08 Tg C in aboveground biomass over the 25-year period. This suggests that the expansion of western juniper had caused significant C accumulation in woody biomass.

The C accumulation rate in woody biomass caused by the expansion of western juniper had not been reported in the literature. However, some studies reported the C accumulation rate in woody biomass caused by the expansion of other species (Table 4.4). For example, Hicke et al. (2004) examined the encroachment of ponderosa pine in Colorado over the period from 1980 to 2001, and reported a C accumulation rate of 0.09 – 0.7 Mg C ha^{-1} yr^{-1} in woody biomass. The C accumulation rate caused by the expansion of western juniper falls within the range of the C accumulation rate reported by Hicke et al. (2004). Anser et al. (2003) studied the encroachment of honey mesquite in Texas drylands during the period from 1937 to 1999, and reported a C accumulation rate of 0.02 Mg C ha^{-1} yr^{-1}.

The C accumulation rate was extrapolated to the entire western juniper woodland in Oregon in order to assess the potential impact of the expansion of western juniper on the regional C budget. I assumed that the C accumulation rate (0.112 Mg C ha^{-1} yr^{-1}) were applicable to the entire juniper woodland in Oregon (1.5 million hectares). On the basis of this assumption, the expansion of western juniper would cause annual accumulation of 0.168 Tg C in aboveground woody biomass.

Table 4.3 Carbon stocks (Tg C) and carbon density (Mg C ha^{-1}) in aboveground woody biomass for western juniper woodlands in the study region.

	Total Carbon (Tg C)	**Density** (Mg C ha^{-1})
1975	0.13	4.59
1989	0.16	5.57
2000	0.21	7.39

Table 4.4 Carbon accumulation rate in woody biomass (Mg C·ha-1·yr-1) caused by woody plant proliferation.

	Region	**Period**	**Species**	**Rates**
Current Study	OR	1975-2000	western juniper	0.112
Hicke et al. (2004)	CO	1980-2001	ponderosa pine	0.09-0.7
Asner et al. (2003)	TX	1937-1999	honey mesquite	0.02

In principle, inventory studies of biomass change produce estimates of annual NPP (Baldocchi 2003). Sources and sinks of CO_2 are usually quantified by net ecosystem exchange (NEE), which is related to NPP on an annual basis as

$$NEE = NPP - R_h$$

where R_h is the heterotrophic respiration or decmoposition of biomass, primarily in the soil. Heterotrophic respiration is difficult to quantify over large areas (Running et al. 2004). NEE depends on the soil C pools available for decomposition, and usually ranges from 10% to 50% of NPP (Baldocchi et al. 2001, Falge et al. 2002).

I only estimated the changes in C stocks in aboveground woody biomass. The changes in C stocks in aboveground woody biomass are close to aboveground NPP. The proportion of belowground NPP may vary as trees age (Eddleman et al. 1994). On average, above- and belowground NPP of western juniper woodland was estimated to be about 80% and 20% of total NPP, respectively (Runyon et al. 1994). Total NPP caused by the expansion of western juniper was approximately 0.14 Mg C ha^{-1} yr^{-1}, assuming that above- and belowground NPP accounted for 80% and 20% of total NPP (Runyon et al. 1994). NEE would be 0.014-0.07 Mg C ha^{-1} yr^{-1}, assuming that NEE accounts for 10% to 50% of NPP (Falge et al. 2000, Baldocchi et al. 2001). Western juniper occupies 1.5 million hectares in Oregon (Kiilsgaard, C., 1999). If the C accumulation rate in ecosystems (0.014-0.07 Mg C ha^{-1} yr^{-1}) were applicable to the entire juniper woodland, the expansion of western juniper would lead to a C sink of 0.02-0.11 Tg C yr^{-1}.

To our knowledge, there was no explicit C budget for Oregon in the literature. In order to assess the potential impact of western juniper expansion on the regional C budget,

I compared the C sink caused by western juniper expansion with the C sinks/sources caused by forest ecosystems in Oregon (Table 4.5).

Cohen et al. (1996) estimated C flux over the 19-year period from 1972 to 1991 for a 1.2-million ha landscape of the PNW region in the central Oregon Cascades Range using forest ecosystem and related models in conjunction with satellite data. 68% of the study region was mapped as forest land in 1988 (Cohen et al. 1995). The forests of this area resulted in a net source of 17.5 Tg C during the 19-year period. The average total net C flux was 1.13 Mg C ha yr with both the live and detrital pools contributing positively to the total net flux and forest products contributing negatively (Cohen et al. 1996).

Wallin et al. (In press) used a simple C model and satellite data to quantify C flux from 4.9 million ha of forested lands in western Oregon. Between 1972 and 1995, the forests in western Oregon were a net C source, averaging 0.67 Mg C ha^{-1} yr^{-1}; between 1991 and 1995, however, the forests resulted in a net accumulation of 0.1 Mg C ha^{-1} yr^{-1} (Wallin et al. In press). The C sink of the forested land was estimated to be 0.49 Tg C yr^{-1}. Thus, the C sink caused by the expansion of western juniper is equivalent to 10% - 51% of the C sink reported by Wallin et al. (In press), although the forested land is 3 times as big as the western juniper woodland.

Law et al. (2004) used a spatially nested hierarchy of field and remote-sensing observations and a process model, Biome-BGC, to produce a C budget for the forested region of Oregon. The simulations suggested that annual net uptake (net ecosystem production (NEP)) for the whole forested region (8.2 million hectares) was 13.8 Tg C (1.68 Mg C ha^{-1} yr^{-1}), and C stocks (both above- and belowground) totaled 2765 Tg C. Net biome production (NBP) on the land, the net effect of NEP, harvest removals, and

wildfire emissions indicated that the study area was a sink (8.2 Tg C yr^{-1}). The estimated C sink caused by the expansion of western juniper is equivalent to only 0.6% - 3% of the C sink reported by Law et al. (2004). It should be noted, however, that the forested land is at least 5 times as big as the western juniper woodland.

Thus, the expansion of western juniper may have a significant impact on the regional C budget in Oregon. The Pacific Northwest region is one of the most productive forested regions in the world, with primary old-growth stands having a total of as much as 650 Mg C ha^{-1} in aboveground and belowground pools (Grier and Logan 1977, Harmon et al. 1986). Other regions experiencing woody plant proliferation in the western US are much less productive than the Pacific Northwest region. Thus, there is a reason to believe that woody plant proliferation may have an even more important role in regional C budgets in other regions. The expansion of western juniper will probably continue to occur in the future. Thus, we can expect that western juniper woodlands will continue to sequester C from the atmosphere and function as a C sink.

Table 4.5 Estimates of C sinks for western juniper woodlands and forest ecosystems in Oregon.

	State	**Ecosystems**	**Area** (10^6 ha)	**Period**	**C sink/source**	
					Mg C/ha/yr	Tg C/yr
This study	OR	Western juniper	1.5	75–00	-0.014 - -0.07	-0.02 - -0.11
Law *et al.* 2004	OR	Forests	8.2	Late 1990s	-1.0	-8.2
Wallin *et al.* In Press	OR	Forests	4.9	91–95	-0.1	-0.49
				88–95	+0.67	+3.28
Cohen *et al.* 1996	OR WA	Forests	10.4	72–91	+1.13	

4.6.4 Uncertainties

There are several uncertainties related to the data and methods used in this analysis that may influence the results presented here. First, there are uncertainties associated with the estimates of percent woody cover derived from Landsat data due to the nature of Landsat data, landscape characteristics, and method. The spatial resolution of Landsat data ranges from 30m to 57m, whereas western juniper is sparsely distributed over the landscape. It is a challenge to accurately estimate percent woody cover within each Landsat MSS/TM/ETM+ pixel. High-resolution satellite data including IKONOS and hyperspectral data (e.g., AVIRIS) may lead to more accurate estimates of woody plant cover. However, the Landsat series of satellites provide the longest coverage of the Earth's surface. Moreover, stepwise linear regression model is not necessarily the best method for estimating percent woody cover. A part of our future work is to continue to explore other methods for estimating percent woody cover including the piecewise regression tree algorithm implemented in Cubist (Rulequest Research) in order to reduce uncertainties associated with estimates of percent woody cover.

Second, there are uncertainties associated with the aboveground woody biomass and crown width data obtained from the PNW-FIA IDB database. Fig. 4.5 shows the uncertainties associated with the relationship between aboveground biomass and crown width, particularly for small trees. Moreover, the aboveground woody biomass was estimated from cubic volume and woody density factors (Forest Inventory & Analysis Program 2004), and thus was not directly measured. Another part of our future work is to obtain more reliable measurements of aboveground biomass so that I can develop a more robust empirical relationship between aboveground biomass and crown width.

Third, there are large uncertainties associated with the C sink estimated for the expansion of western juniper. I only estimated the changes in aboveground woody biomass, and did not consider the changes in belowground biomass. I assumed that above- and belowground NPP of western juniper woodland was estimated to be about 80% and 20% of total NPP, respectively (Runyon et al. 1994). However, the proportion of belowground NPP may vary as trees age (Eddleman et al. 1994). Another assumption that NEE accounts for 10% to 50% of NPP (Falge et al. 2000, Baldocchi et al. 2001) further increased the uncertainty associated with the estimated C sink caused by western juniper expansion.

4.7 Conclusions

I quantified regional changes in woody plant cover and aboveground C pools across 650 km^2 of western juniper woodland in central Oregon from 1975 to 2000. Over the study region, woody plant increased from 7.9% in 1975 to 11.55% in 2000. Western juniper expanded at the rate of 0.15% per year over the 25-year period. The expansion of western juniper caused C accumulation of 0.112 Mg C ha^{-1} yr^{-1} in aboveground woody biomass. If the C accumulation rate observed in the case study region were applicable to the entire western juniper woodlands in Oregon, western juniper expansion would cause net accumulation of 0.168 Tg C yr^{-1} in aboveground woody biomass. The resulting C sink in ecosystems was estimated to be 0.02-0.11 Tg C yr^{-1}. Western juniper expansion may have a significant impact on the regional C budget in Oregon.

4.8 Acknowledgements

Landsat data were obtained from the Global Land Cover Facility (http://www.landcover.org); color infrared aerial photographs were obtained from USGS

EarthExplorer; the DOQ was obtained from the Oregon Geospatial Enterprise Office; the PNW-FIA Integrated Database was kindly provided by Forest Inventory & Analysis Program, Pacific Northwest Research Station. Bo Xiao, a freshman at the University of North Carolina at Chapel Hill, helped us collect field data. I also thank Dr. Conghe Song, Department of Geography, University of North Carolina at Chapel Hill, for providing equipment and valuable suggestions for field work.

4.9 Chapter Synopsis

4.9.1 Background

The balance between herbaceous and woody vegetation in arid and semiarid regions has shifted to favor trees and shrubs during the past 150 years (Archer 1994) because of fire suppression (Houghton et al. 2000, Tilman et al. 2000), over-grazing (Archer 1989), climate change (Brown et al. 1997), atmospheric CO_2 enrichment (Polley et al. 2002), nitrogen deposition (Köchy & Wilson 2001), and a combination of two or more of these factors (Van Auken 2000). The expansion of woody plant cover in arid and semi-arid regions has important implications for the US C budget. Neither the rates of change nor the geographical extent of the phenomenon have been systematically quantified (Anser et al. 2003), not to mention the resulting C uptake and the implications on regional C budgets. Regional-scale analyses are needed to reduce the uncertainty in the C sink resulting from woody plant proliferation.

4.9.2 Synopsis

In Chapter 4, I presented a regional-scale analysis of the rates of woody plant proliferation and the resulting C uptake. First, I quantified regional changes in woody

plant cover and aboveground C pools across 650 km^2 of western juniper woodland in central Oregon from 1975 to 2000. Percent woody cover was estimated from Landsat data for 1975, 1989, and 2000, respectively. Over the study region, woody plant increased from 7.9% in 1975 to 11.55% in 2000. Western juniper expanded at the rate of 0.15% per year over the 25-year period.

Second, I developed a pixel-level empirical relationship between total aboveground biomass and canopy cover from forest inventory data and field measurements. This empirical relationship was used to estimate total aboveground biomass for each pixel from the percent woody cover derived from Landsat data for 1975, 1989, and 2000, respectively. The results suggest that the expansion of western juniper caused C accumulation of 0.112 Mg C ha^{-1} yr^{-1} in aboveground woody biomass. Total C stock in aboveground woody biomass increased from 0.13 Tg in 1975 to 0.21 Tg in 2000. This suggests that western juniper expansion led to significant C accumulation in woody biomass.

Third, I assessed the potential impact of western juniper expansion on the regional C budget by assuming that the C accumulation rate observed in the case study region was applicable to the entire juniper woodlands in Oregon. If the C accumulation rate were applicable to the entire juniper woodlands, western juniper expansion would cause net accumulation of 0.168 Tg C yr^{-1} in aboveground woody biomass. The resulting C sink in ecosystems was estimated to be 0.02-0.11 Tg C yr^{-1}. Thus, western juniper expansion may have a significant impact on the regional C budget in Oregon.

4.9.3 Limitations

There are several limitations regarding the analysis presented in this chapter. First, there are uncertainties associated with the estimates of percent woody cover derived from Landsat data due to the nature of Landsat data, landscape characteristics, and the method used to estimate percent woody cover. Western juniper is sparsely distributed over the landscape. Thus, a pixel in a Landsat image (30-57m resolution) includes woody plant cover and soil background. It is a challenge to accurately estimate percent woody cover within each Landsat MSS/TM/ETM+ pixel. The uncertainties associated with percent woody cover will lead to uncertainties in the estimates of the rates of western juniper expansion and the resulting C uptake.

Second, there are uncertainties associated with the aboveground biomass data obtained from the PNW-FIA IDB database. In this database, the aboveground biomass was estimated from cubic volume and woody density factors, and thus was not directly measured (Forest Inventory & Analysis Program 2004). The uncertainties associated with aboveground biomass will lead to uncertainties in the estimates of aboveground biomass and C stocks.

Third, there are large uncertainties associated with the C sink estimated for the expansion of western juniper. I only estimated the changes in aboveground woody biomass, and did not consider the changes in belowground biomass. I assumed that above- and belowground NPP of western juniper woodland was estimated to be about 80% and 20% of total NPP, respectively (Runyon et al. 1994). However, the proportion of belowground NPP may vary as trees age (Eddleman et al. 1994). Another assumption that NEE accounts for 10% to 50% of NPP (Falge et al. 2000, Baldocchi et al. 2001)

further increased the uncertainty associated with the estimated C sink caused by western juniper expansion.

4.9.4 Future directions

My future work for western juniper expansion will focus on the following aspects. First, I will extend the analysis from the case study region to the entire western juniper woodlands in Oregon. As with the case study, increases in woody plant cover and C stocks in aboveground woody biomass will be estimated based on satellite data, forest inventory data, and field measurements. Second, I will obtain more reliable measurements of aboveground biomass so that a more robust relationship between aboveground biomass and crow width can be developed for western juniper. Third, I will develop an allometric relationship between belowground woody biomass and crown width for western juniper, and then use this relationship to estimate the C stocks in belowground woody biomass. The total C uptake measured by NPP in both above- and below-ground woody biomass will thus be estimated. Fourth, the century model (Parton et al. 1987) will be used to simulate soil decomposition. The estimates of both NPP and soil decomposition will lead to estimates of NEP that measures the net C uptake in ecosystems. Finally, I expect to explore the drivers of western juniper expansion. A dynamic vegetation model, MC1 (Bachelet et al. 2000), will be used to simulate the vegetation distribution and ecosystem fluxes of C. MC1 was created by combining the MAPSS model (Neilson 1995), the CENTURY model (Parton et al. 1987), and a fire module, MCFIRE (Lenihan et al. 1998). The impacts of fire suppression, grazing, and climate on western juniper expansion will be examined through the simulations.

4.10 References

Adams, J. B., Smith, M. O., & Johnson, P. E. (1986). Spectral mixture modeling: a new analysis of rock and soil types at the Viking Lander 1 site. *J. Geophys. Res., 91*, 8098-8112.

Adams, J. B., Sabol, D. E., Kapos, V., Filho, R. A., Roberts, D. A., Smith, M. O., & Gillespie, A. R. (1995). Classification of multispectral images based on fractions of endmembers: application to land-cover change in the Brazilian Amazon. *Remote Sens. Envrion., 52*, 137-154.

Anys, H., Bannari, A., He, D.C. et al., 1994. Texture analysis for the mapping of urban areas using airborne MEIS-II images. In: *First International Airborne Remote Sensing Conference and Exhibition 3*, Strasbourg, France, pp. 231-245.

Archer, S., 1989. Have southern Texas savannas been converted to woodlands in recent history*? American Naturalist*, **134**, 545-561.

Archer, S., 1994. Woody plant encroachment into southwestern grasslands and savannas: rates, patterns and proximate causes. In: *Ecological Implications of Livestock Herbivory in the West* (eds Vavra M., Laycock W., Piper R.), pp. 13-68. Society for Range Management, Denver, CO.

Asner, G.P., Archer, S., Hughes, R.F., Ansley, J., & Wessman, C.A., 2003. Net changes in regional woody vegetation cover and carbon storage in Texas drylands, 1937-1999. *Global Change Biology*, **9**, 316-335.

Azuma, D.L., Hiserote, B.A., Dunham, P.A., 2005. The western juniper resource of eastern Orego, 1999. Resour. Bull. PNW-RB-249. Portland, OR: U.S. Department of Agriculture, Forest Service, Pacific Northwest Research Station. 18p.

Bachelet, D., Lenihan, J.M., Daly, C., & Neilson, R.P., 2000. Interactions between fire, grazing and climate change at Wind Cave National Park, SD. *Ecological Modeling*, **134**, 229-244.

Bailey, RG., 1998. *Ecoregions: the Ecosystem Geography of the Oceans and Continents*. Springer, New York.

Baldocchi, D., Falge, E., Gu, L., Olson, R., Hollinger, D. et al., 2001. FLUXNET: A new tool to study the temporal and spatial variability of ecosystem-scale carbon dioxide, water vapor, and energy flux densities. *Bulletin of the American Meteorological Society*, **82**, 2415-2434.

Baldocchi, D.D., 2003. Assessing the eddy covariance techniques for evaluating carbon dioxide exchange rates of ecosystems: past, present, and future. *Global Change Biology*, **9**, 479-492.

Bedell, T.E., Eddleman, L.E., Deboodt, T., & Jacks, C., 1993. Western Juniper – Its Impact and Management in Oregon Rangelands. EC 1417. Oregon State University Extension Service, Corvallis, OR, 15pp.

Belsky, A.J., 1996. Viewpoint: Western juniper expansion: Is it a threat to arid northwest ecosystems? *Journal of Range Management*, **49**, 53-59.

Briggs, J.M., Knapp, A.K., & Brock, B.L., 2002a. Expansion of woody plants in tallgrass prairie: a fifteen-year study of fire and fire-grazing interactions. *American Midland Naturalist*, **147**, 287-294.

Briggs, J.M., Hoch, G.A., & Johnson, L.C., 2002b. Assessing the rate, mechanisms, and consequences of the conversion of tallgrass prairie to Juniperus virginiana forest. *Ecosystems*, **5**, 578-586.

Brown, J.R., & Archer, S., 1999. Shrub invasion of grassland: recruitment is continuous and not regulated by herbaceous biomass or density. *Ecology*, **80**, 2385-2396.

Brown, J.H., Valone, T.J., & Curtin, C.G., 1997. Reorganization of an arid ecosystem in response to recent climate change. *Proc. Natl. Acad. Sci. USA*, **94**, 9729-9733.

Burkhardt, J.W., Tisdale, E.W., 1969. Nature and successional status of western juniper invasion in Idaho. *Journal of Range Management*, **22**, 264-270.

Burkhardt, J.W., Tisdale, E.W., 1976. Causes of juniper invasion in southwestern Idaho. *Ecology*, **57**, 472-484.

Burgess, T.L., 1995. Desert grassland, mixed-shrub savanna, shrub-steppe, or semi-desert scrub? The dilemma of coexisting growth forms. In: *The Desert Grasslands* (eds McClaran M.P., van Devender T.R.), pp. 31-67. University of Arizona Press, Tucson.

Caraher, D.L., 1978. The spread of western juniper in central Oregon. In: Proceedings of the western juniper ecology and management workshop (eds Martin RE, Dealy JE, Caraher DL), General Technical Report PNW-74, pp. 1-7. United States Department of Agriculture Forest Service, Portland, OR.

Chavez, P. S., Jr. (1989). Radiometric calibration of Landsat Thematic Mapper multispectral images. *Photogramm. Eng. Remote Sens.,* **55**, 1285-1294.

Chittester, J.M. and C.D. MacLean. 1984 Cubic-Foot Tree Volume Equations and Tables for Western Juniper. PNW-420. 8 pp.

Cohen WB, Spies TA, Fiorella M. 1995. Estimating the age and structure of forests in a multi-ownership landscape of western Oregon, U.S.A. *International Journal of Remote Sensing,* **16**: 721-746.

Cohen, W.B., Harmon, M.E., Wallin, D.O., & Fiorella, M., 1996. Two decades of carbon flux from forests of the Pacific Northwest. *Bioscience*, **46**, 836-844.

Cowlin, R.W., Briegleb, P.A., Moravets, F.L., 1942. Forest resources of the ponderosa pine region of Washington and Oregon. Misc. Publ. 490. Washington, DC: U.S. Department of Agriculture, Forest Service. 99 p.

Driscoll, R.S., 1964a. A relict area in central Oregon juniper zone. *Ecology*, **45**, 345-353.

Driscoll, R.S., 1964b. Vegetation-soil units in the central Oregon juniper zone. USDA, Pac. NW For. and Range Exp. Sta. US For. Ser. Res. Pap. PNW 19, 60 pp.

Dyksterhuis, E.L., 1981. Soil Survey of Grant County, Oregon, Central Part. USDA, Soil Conserv. Serv.

Eddleman, L.E., 1987. Establishment and stand development of western juniper in central Oregon. In: Procceedings of the Pinyon-Juniper Conference (ed. Everett RL), General Technical Report INT-215, pp. 255-259. United States Department of Agriculture, Ogden, UT.

Eddleman, L.E., Miller, P.M., Miller, R.F., & Dysart, P.L., 1994. Western juniper woodlands (of the Pacific Northwest): science assessment. Unpublished scientific contract report solicited by and on file with the Interior Columbia Basin Ecosystem Management Project, Walla Walla, Washington, 132 pp.

Falge, E., et al. 2002. Phase and amplitude of ecosystem carbon release and uptake potentials as derived from FLUXNET measurements. *Agriculture and Forest Meteorology*, **113**, 75-95.

Fisher, C.E., 1950. The mesquite problem in the Southwest. *Journal of Range Management*, **3**, 60-70.

Forest Inventory & Analysis Program, 2004. The PNW-FIA Integrated Database User Guide: A Database of Forest Inventory Information for California, Oregon, and Washington. Version 1.4-1. Pacific Northwest Research Station, Portland, Oregon.

Gedney, D.R., Azuma, D.L., Bolsinger, C.L., & McKay, N., 1999. Western juniper in eastern Oregon. Gen. Tech. Rep. PNW-GTR-464. Portland, OR: U.S. Department of Agriculture, Forest Service, Pacific Northwest Research Station. 53p.

Gifford, G.F., 1987. Myths and fables and the pinyon-juniper type. In: Proceedings of the Pinyon-Juniper Conference (ed. Everett RL), General Technical Report INT-215, pp. 34037. United States Department of Agriculture, Ogden, UT.

Green, G.L., 1975. Soil survey of trout Creek-Shaniko area, Oregon. USDA, Soil Con. SErv., US Gov. Prin. Office. 1975-O-524-786.

Grier CC, Logan RS. 1977. Old growth Douglas fir communities of a western Oregon watershed: biomass distribution and production budgets. *Ecological Monographs,* **47**, 373-400.

Harmon ME, et al. 1986. Ecology of coarse woody debris in temperate ecosystems. *Recent Advances in Ecological Research*, **15**: 133-302.

Hicke, J.A., Sherriff, R.L., Veblen, T.T., & Asner, G., 2004. Carbon accumulation in Colorado ponderosa pine stands. *Canadian Journal of Forest Research*, **34**, 1283-1295.

Houghton, R.A., Hackler, J.L., & Lawrence, K.T., 1999. The U.S. carbon budget: contributions from land-use change. *Science*, **285**, 574-578.

Houghton, R.A., Hackler, J.L., & Lawrence, K.T., 2000. Changes in terrestrial carbon storage in the United States. 2: The role of fire and fire management. *Global Ecology & Biogeography*, **9**, 145-170.

Huang, C., Yang, L., Wylie, B, & Homer, C., 2001. A strategy for estimating tree canopy density using Landsat ETM+ and high resolution images over large areas. Proceedings of the Third International Conference on Geospatial Information in Agriculture and Forestry, Denver, Colorado, 5-7 November, 2001. CD-ROM, 1 disk.

Josaitis, R.M., 1991. The effects of western juniper occupancy on changes in soil characteristics in relation to shrub and grass establishment in Owyhee County, Idaho. Thesis. University of Idaho. 109 pp.

Karl, M.G., & Leonard, S.G., 1996. Western Juniper (*Juniperus occidentalis* ssp. *occidentalis*) in the Interior Columbia Basin and portions of the Klamath and Great Basin: Science Assessment. 2nd draft, March 17, 1996. Interior Columbia Basin Ecosystem Management Project Science Integration Team, Terrestrial Staff, Range Task Group.

Knapp, P.A., & Soulé, P.T., 1998. Recent Juniperus occidentalis (western juniper) expansion on a protected site in central Oregon. *Global Change Biology*, **4**, 347-357.

Kiilsgaard, C., 1999. Manual and Land Cover Type Descriptions: Oregon Gap Analysis 1998 Land Cover for Oregon. Oregon Natural Heritage Program, Portland, OR.

Köchy, M., & Wilson, S.D., 2001. Nitrogen deposition and forest expansion in the northern Great Plains. *Journal of Ecology*, **89**, 807-817.

Law, B.E., Turner, D., Campbell, J., Sun, O.J., Tuyl, S.V. et al., 2004. Disturbance and climate effects on carbon stocks and fluxes across western Oregon USA. *Global Change Biology*, **10**, 1429-1444.

Lenihan, J.M., Daly, C., Bachelet, D., Neilson, R.P., 1998. Simulating broad-scale fire severity in a dynamic global vegetation model. *Northwest Sci*., **72**, 91-103.

Lentz, R.D., & Simonson, G.H., 1986. A detailed soils inventory and associated vegetation of Northern Great Basin Experimental Station. Spec. Rpt. 760. Agr. Exp. Sta., Oregon State Univ., Corvallis. 184 pp.

Markham, B. L., & Barker, J. L. (1987). Radiometric properties of U.S. processed Landsat MSS data. *Remote Sensing of Environment,* **22**, 39-71.

Martin, R.E., 1978. Fire manipulation and effects in western juniper (Juniperus occidentalis) Hook. pp. 121-136. IN: Proc. West. Juniper Ecol. and Manage. Workshop. Bend, OR. 1977. USDA For. Ser. Gen. Tech Rpt. PNW-74.

Martin, R.E., & Johnson, A.H., 1979. Fire management of Lava Beds National Monument. pp. 1209-1217. IN: Linn, R.M. (ed.). Proc. of the First Conference of Science and Research in the National Parks. USDI Nat. Park Serv., Transactions Proc. Serial No. 5.

McDonald, A. J., Gemmell, F. M., & Lewis, P. E. (1998). Investigation of the utility of spectral vegetation indices for determining information on coniferous forests. *Remote Sensing of Environment*, **66**, 250-272.

Miller, R.F., Rose, J.A., 1995. Historic expansion of Juniperus occidentalis (western juniper) in southeastern Oregon. *Great Basin Naturalist*, **55**, 37-45.

Miller, R.F., Wigand, P.E., 1994. Holocene changes in semiarid pinyon-juniper woodlands. *BioScience*, **44**, 465-474.

Moran, M. S., Jackson, R. D., Slater, P. N., & Teillet, P. M. (1992). Evaluation of simplified procedures for retrieval of land surface reflectance factors from satellite sensor output. *Remote Sensing of Environment*, **41**, 169-184.

Neilson, R.P., 1995. A model for predicting continental-scale vegetation distribution and water balance. *Ecol. Appl.*, **5**, 362-385.

Pacala, S.W., Hurtt, G.C., Baker, D., Peylin, P., Houghton, R.A. et al., 2001. Consistent land- and atmosphere-based U.S. carbon sink estimates. *Science*, **292**, 2316-2320.

Parton, W.J., Schimel, D.S., Cole, C.V., & Ojima, D.S., 1987. Analysis of factors controlling soil organic matter levels in Great Plains grasslands. *Soil Sci. Soc. Am. J.*, **51**, 1173-1179.

Polley, H.W., Johnson, H.B., & Tischler, C.R., 2002. Woody invasion of grasslands: evidence that CO_2 enrichment indirectly promotes establishment of Prosopis glandulosa. *Plant Ecology*, **164**, 85-94.

Price, J. C. (1987). Special issue on radiometric calibration of satellite data. *Remote Sensing of Environment*, **22**, 1-158.

Rappole, J.H., Russell, C.E., & Fulbright, T.E., 1986. Anthropogenic pressures and impacts on marginal, neotropical, semiarid ecossytems: the case of south Texas. *Science of the Total Environment*, **55**, 91-99.

Running, S.W., Nemani, R.R., Heinsch, F.A., Zhao, M., Reeves, M., & Hashimoto, H., 2004. A continuous satellite-derived measure of global terrestrail primary production. *Bioscience*, **54**, 547-560.

Runyon, J., Waring, R.H., Goward, S.N., & Welles, J.M., 1994. Environmental limits on net primary production and light-use efficiency across the Oregon transect. *Ecological Applications*, **4**, 226-237.

Sauerwein, W.J. 1982. Western juniper site index curves. Woodland Tech. Note No. 14. Portland, OR: U.S. Department of Agriculture, Soil Conservation Service; 1982, 4 p.

Schlesinger, W.H., 1997. *Biogeochemistry: An Analysis of Global Change*. Academic Press, New York.

Schlesinger, W.H., Reynolds, J.F., Cunningham, G.L., Huenneke, L.F., Jarrell, W.M., et al., 1990. Biological feedbacks in global desertification. *Science*, **247**, 1043-1048.

Shinn, D.A., 1989. Historical perspective on range burning in the inland pacific Northwest. *Journal of Range Management*, **33**, 415-422.

Smith, M. O., Ustin, S. L., Adams, J. B., & Gillespie, A. R. (1990). Vegetation in deserts: I. A regional measure of abundance from multispectral images. *Remote Sensing of Environment,* **31**, 1-26.

Song, C., Woodcock, C.E., Seto, K.C., Lenney, M.P., & Macomber, S.A., 2001. Classification and change detection using Landsat TM data: when and how to correct atmospheric effects? *Remote Sensing of Environment*, **75**, 230-244.

Soulé, P.T., & Knapp, P.A., 1999. Western juniper expansion on adjacent disturbed and near-relict sites. *Journal of Range Management*, **52**, 525-533.

Soulé, P.T., Knapp, P.A., & Grissino-Mayer, H.D., 2003. Comparative rates of western juniper afforestation in south-central Oregon and the role of anthropogenic disturbance. *Professional Geographer*, **55**, 43-55.

Teillet, P. M., & Fedosejevs, G. (1995). On the dark target approach to atmospheric correction of remotely sensed data. *Canadian Journal Remote Sensing,* **21**, 373-387.

Tilman, D., Reich, P., Phillips, H., Menton, M., Patel, A., et al., 2000. Fire suppression and ecosystem carbon storage. *Ecology*, **81**, 2680-2685.

Van Auken, W.O., 2000. Shrub invasions of North American semiarid grasslands. *Annual Review of Ecology and Systematics*, **31**, 197-216.

Vaitkus, M.R., & Eddleman, L.E., 1991. Tree size and understory phytomass production in a western juniper woodland. *Great Basin Naturalist*, **51**, 236-243.

Wallin, D.O, M. Harmon, W. Cohen (in press) Modeling regional-scale carbon dynamics in Pacific Northwest forests: 1972-95. Pages xx-xx *In:* O. Krankina and M.E. Harmon (eds.) Carbon Dynamics of Two Forest Regions: Northwestern Russian and the Pacific Northwest. Springer-Verlag, New York.

Waring, R.H., & Peterson, D.L., 1994. Oregon Transect Ecosystem (OTTER) Project. *Ecological Applications*, **4**, 210.

Williams, C.N., Jr., M.J. Menne, R.S. Vose, and D.R. Easterling. 2005. United States Historical Climatology Network Monthly Temperature and Precipitation Data. ORNL/CDIAC-118,NDP-019. Available on-line [http://cdiac.ornl.gov/epubs/ndp/ushcn/usa_monthly.html] from the Carbon Dioxide Information Analysis Center, Oak Ridge National Laboratory, U.S. Department of Energy, Oak Ridge, Tennessee.

Xiao, J., & Moody, A., 2005. A comparison of methods for estimating fractional green vegetation cover within a desert-to-upland transition zone in central New Mexico, USA. *Remote Sensing of Environment*, **98**, 237-250.

Yang, L., Huang, C., Homer, C. G., Wylie, B. K., & Coan, M. J. (2003). An approach for mapping large-area impervious surfaces: synergistic use of Landsat-7 ETM+ and high resolution imagery. *Canadian Journal of Remote Sensing,* **29**, 230-240

Chapter 5

Conclusions

5.1 Conclusions

More and more evidence suggest that global warming will be a real threat to the stability of the world's ecosystems (Jutro 1991, Masek 2001). Global warming is primarily attributed to the dramatic rise of atmospheric CO_2 concentration due to anthropogenic activities (IPCC 2001). The two major sources of CO_2 in the atmosphere are the combustion of fossil fuels and tropical deforestation (IPCC 2001). However, not all the C released by anthropogenic activities is absorbed by the atmosphere. For example, there is general agreement that terrestrial ecosystems sequester a large amount of CO_2 from the atmosphere and thus provide a large C sink although the magnitude, distribution, and mechanisms of this sink remain uncertain (Battle et al. 2000, Schimel et al. 2001). Changes in vegetation productivity, especially at regional or larger scales, affect atmospheric CO_2 concentrations, and produce variability in global C budgets and uncertainty in their approximation (Tans et al. 1990, Schimel et al. 1996).

Regionally, net C uptake has been attributed to increases in vegetation productivity. However, the patterns and distribution of increases in vegetation productivity are not well understood. Understanding the modes and drivers of changes in terrestrial plant productivity can, therefore, help us to understand the variability in global C budgets. In

this dissertation, I looked at increases in vegetation productivity and responses to climate variability at multiple spatial scales. The overall research question of my dissertation is: What are the rates and climatic correlates of increases in vegetation productivity at regional or larger scales? I attempted to address this question using satellite data, ground-based climatology data, forest inventory data, and field measurements.

There is growing evidence that vegetation productivity has been increasing during the past two decades, suggesting that the earth has become greener due to natural factors and anthropogenic activities (Fan et al. 1998, Bousquet et al. 1999, Zhou et al. 2001, Goodale et al. 2002). However, the investigation of large-scale increases in vegetation productivity has been largely limited to northern high latitudes (e.g., Myneni et al. 1997, Zhou et al. 2001). The trends and patterns of changes in vegetation productivity in other geographical regions are not well understood. My dissertation showed that vegetation productivity also significantly increased in forested and agricultural regions in the northern middle latitudes (e.g., US and China) and the tropics (Chapter 2) as well as in some arid and semi-arid regions, particularly in the US west (Chapters 2 & 4). As with enhanced plant growth in northern high latitudes (e.g., Myneni et al. 1997, Zhou et al. 2001), the observed increases in vegetation productivity in other geographical regions (Chapters 2 & 4) may have also led to significant C accumulation in ecosystems, and thus have important implications for the global C cycle. For example, regional C sinks may exist in the tropics due to regional increases in vegetation productivity (Chapter 2) despite the general consensus that tropical ecosystems are a large C source (e.g., IPCC 2001). The terrestrial C sink at the global scale may be bigger than expected (Schimel et al. 2001).

With a better understanding of the distribution and patterns of increases in vegetation productivity, the next step is naturally to examine the drivers behind these changes. Increases in vegetation productivity have been attributed to climate change (Nemani et al. 2002), CO_2 enrichment (Hamilton et al. 2002), N deposition (Nadelhoffer et al. 1999), forest plantations (Goodale et al. 2002), forest regrowth after agricultural abandonment (Caspersen et al. 2000), fire suppression (Houghton et al. 2000), and woody plant proliferation (Houghton et al. 1999, 2000, Pacala et al. 2001). However, the relative contributions of these mechanisms still remain uncertain. Focusing on the influences of two of these drivers including climate change and woody plant proliferation on vegetation productivity, this dissertation showed that (1) temperature is leading climatic factor of increases in vegetation productivity, and vegetation productivity responds to climate variability in a manner that varies by biome type (Chapters 2 & 3); (2) regionally, woody plant proliferation has led to increases in vegetation productivity, and thus has a significant impact on C budgets, at least in the US (Chapters 2 & 4). Other factors, such as CO_2 fertilization (Hamilton et al. 2002), forestry plantations (Goodale et al. 2002), forest regrowth (Caspersen et al. 2000), and trends in agricultural practices (Xiao & Moody 2004) also contribute substantially to increases in vegetation productivity (Chapter 2). Further studies are needed to asess the relative contributions of the mechanisms above to the observed increases in vegetation productivity.

Among the modes of increases in vegetation productivity, woody plant proliferation is unique and deserves special attention in that this phenomenon increases in stem density and/or represents a transition between biome types, and has important implications for the US C budget. For example, Houghton et al. (1999, 2000) and Pacala et al. (2001)

attributed approximately 21-40% of the US C sink woody plant proliferation. However, these studies emphasized the large uncertainty in their estimates, and called for regional-scale analyses of the rates and C consequences of woody plant proliferation (Anser et al. 2003). In Chapter 4, I presented a regional-scale analysis of western juniper expansion in central Oregon, suggesting that western juniper expansion may have a significant impact on the regional C budget. This is an important step towards explictly quantifying the C sink resulting from woody plant proliferation in the US west. More regional-scale studies are needed to reduce the uncertainty in the estimates of the C sink (e.g., Houghton et al. 1999, 2000, Pacala et al. 2001). The good news is that Landsat satellite imagery has great potential for estimating the rates and geographical extent of woody plant proliferation at regional or larger scales (Chapter 4). These regional-scale efforts based on satellite data ground-based measurements will better characterize the rates and C consequences of woody plant proliferation, and thus reduce the uncertainties associated with the size of the US C sink.

This dissertation characterizes the increases in vegetation productivity and responses to climate variability at multiple scales. It should be noted that, however, increases in vegetation productivity inferred from satellite data (Chapters 2 & 4) can not be directly interpreted as changes in ecosystem C stocks. Dynamics in ecosystem C stocks are usually characterized by NEE. In addition, this dissertation focuses on the influences of climate variability and woody plant proliferation on vegetation productivity (Chapters 2 & 3), and other factors such as CO_2 enrichment, forest regrowth, and fire suppression are not explicitly explored. Multidisciplinary studies on the basis of satellite data, biogeochemical models, and ground-based measurements (e.g., LTER, FLUXNET, and

forest inventory data) will lead to a better understanding of the distribution, patterns, and drivers of vegetation dynamics as well as the resulting changes in ecosystem C storage.

5.2 References

Battle, M., Bender, M.L., Tans, P.P., White, J.W.C., Ellis, J.T., Conway, T., & Francey, R.J., 2000. Global sinks and their variability inferred from atmospheric O_2 and $\delta^{13}C$. *Science*, **287**, 2467-2470.

Bousquet, P., Ciais, P., Peylin, P., Ramonet, M., & Monfray, P., 1999. Inverse modeling of annual atmospheric CO_2 sources and sinks. 1. Method and control inversion. *Journal of Geophysical Research*, **104**, 26161-26178.

Caspersen, J.P., Pacala, S.W., Jenkins, J.C., Hurtt, G.C., Moorcroft, P.R., & Birdsey, R.A. 2000. Contributions of land-use history to carbon accumulation in U.S. forests. *Science*, **290**, 1148-1151.

Fan, S., Gloor, M., Mahlman, J., Pacala, S., Sarmiento, J., Takahashi, T., and Tans, P., 1998, A large terrestrial carbon sink in North America implied by atmospheric and oceanic carbon dioxide data and modes. *Science,* **282**, 442-446.

Goodale, C.L., Apps, M.J., Birdsey, R.A., Field, C.B., Heath, L.S. et al. 2002. Forest carbon sinks in the northern hemisphere. *Ecological Applications*, **12**, 891-899.

Hamilton, JG, DeLucia, EH, George, K et al. 2002. Forest carbon balance under elevated CO_2. *Oecologia*, **131**, 250-260.

Houghton, R.A., Hackler, J.L., & Lawrence, K.T. 1999. The U.S. carbon budget: contributions from land-use change. *Science*, **285**, 574-578.

Houghton, R.A., Hackler, J.L., & Lawrence, K.T. 2000. Changes in terrestrial carbon storage in the United States. 2: The role of fire and fire management. *Global Ecology & Biogeography*, **9**, 145-170.

Intergovernmental Panel on Climate Change (IPCC), 2001. *Climate Change 2001: The Scientific Basis*. Contribution of Working Group I to the Third Assessment Report of the Intergovernmental Panel on Climate Change (IPCC). J. T. Houghton, Y. Ding, D.J. Griggs, M. Noguer, P. J. van der Linden and D. Xiaosu (Eds.). Cambridge University Press, UK. pp 944.

Jutro, P.R., 1991. Biological diversity, ecology, and global climate change. *Environmental Health Perspectives*, **96**, 167-170.

Masek, J.G., 2001. Stability of boreal forest stands during recent climate change: evidence from Landsat satellite imagery. *Journal of Biogeography*, **28**, 967-976.

Myneni, R.B., Keeling, C.D., Tucker, C.J., Asrar, G., & Nemani, R.R., 1997. Increased plant growth in the northern high latitudes from 1981 to 1991. *Nature*, **386**, 698-702.

Nadelhoffer, KJ, Emmett, BA, Gundersen, P et al. 1999. Nitrogen deposition makes a minor contribution to carbon sequestration in temperate forests. *Nature*, **398**, 145-148.

Nemani, R., White, M., Thornton, P., Nishida, K., Reddy, S., Jenkins, J., & Running, S. 2002. Recent trends in hydrologic balance have enhanced the terrestrial carbon sink in the United States. *Geophysical Research Letters*, **29**, 1468, doi:10.1029/2002GL014867.

Pacala, S.W., Hurtt, G.C., Baker, D., Peylin, P., Houghton, R.A., et al. 2001. Consistent land- and atmosphere-based U.S. carbon sink estimates. *Science*, **292**, 2316-2320.

Schimel, D.S., Alves, D., Enting, I., Himann, M., Joos, F., Raynaud, D., and Wigley, T., 1996, CO2 and the carbon cycle, in *Climate Change 1995: The Science of Climate Change*, edited by J. T. Houghton et al., pp. 76-86, Cambridge University Press, New York, 1996.

Schimel, D.S., House, J.I., Hibbard, K.A., Bousquet, P., Ciais, P. et al., 2001. Recent patterns and mechanisms of carbon exchange by terrestrial ecosystems. *Nature*, **414**, 169-172.

Tans, P. P., Fung, I. Y., and Takahashi, T. 1990. Observation constraints on the global atmospheric CO_2 budget. *Science*, **247**, 1431-1438.

Xiao, J., & Moody, A., 2004. Trends in vegetation activity and their climatic correlates: China 1982 to 1998. *International Journal of Remote Sensing*, **25**, 5669-5689.

Zhou, L., Tucker, C.J., Kaufmann, R.K., Slayback, D., Shabanov, N.V., and Myneni, R.B., 2001, Variations in northern vegetation activity inferred from satellite data of vegetation index during 1981 to 1999. *Journal of Geophysical Research,* **106**, 20069-20083.